NASA Contractor Report CR-195395

Two Rotor Stratified Charge Rotary Engine (SCRE) Engine System Technology Evaluation

T. Hoffman, J. Mack and R. Mount
Rotary Power International, Inc.
Wood-Ridge, New Jersey

October 1994

Prepared for
Lewis Research Center
Under Contract NAS3-26920

Two Rotor Stratified Charge Rotary Engine

(SCRE) Engine System Technology Evaluation

TABLE OF CONTENTS

8.0 Conclusions
- 8.1 Engine Performance Status
- 8.2 Engine Mechanical Status
- 8.3 Accessories System Status
- 8.4 Overall Summary and Engine Status

9.0 Recommendations

10.0 Appendix

1.0 INTRODUCTION

1.0 INTRODUCTION

A final report is provided for Contract NAS3-26920. This contractual effort was the fourth phase in an overall, consecutive contracts, multi-phase program (1983-1994) addressing Stratified Charge Rotary Engine (SCRE) technology enablement. The NASA long range, overall program objectives are the establishment of an advanced aircraft engine technology base for general aviation of the mid-1990's and beyond.

Contract NAS3-26920 focused on the evaluation of the two rotor SCRE system technology.

The program utilized the concepts and hardware deriving from the research and technology efforts in prior contracts, NAS3-25945 (Phase III) and NAS3-24628 (Phase II). The basic technical approach was to identify and refine those component concepts proven most effective in achieving performance goals in the prior programs, and integrate these components into an overall two rotor core engine configuration, Figure No. 1.0-1. The program objectives were to demonstrate 340 BHP (254 kW) at take-off conditions using Jet-A fuel. This entailed two rotor engine system components including the basic power section, fuel injection system, turbocharger and ignition system. Cruise conditions as defined here relate to typical aircraft engine maximum cruise condition, i.e. 75% of take-off or 255 HP (190kW).

The objective of demonstrating Take-off power of 340 BHP (254kW) while operating on Jet-A fuel was accomplished. In addition to this demonstration on the two rotor system, supportive component testing with the single rotor research rig engine also achieved demonstration of the same HP/cu.in. level, i.e. 4.25 HP (3.17kW)/cu.in. or 170 BHP (127kW).

A specific fuel consumption of 0.49 LBS/BHPHr (298 GRS/kW-Hr) was achieved at the 75% or maximum cruise condition vs. the objective of 0.435 LBS/BHP-Hr.(265 GRS/kW-Hr). Lower values were achieved with the supportive single rotor research rig engine reflecting the potential to achieve that level through additional refinement and testing with the two rotor machine.

The program was initiated on January 21, 1993 and was completed on schedule in October 1994.

ADVANCED ENGINE CONFIGURATION

NAS3-26920

MODEL 2013R **340 BHP/8000 RPM**

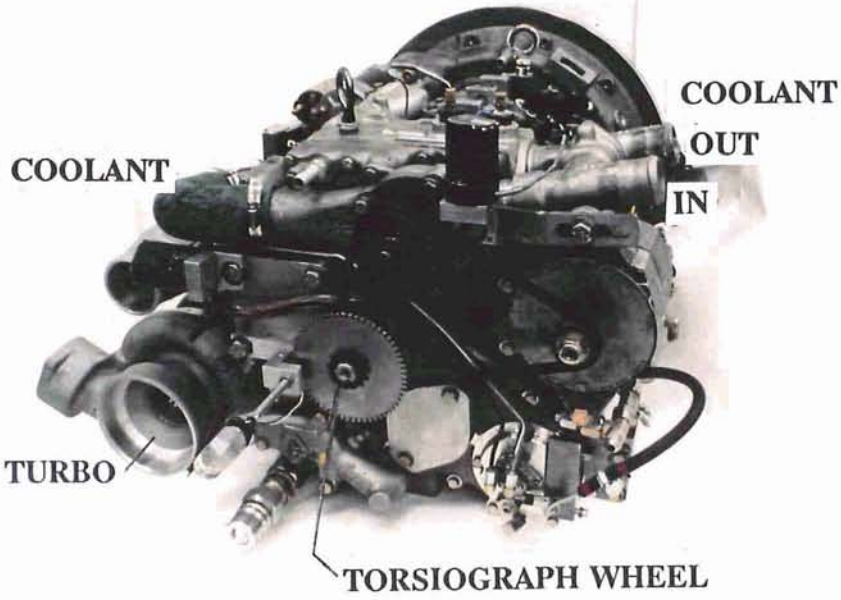

ORIGINAL PAGE
COLOR PHOTOGRAPH

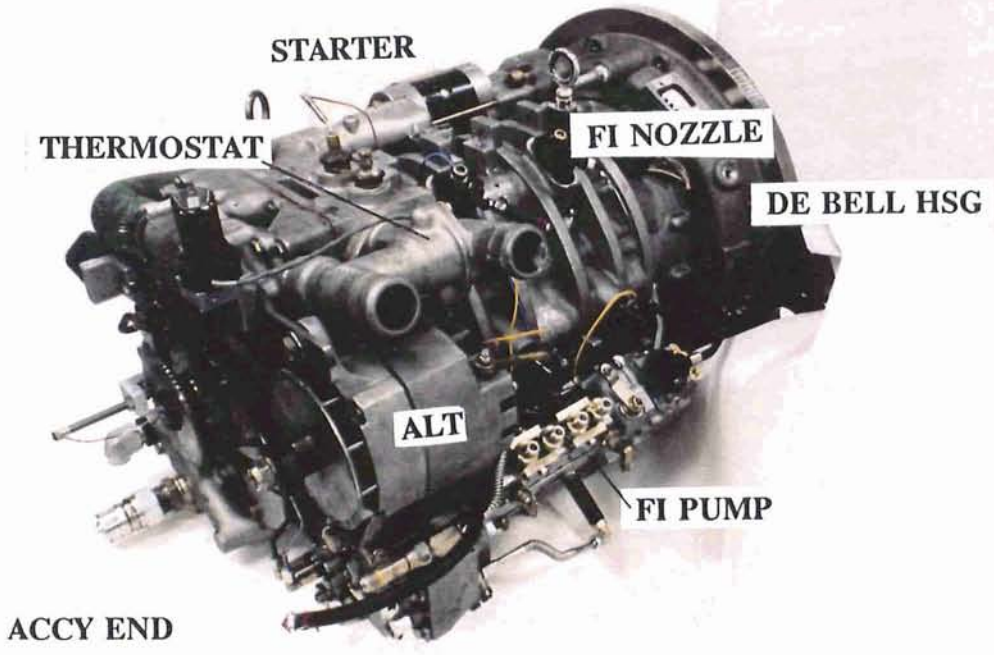

Figure No. 1.0-1

2.0 EXECUTIVE SUMMARY

2.0 EXECUTIVE SUMMARY

NASA Contract No. NAS3-26920, entitled "Two Rotor Stratified Charge Rotary Engine (SCRE) Engine System Technology Evaluation" was a logical extension of and a continuation of research work conducted in prior contracts NAS3-25945, NAS3-24628 and NAS3-23056. The primary objective of these successive efforts has been the advancement of technologies necessary to attain an affordable, Jet-A fueled engine for General Aviation in the mid-1990's and beyond timeframe. In this particular contract, component research technologies deriving from the earlier research work were refined and integrated into a two rotor engine system for an evaluation of that technology.

A demonstration of Take-off power at 340 BHP (254kW) operating on Jet-A fuel was achieved. A demonstration of specific fuel consumption at 75% power, maximum cruise of 0.49 LBS/BHP-Hr (298 GRS/kW-Hr) was achieved. An advanced electronic high speed unit injector fuel injection system was defined, procured and tested as part of the program.

2.1 Schedule

The program was initiated on January 21, 1993 and completed in October 1994. The master schedule, reflecting task definitions and timing is presented in Figure No. 2.1-1.

2.2 Milestones

Four milestones were defined for the program and are summarized here:

Milestone No.	Objective	Result
1	Advanced Core Engine Configuration Review	Completed on schedule May 1993
2	Advanced Engine Systems Configuration Review	Completed on schedule August 1993
3	Completion of Advanced Engine Fabrication and Installation	Completed February 1994 (2 wks late vs January 1994 target)
4	Advanced Engine Testing Complete	Completed September 1994 (vs July 1994 target, extension of testing coordinated with NASA

ROTARY POWER INTERNATIONAL, INC.
NASA Contract NAS3 - 26920
Two Rotor Stratified Charge Rotary Engine
(SCRE) Engine System Technology Evaluation

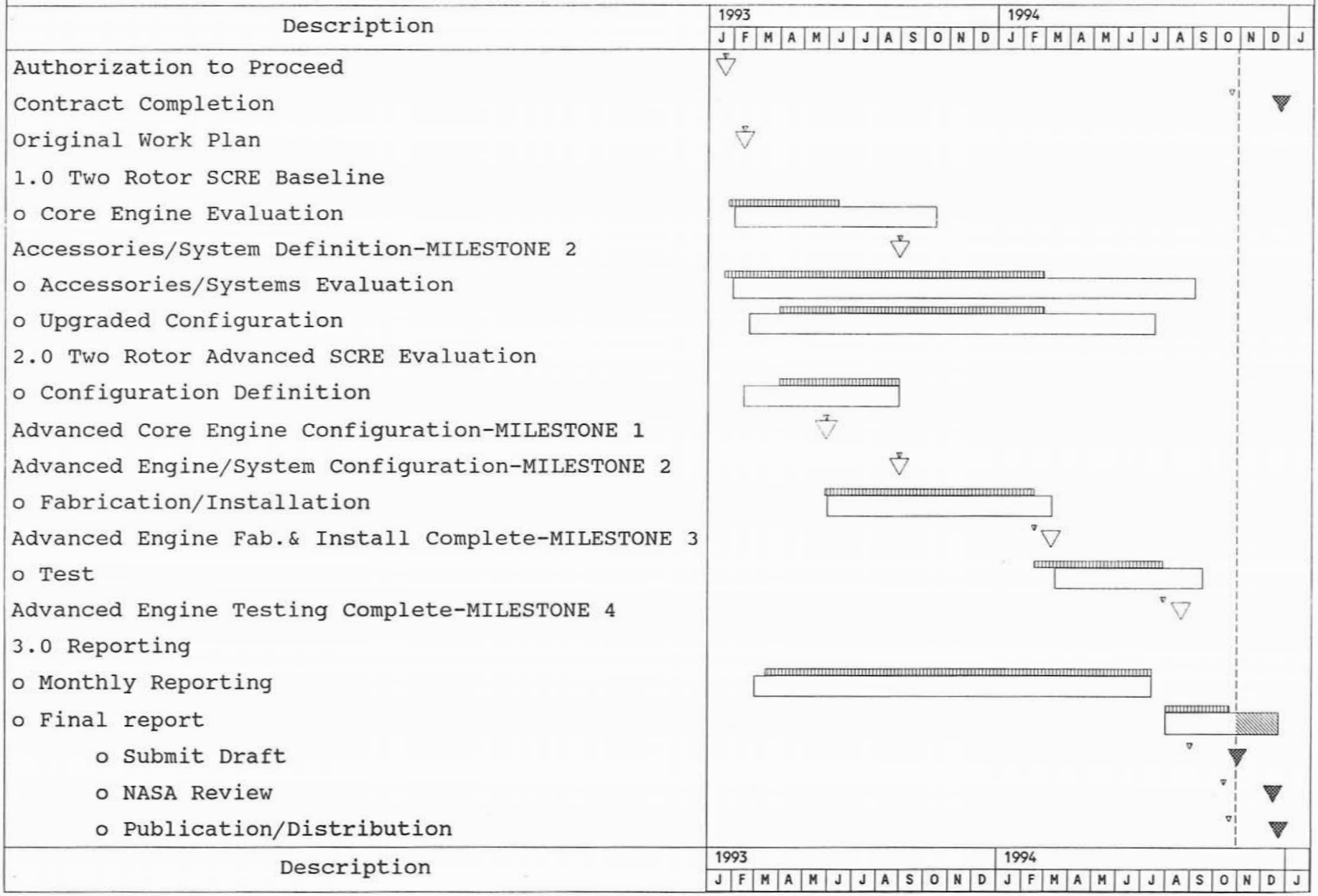

2.3 GENERAL BACKGROUND

Early studies directed by NASA Lewis Research Center (Contract NAS3-21285, Circa 1982) identified the Stratified Charge Rotary Engine as the leading candidate for an advanced, non-aviation gasoline dependent general aviation engine for the mid-1990's and beyond. An industry wide fuels conference conducted by NASA Lewis Research Center at that time noted the ever increasing limitations in the availability of high octane aviation fuels. An engine capable of operating with Jet-A fuel, combined with low cost and high efficiency was deemed necessary. The Stratified Charge Rotary Engine was identified as a candidate meeting those requirements. Three successive phases of technology enablement were conducted prior to the current contractual effort reported herein. These are briefly summarized in this section (Phases I, II and III) for continuity.

Figure No. 2.3-1 depicts the basic operating cycle for the Stratified Charge Rotary Engine, utilizing a pilot injector located in close proximity to a spark plug and a separate main injector.

Figure No. 2.3-2 presents an enlarged view of the basic injection-ignition geometry. The pilot injector provides a small quantify of fuel (less than 5% of the total fuel flow) and maintains a constant volume per stroke. A stoichiometric mixture is created at the spark plug pilot injector region for spark ignitable conditions independent of fuel type. A wide variation in fuel flow as a function of load demand can then be introduced by the main injector into the pilot initiated combustion. This separation of main injector and pilot injector permits optimization of conditions in the light off zone.

Figure No. 2.3-3 presents a general arrangement of a two rotor, Stratified Charge Rotary Aircraft Engine based upon the early NASA studies. This general configuration was used in studies conducted by Cessna and Beech under NASA Lewis Research Center's direction to investigate aircraft performance and operating cost characteristics.

PHASE I CONTRACT

The Phase I Contract NAS3-23056 was conducted during the period of 1983-1985 initially by Curtiss-Wright Corporation (through January 1984) and subsequently by the Rotary Engine Division of John Deere Technologies International, Inc.

During Phase I, a high performance single rotor research rig engine was designed, procured and check-out tested. The research rig engine was designed for 200BHP (150kW) at speeds up to 9600RPM and peak internal pressures of up to 1400psi (9653kPa). Basic performance and multi-fuel operation was demonstrated.

Direct Injected Stratified Charge Combustion Cycle

Note: Events shown for one flank only for clarity. Other two flanks follow same cycle.

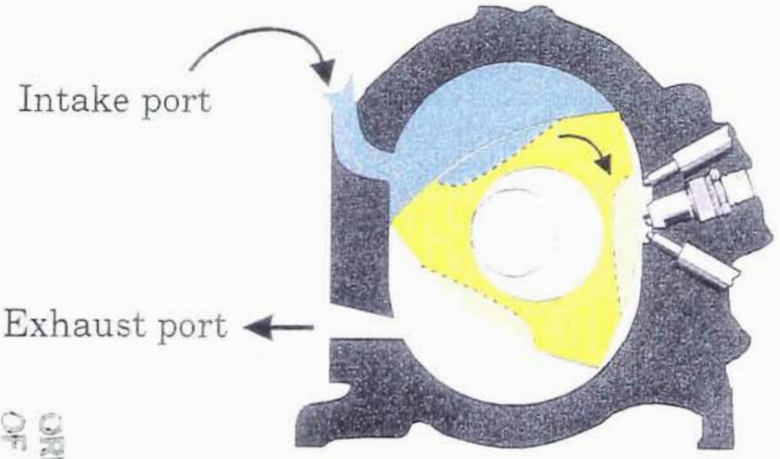

INTAKE

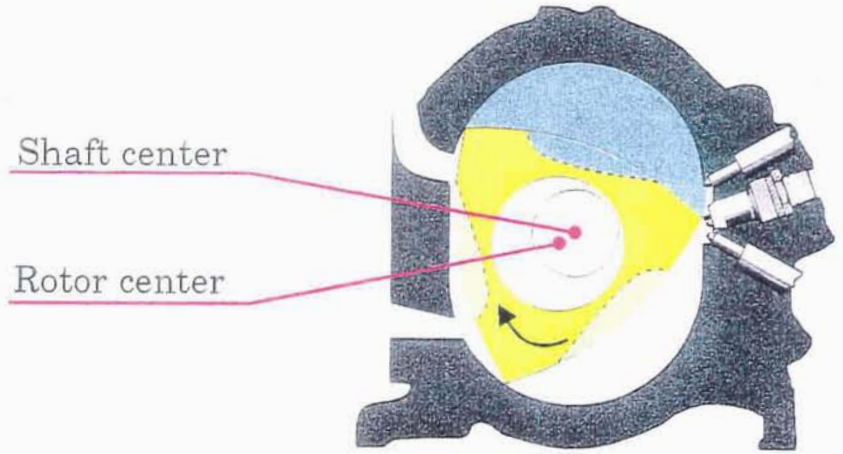

COMPRESSION

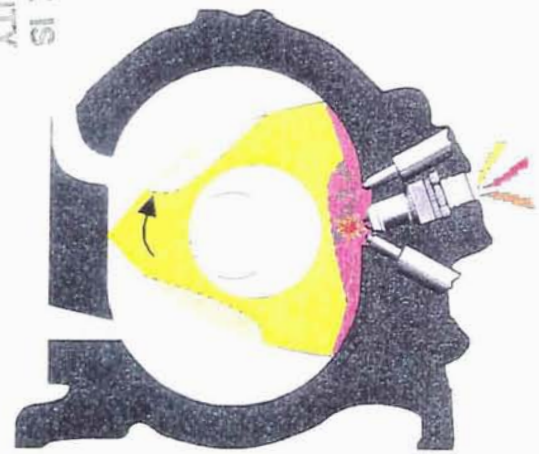

IGNITION

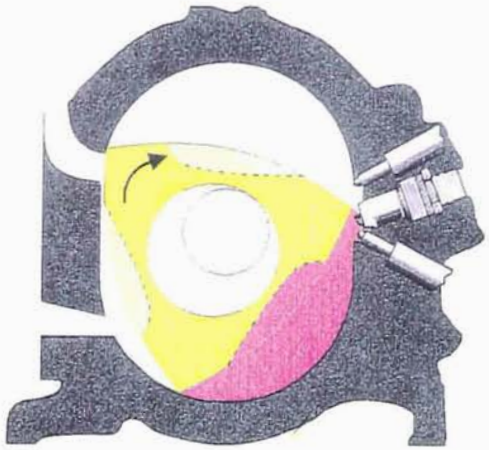

EXPANSION

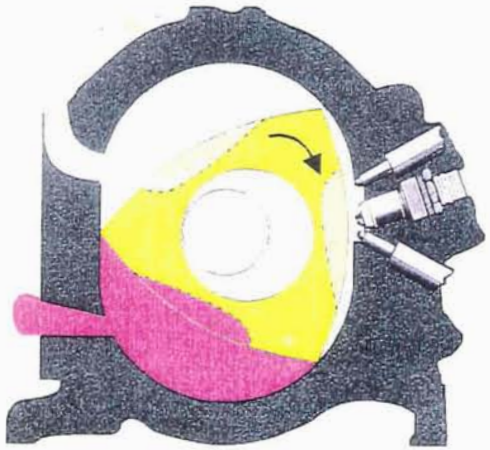

EXHAUST

FIG. 2.3-1

Stratified Charge Ignition System

- Competitive fuel consumption
- Cold starting capability
- Broad operating range
- Independent from Cetane number

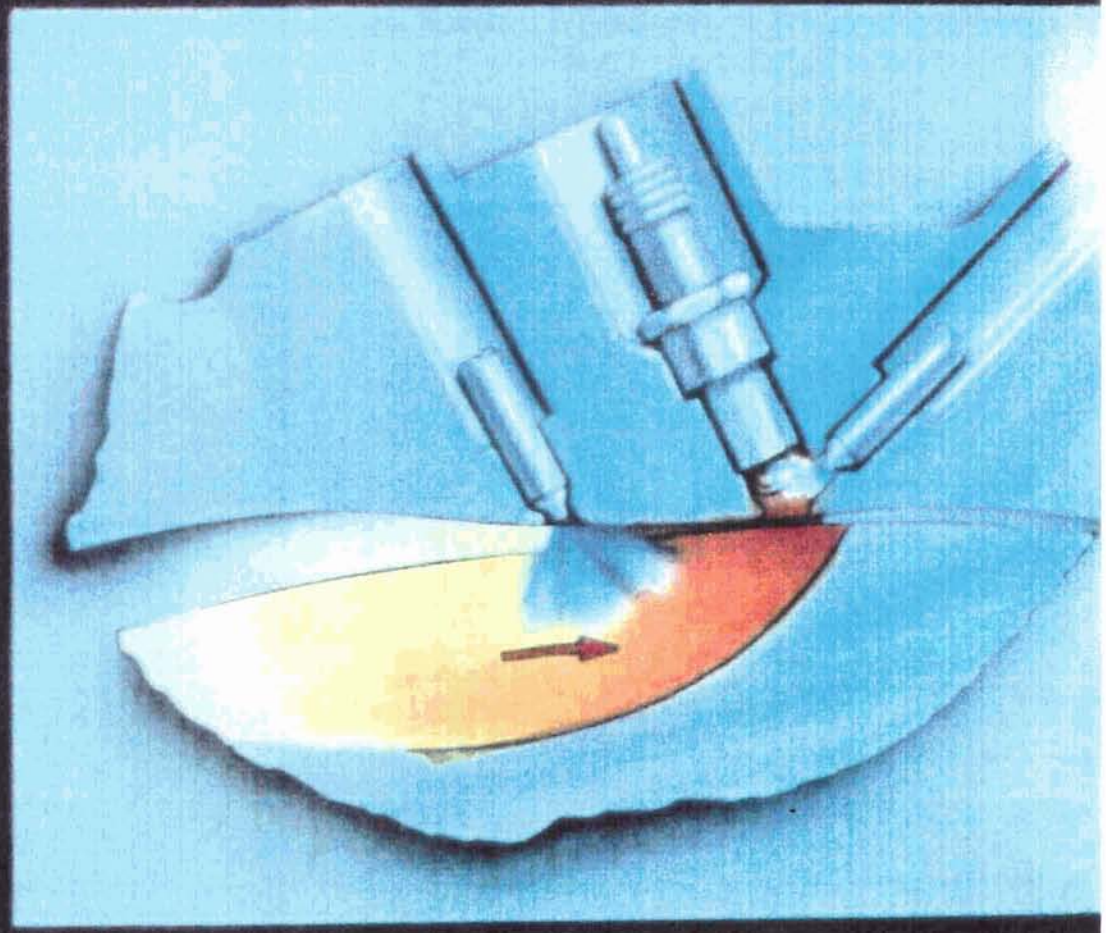

Figure 2.3-2

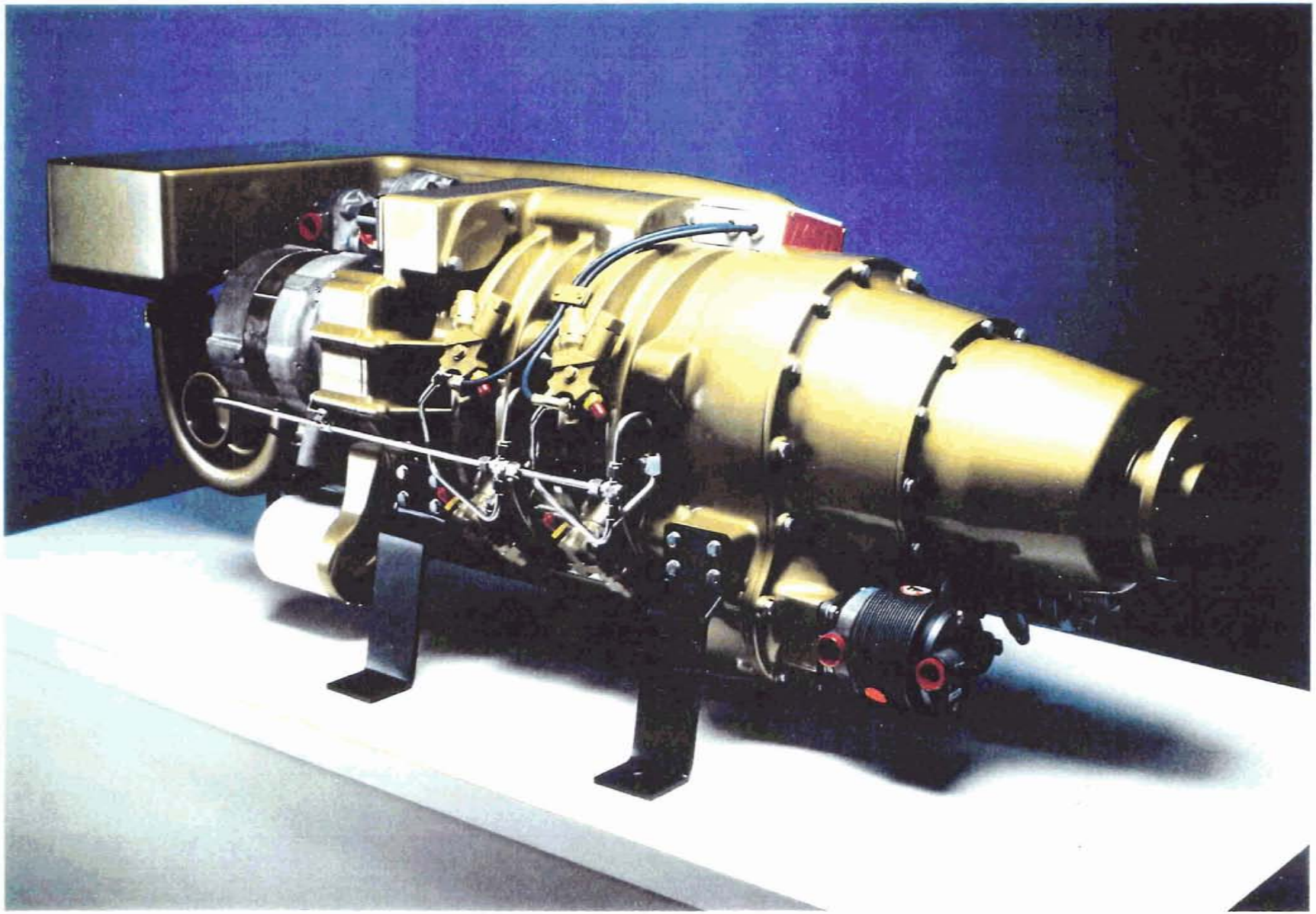

ORIGINAL PAGE IS
OF POOR QUALITY

2013R AVIATION ENGINE
GENERAL ARRANGEMENT

Figure 2.3-3

NASA SCRE CRITICAL TECHNOLOGY ENABLEMENT

MAXIMUM POWER

2013R SCORE 70 ENGINE

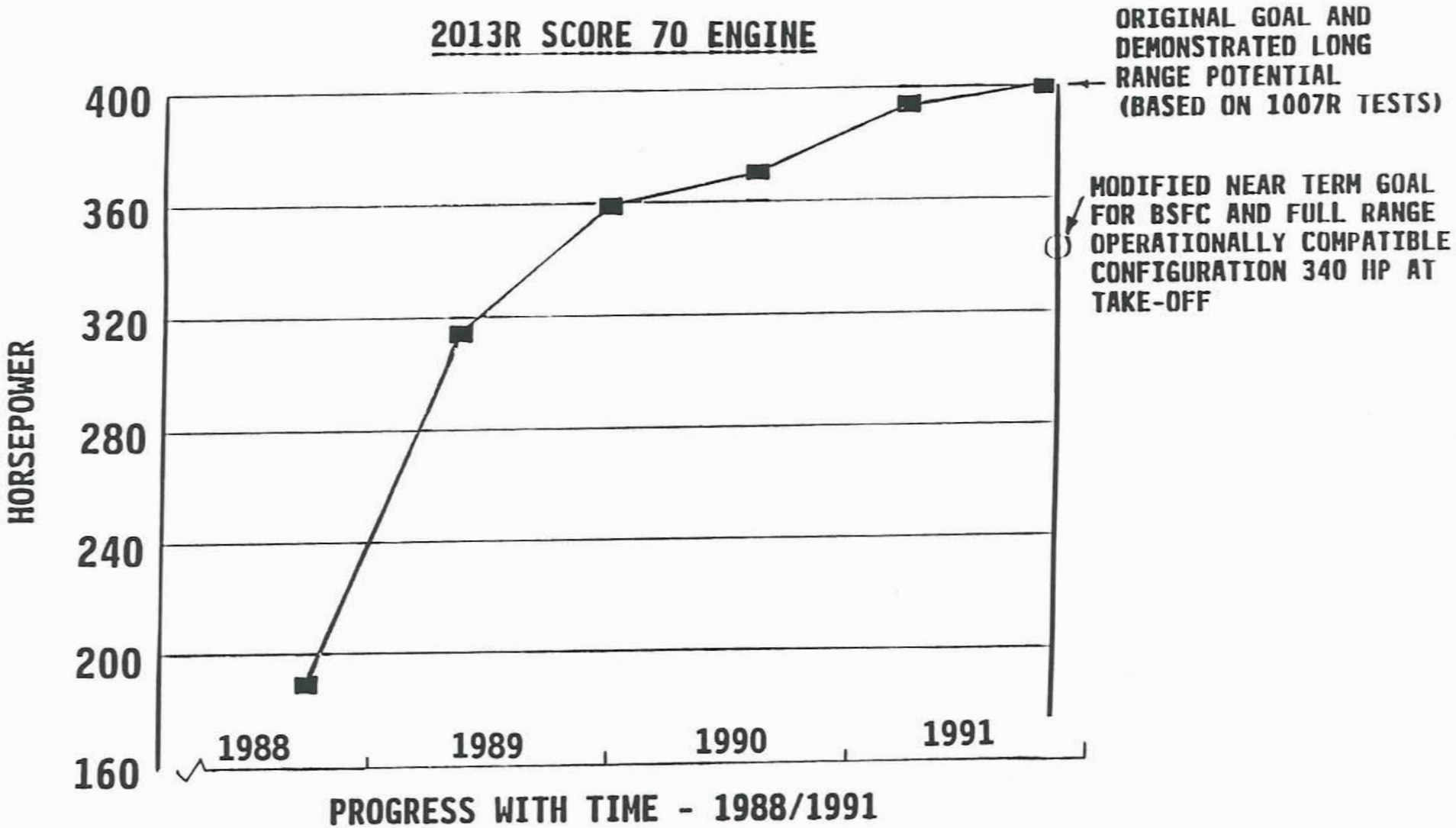

FIG. 2.3-4

NASA SCRE CRITICAL TECHNOLOGY ENABLEMENT

BRAKE SPECIFIC FUEL CONSUMPTION

2013R SCORE 70 ENGINE

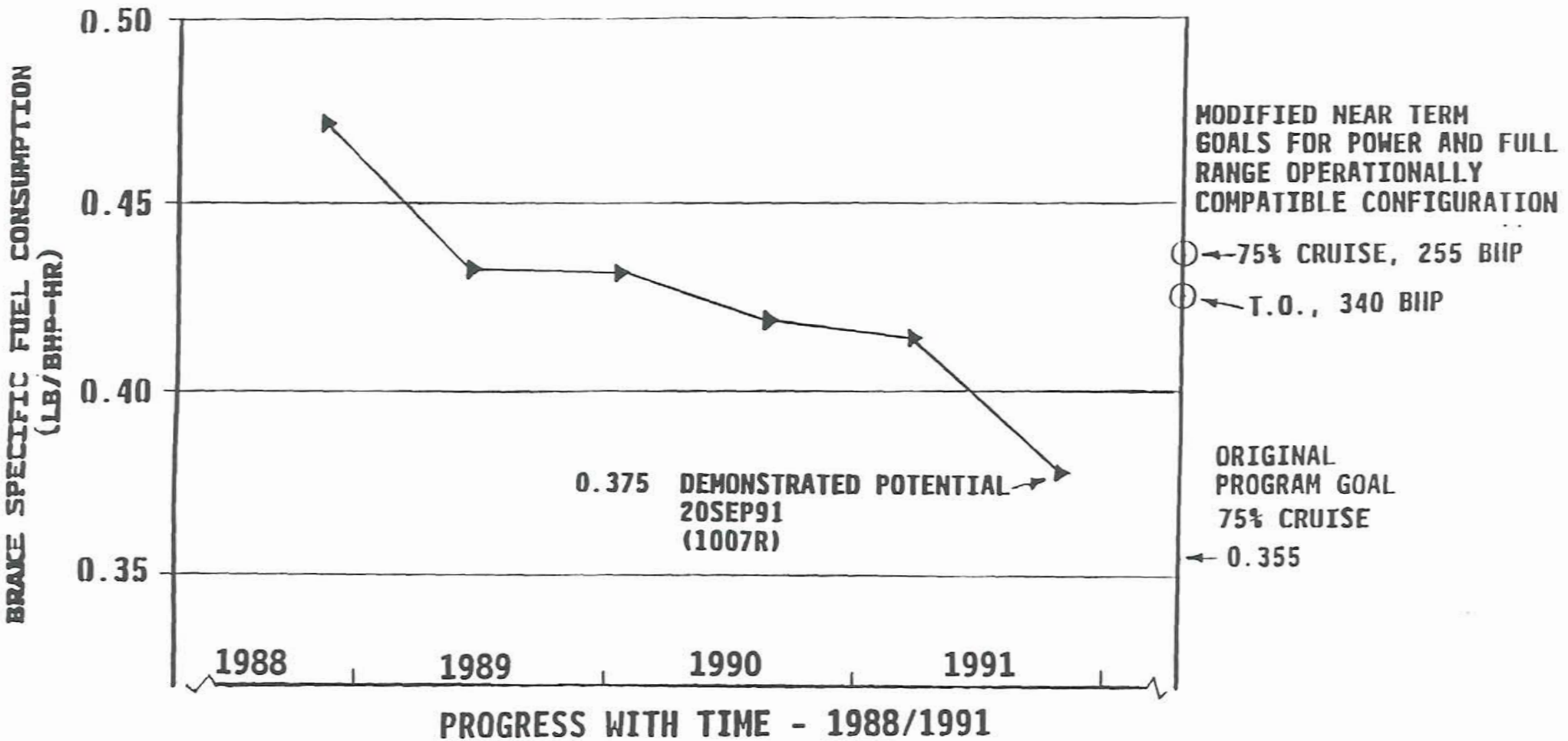

FIG. 2.3-5

PHASE II CONTRACT

The Phase II Contract NAS3-24628 utilized the research rig engine as a vehicle for examining component technologies. An advanced electronically controlled fuel injection system was procured and tested. Power output of 4.3HP/cu.in(194kW/ℓ) was demonstrated exceeding the contract objectives of 4.0HP/cu.in (180kW/ℓ). Subsequently, a revised long range goal of 5HP/cu.in. (230kW/ℓ) was established as an objective. A fuel consumption at cruise of 0.42 Lbs/BHP-HR (256 Grs/Kw-HR) was achieved on Jet-A, diesel and aviation gasoline fuels. During the Phase II effort, Computational Fluid Dynamics (CFD) studies were utilized extensively at John Deere Technologies International, Inc. and at NASA supporting contractors and grantees to guide the improved fuel economy thrust.

During the Phase II effort,discussions between NASA, JDTI, inc. and Naval Air Development Center, Warminster, PA resulted in USN participation in the technology enablement efforts. This activity involved preparation of an engine performance model and design of a twin rotor core power section aimed at 250BHP (188kW) at 66,000 Ft. (20km) altitude.

PHASE III CONTRACT

The Phase III Contract NAS3-25945 addressed critical technology enablement in the areas of advanced, higher speed Computational Fluid Dynamics (CFD) analyses via three-dimensional combustion modeling; airframe mission modeling; design of a reference engine; friction reduction; improved tribology/sealing methods; control system modeling; lightweight/low conductivity parts; catalytic surfaces; advanced fuel injection and an extensive effort to define the turbomachinery system including the consideration of turbo-compounding.

Significant progress was demonstrated in the power density and efficiency regimes during this contract. Figure numbers 2.3-4 and 2.3-5 present maximum power and cruise specific fuel consumption achievements respectively over the course of the program. These tests were conducted with the 1007R single rotor research engine with appropriate correction to the twin rotor, 2013R engine basis. These tests concentrated on investigating power and BSFC capabilities independently , hence no one discrete configuration performed both power and BSFC achievements simultaneously.

CONTRACT NAS3-26920

Contract NAS3-26920 for which this final report is provided integrated a variety of component technologies into a two rotor configuration and conducted a technology evaluation of the two rotor, core aircraft engine system.

3.0 INTRODUCTION AND OUTLINE OF TECHNICAL WORK

3.0 INTRODUCTION AND OUTLINE OF TECHNICAL WORK

3.0.1 Background and Intent. During the several previous NASA-sponsored stratified charge rotary engine programs, various advances to the technology have been conceived and demonstrated using single-rotor laboratory (rig) engines. During the same time period, a two-rotor version of the engine having a lower specific output was developed by RPI and its predecessors for the commercial/industrial market. During the previous program, the two rotor engine design was modified for higher speeds by the addition of an outboard main bearing at the drive end. The appropriate hardware (longer crankshaft, drive end support housing, bearings etc.) were procured and the engine was built and briefly tested.

The ultimate goal is to advance the two rotor engine technology to the point that it offers features and performance superior to that of existing aviation propulsion systems. This is to be accomplished by incorporating the best features demonstrated on the single rotor rig engines. The resulting power plant offers an attractive combination of high specific output and good mission fuel consumption not available in other products.

3.0.2 Summary of Technical Work.

3.0.2.1 Methodology and overall approach. With the goal to demonstrate the Advanced Core Engine maximum power and maximum cruise fuel consumption goals the work began with engineering review of the facts at hand and assessments of the status and capabilities of the design and hardware. The intent was to achieve the goals within limitations, primarily engine speed and maximum combustion pressures, such that reasonable engine life would co-exist with the achievement of the performance goals. As a consequence, pressure limits were set as well as were other target parameters such as intercooled air temperature, coolant and oil temperatures, etc.

Identified at this time were the components expected to require design changes and procurement to enable the required engine performance in terms of both mechanical integrity and engine power and fuel efficiency. The items requiring new effort included the basic engine components of rotor housing and rotor for the purposes respectively of modifying the air inlet and exhaust porting and to raise the compression ratio. With the requirement of new rotor castings and pattern modifications, it was found that an option of rotor material could be obtained and evaluated at little extra cost. Thus rotors were procured of both cast 4140 steel and of cast 17-4PH stainless steel.

Major items external to the engine included the determination of an appropriate turbocharger and alternatives to provide for variations in the likely event that the first match would not be optimum. Another item was the ignition unit: because the prior sources of ignition had expressed that they would be unwilling to provide new units, an alternative source was required. It was established that the inlet and exhaust manifolds available for the two-rotor engine as it presently existed (one unit previously built) were

inappropriate and inadequate for the power levels anticipated, thus new manifolds were designed and procured.

The most ambitious of the accessory systems addressed to was the fuel injection system. Fuel injection systems are typically totally incapable of the speeds required for a high-output rotary engine and tend to become limiting factors. It was decided that a bold approach was appropriate and the development of a high speed electronically controlled unit injector system was commenced. As will be seen, this system was designed, procured and successfully engine tested to the point of proving its viability.

Each of the accessory items is discussed in a section of this report.

A cross section drawing of the Advanced Core Engine is provided as Figure 3.0.2-1.

3.0.2.2 Test Phase. The engine test phase, the largest portion of the contractual effort, was divided into several mutually complementary components.

a. Single Rotor Component Evaluation Engine

Much evaluation was accomplished with the Single-Rotor Component Evaluation Engine, to provide required advanced information for design and parameter choices, to select by trial the optimum porting, to evaluate compression ratios, to act as the vehicle for first evaluation of various components, and for numerous other required actions as is reported in the appropriate section of this report. Four single rotor test engines were built in sequence to accomplish the desired evaluations and select components for two-rotor engine testing to follow.

With the Single Rotor Engine the max cruise fuel efficiency goal was essentially achieved on the basis of conversion to two-rotor engine equivalency. Also with the single-rotor engine the new (HSUI) fuel injection system was made operational prior to installation on the Advanced Engine.

b. Two-Rotor Baseline Engine

Initial two-rotor engine testing was with the Baseline Engine from the previous contract NAS3-25945. Testing of this engine was to provide on the most immediate basis information at higher rotational speeds than previous run with the two-rotor, total engine (with accessories and drives, etc.) while designing and procuring the advanced components. Three Baseline engines were tested in series beginning with the one built and briefly tested in the prior program.

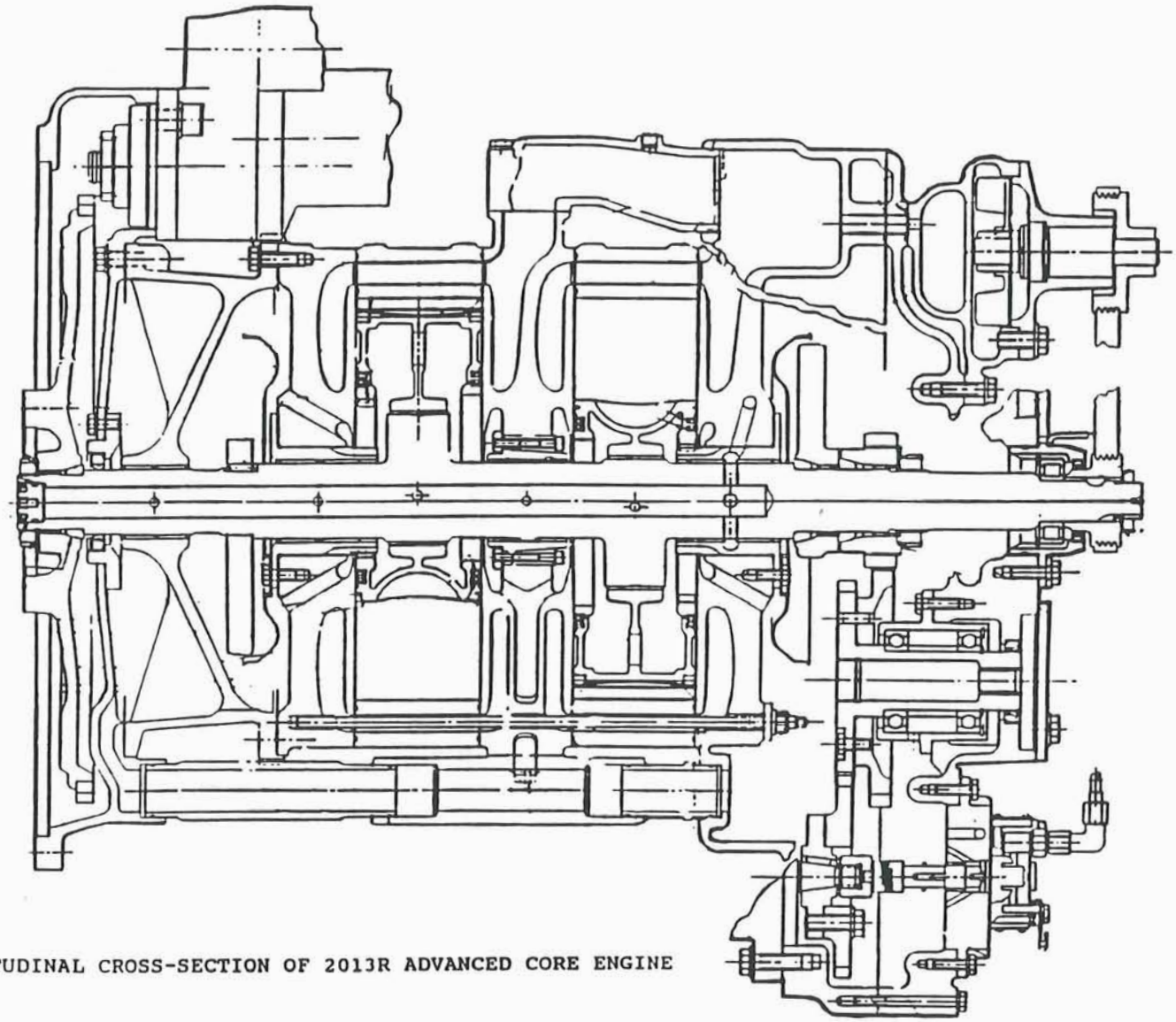

LONGITUDINAL CROSS-SECTION OF 2013R ADVANCED CORE ENGINE

Figure 3.0.2-1

c. Upgraded Two-Rotor Baseline Engine

As Planned, the Baseline Engine was upgraded to allow continuation of the test to higher power and to introduce new components as they became available. Two builds of the upgraded engine were tested. During the Baseline and Upgraded Baseline testing, several, mostly unexpected, mechanical difficulties were identified either as failures or by observation of the tested hardware. As a result, significant effort was expended in achieving mechanical operation up to the rated speed and power. Several improvements were introduced and evaluated during this contractual period. The majority of these are considered to be very satisfactorily resolved while one or two are identified as concerns for further improvement. These items are all discussed in following sections of this report.

d. Advanced Core Engine

The final phase was the demonstration of the Advanced Core Engine. This basic "core" engine did not include specific application equipment such as the propeller drive. Four Advanced Core engines were built in series. The take-off rating of 340 BHP (254 kW) at 8000 RPM was demonstrated. Also, operation and performance at the maximum cruise condition of 255 BHP (190 kW) at 7000 RPM was demonstrated. Details are provided in following sections.

In total it is considered that through these test phases, the new components were proven, the great majority of the mechanical difficulties encountered were effectively corrected, and the capability of the engine was demonstrated.

The multiple facets of this effort are diagrammed in Figure 3.0.2-2 which charts the activities just discussed and indicates the inter-relationships.

3.0.2.3 Accomplishments in Brief

Goals and Milestones were achieved:

* The Advanced Core Engine was defined, procured, built and tested.
* Rated take-off power was demonstrated.
* Maximum Cruise condition was repeatedly achieved although the fuel efficiency goal, basically demonstrated with the single rotor test engine, was not achieved with the two-rotor engine.
* Several mechanical problems identified were corrected.
* A new fuel injection system capable of high engine speed and control functions was defined and demonstrated.
* Capability and feasibility of the basic core engine for aircraft application was established.
* Technical data was obtained, which provided a basis for enabling further improvements.

Two Rotor Stratified Charge Rotary Engine (SCRE) Engine System Technology Evaluation

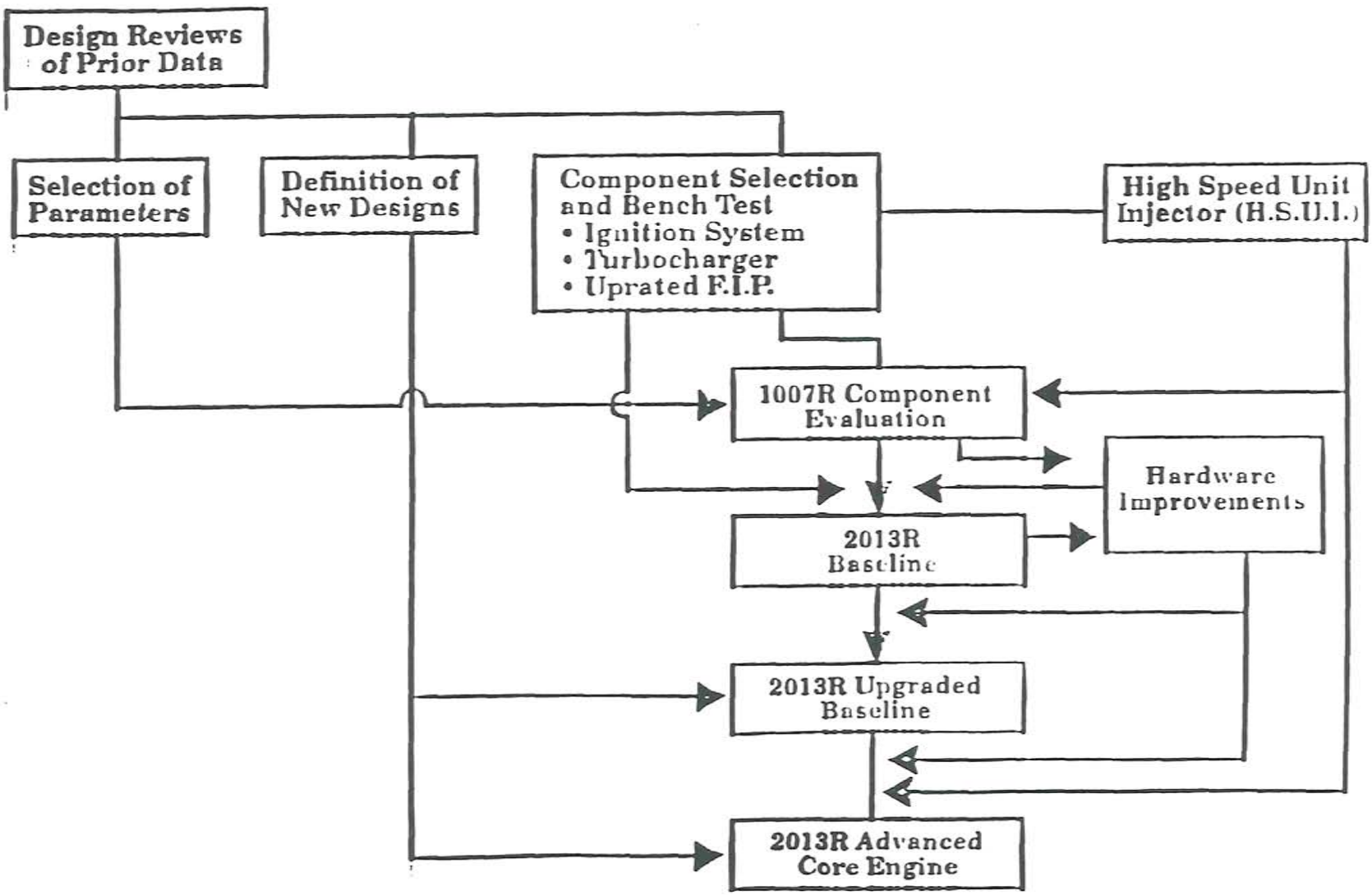

Figure 3.0.2-2

3.1 - BASELINE ENGINE

3.1.1 Introduction. The goal of this contract was to advance the technology of the engine such that a takeoff rating of 340 HP (254 kW) and a specific fuel consumption of 0.435 lb/hp-hr (265 g/kW-hr) at the 75% maximum cruise rating can be demonstrated. The starting point is the Baseline Engine which refers to a variation of a commercial/industrial two rotor engine with a rating of 200 HP (149 kW) at 6000 rpm. This effort draws upon technology advances demonstrated using the single rotor laboratory engines of the current and previous NASA programs.

For this program, a series of two rotor engine tests was planned. The first of these was to evaluate the baseline engine at the commercial/industrial rating and then proceed to higher speeds and loads. Information obtained during the baseline test was used to guide changes to the configuration such that the output and fuel consumption would be improved. Certain of these improvements, as allowed by hardware availability, were incorporated into the upgraded baseline engine. This upgraded configuration was then also performance tested. The results of both baseline tests were used to determine the configuration of the Advanced Engine, which is reported in a later section.

3.1.2 Engine Configuration. The baseline NASA 2013R is a two rotor, stratified charge rotary combustion engine utilizing the four stroke cycle. It is liquid cooled and has a dry sump lubrication system. This engine is more specifically defined by the bill of materials NR10250 and engine basic drawing LS34190.

The power section consists of two 7.5:1 compression ratio rotors, two rotor housings, two end housings, an intermediate housing, a crankshaft and the appropriate seals, bearings and hardware. The drive end incorporates an additional outboard support bearing for increased speed capability.

The fuel system consists of a fuel injection pump assembly, main and pilot fuel injection nozzles, high pressure lines, return lines and a filter. Other accessories include a Mitsubishi TD08H-23K-33 cm^2 turbocharger and a glow ignition system consisting of two NGK CZ02 glow plugs, two adapter bushings and control unit. Near the conclusion of the baseline test, the engine was changed to spark ignition.

The coolant and lube systems consist of engine-driven pumps which circulate the fluids within the engine and to the external systems. The heat exchangers, filters and sumps are part of the test cell equipment.

3.1.3 Purpose of Test. This test was planned to evaluate the baseline engine as defined, procured, assembled and briefly tested during the previous program. This engine lacked many of the advanced features tested previously on the single rotor rig engine. Those features deemed necessary to meet the performance goals were introduced later in the program as the hardware became available.

The baseline test plan included four distinct phases. The first phase was a test cell shakedown since the cell had been inactive for twelve months and was last configured for a single rotor rig engine. The second phase was a baseline performance test using the engine configured as it was at the end of the previous program. It was anticipated that the fuel injection system will not be able to deliver sufficient fuel to achieve the performance goals. To address this shortcoming, the third phase was planned to map the engine with an upgrade to the fuel injection pump. Also upgrades to the charge air system were evaluated during subsequen tests.

3.1.4 Testing Performed. The test cell preparation included installation of the proper engine mounting structure, cleaning and servicing of the various fluid systems, servicing of the dynamometer and related systems and calibration of all instrumentation.

During the first start attempt the engine overshot the 8000 rpm limit to approximately 8400 rpm due to the combination of slow dynamometer response, manual fuel control and improper overspeed protection. Damage was limited to the fuel injection pump which seized a main plunger. The pump was rebuilt and the engine operated at moderate speeds and loads to verify systems operation. Corrections to the instrumentation, control and engine support systems were made as required including the overspeed shutdown modes. The fuel injection timing appeared to be too advanced and was retarded prior to the baseline mapping test.

At approximately ten hours into the test, the baseline engine performance mapping began. The engine was operated at 4000, 5000, 6000, 6500, 7000 and 7200 rpm and at various loads up to 179 psi (12.3 bar) brake mean effective pressure (BMEP). To maintain fuel injector line pressures below 10000 psi (700 bar), the original main nozzles were replaced with tips having the same 6 hole, "A" pattern but with 0.010" orifices rather than 0.008". The engine was again mapped over a range of speeds and loads.

Just after operating the engine at 7000 rpm, 162 psi (11.2 bar) BMEP, 231 HP (172 Kw), the drive end support bearing failed. In addition to the failure of this bearing, several other failures were noted upon engine disassembly: drive end rotor gear, loose drive end rotor gear attachment screws, broken center main bearing bolts and rotation of both rotor bearings. Corrective actions were defined and implemented for each of these items. These are described in further detail in Section 3.2.5. Engine total test time was 28:05 hours in addition to the approximately 10 hours accumulated during the previous program.

Further Testing. The engine was rebuilt and it designation changed to 65201-2. The original intake manifold "Y" was replaced with a larger diameter design, refer to Figure 3.1.4-1. The engine was operated at speeds from 4000 to 7000 rpm at low and moderate loads. The combustion pressure traces showed rates of rise and peak pressures which were higher than expected. This was especially the case when the fuel rack was increased above 75% at which point the main injection timing jumped (advanced) approximately 10° crankangle. This resulted in extremely high combustion pressures, on the order of 1900 psi (131 bar), followed by a condition referred to as "fall-off". The indications of fall-off are higher frequency pressure waves in the intake manifold (audible noise in this instance), a loss of airflow and a loss of power. The generally-accepted mechanism is that the trailing apex seal lifts from the trochoid surface and hot gas from the higher pressure combustion zone

ORIGINAL CONFIGURATION

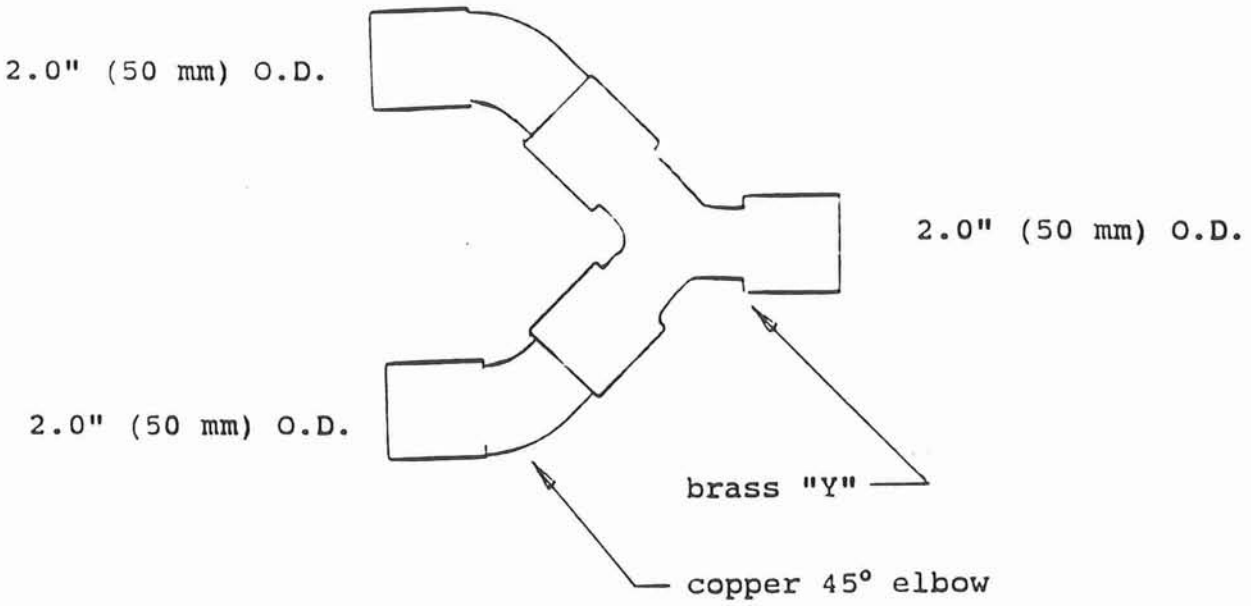

IMPROVED CONFIGURATION

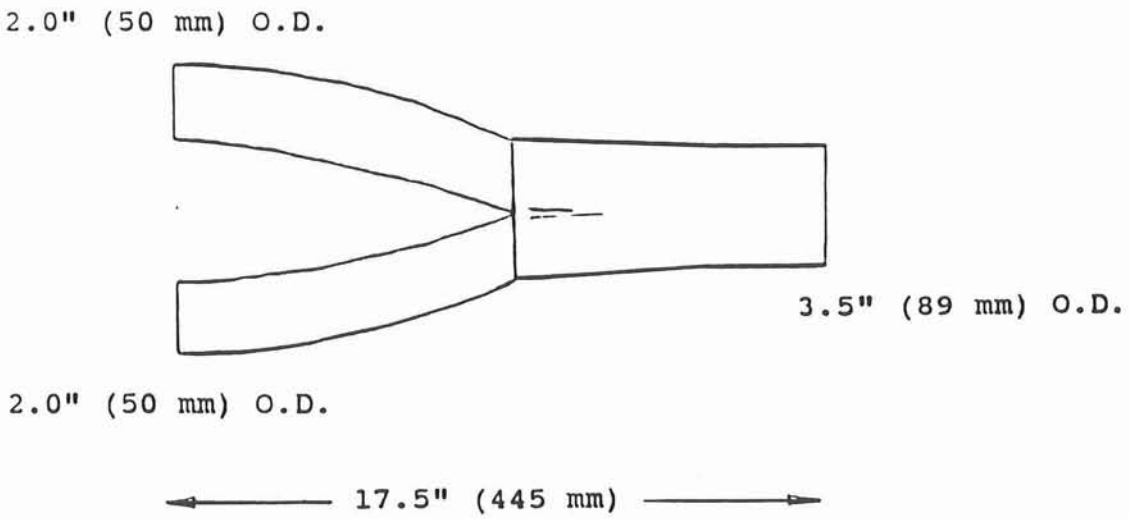

Figure 3.1.4-1 Intake Manifold Configurations - Baseline Engines

transfers into the compression zone. The gas passing over the apex seal increases the seal temperature and likely removes any lubricant leading to accelerated seal wear. Fall-off was encountered several times and is believed responsible for the flatting of the ADE apex seals. The engine was removed from test rather than risk severe damage of major components should the apex seals fail catastrophically. Total engine test time for this rebuild was 16:45 hours.

The engine was rebuilt with new apex seals and its designation changed to 65201-3. The fuel injection pump was tested on the pump rig and adjusted to eliminate the timing jump and to correct the main-to-pilot timing. The pump was advanced slightly and the engine mapped at 5000, 6000 and 7000 rpm. Maximum power achieved was limited to 201 HP (150 kW) due to peak combustion pressures approaching the 1420 psi (98 bar) limit and an engine air inlet temperature exceeding the 140°F (60°C) limit.

The combustion pressure limit of 1420 psi was established to ensure rotor housing life on the order of hundreds of hours at the cruise condition. This pressure limit is increased to 1750 psi (120 bar) for the takeoff condition since a reduced rotor housing life is acceptable given the reduced time the engine will operate at that condition. The air inlet temperature limit is somewhat arbitrary and was chosen midway between the 110°F (43°C) typical of our experience base and 170°F (77°C) which is generally accepted as the point above which power loss is expected.

The glow plug ignition system was replaced with a spark ignition system. The engine was again mapped at 5000, 6000 and 7000 rpm. The change to spark ignition resulted in improved fuel consumption, engine starting and quality of combustion pressure trace. Similar to the previous testing, the maximum power achieved was limited to 213 HP (159 Kw), 7000 rpm, 149 psi (10.3 bar) BMEP. In this case the limiting factors were observed combustion pressure peaks as high as 1450 psi (100 bar) and air inlet temperatures as high as 151°F (66°C).

While operating at 7000 rpm, the spark ignition system was observed to be firing only every other revolution. While this did not result in noticeable combustion variation, it did signal that some component of the ignition system was beyond its capacity. To remedy the situation, the spark duration was reduced. While warming-up the engine to verify this change, the gear mesh at the engine's drive end rotor failed. Disassembly revealed that the rotor gear and the stationary gear had failed. A small portion (5mm x 10mm) of the anti-drive end rotor bearing liner had de-laminated from the shell. Total engine test time for this rebuild was 15:00 hours.

3.1.5 Performance of Baseline Engine. The engine as originally configured produced results as shown in the table below:

Run	Speed	Power	BMEP	BSFC	PFP	Inlet Air
	rpm	BHP (kW)	psi (bar)	lb/hp-hr (g/kW-hr)	psi (bar)	°F (°C)
34	6000	199 (148)	162 (11.2)	.457 (278)	1200 (82.7)	112 (44)
35	6000	217 (162)	177 (12.2)	.461 (280)	1400 (96.5)	119 (48)
43	6500	224 (167)	169 (11.7)	.481 (293)	1200 (82.7)	122 (50)
44	7000	223 (166)	156 (10.8)	.516 (314)	1000 (68.9)	127 (53)
SF*	6000	200 (149)	163 (11.2)	.45 (274)	N/A (N/A)	121 (49)

*The SF refers to the maximum power achieved during the previous program on the SuperFlow dynamometer (this program used a different test stand, identified as TC20-5, for all two rotor engine testing). This is the power rating of the engine as developed for commercial/industrial applications.

At this point, it was concluded that the engine was performing as anticipated. As originally configured, the baseline engine was output-limited by the fuel injection system as was expected. If the fuel rack was increased further, the engine would lose power as the fuel pump went into the start-retard mode.

Effects of Increased Main Nozzle Orifice Area. The maximum flow rate of a fuel injection system is limited, to a certain extent, by the orifice area of the main injectors. This is particularly true if there is a pressure limitation as is the case here. To determine if significant improvement was available through increased nozzle orifice area, the original 6 hole x 0.008" main nozzles were replaced with 6 x 0.010" nozzles of the same spray pattern. For comparison with the baseline data presented in the table above, the performance with the larger main nozzles was as follows:

Run	Speed	Power	BMEP	BSFC	PFP	Inlet Air
	rpm	BHP (kW)	psi (bar)	lb/hp-hr (g/kW-hr)	psi (bar)	°F (°C)
56	6000	217 (162)	177 (12.2)	.459 (279)	1600 (110.3)	N/A (N/A)
59	7000	231 (172)	162 (11.2)	.526 (320)	1400 (96.5)	147 (64)

Comparison of the data of the two tables reveals substantially higher peak firing pressure but similar fuel consumption. What is not shown in the tables is that the larger main nozzle

affected the injection timings. At the 6000 rpm point shown above, the start of main injection was advanced 5° and the duration was reduced 4° crankangle. Oddly, the pilot injection advanced a similar amount. In general, advancing timing will increase the peak firing pressure; however, it cannot be determined whether this alone is responsible for the full amount of the increase or whether the increase is due in part to the higher injection rate which results from the larger orifice area.

Effects of Larger Intake Manifold. The original manifold "Y" section had a 1.63" (41.4 mm) ID inlet and two outlets of the same size. This restriction resulted in high pressures in the charge air system upstream of the "Y". In particular, the compressor outlet pressure was 52.7 in-Hg at the 7000 rpm 231 BHP (172 kW) condition shown in the table above. It was anticipated that a lower restriction manifold would be beneficial because it would allow operation at a more efficient point on the compressor map.

A larger "Y" section was fabricated having a 3.5" (89 mm) inlet and 2" (50 mm) outlets. The transition is smoother with a substantially smaller included angle. All testing after the first build was accomplished with this larger "Y". The most appropriate means to examine the effect of this change is through volumetric efficiency. To generate the plots presented in Figure 3.1.5-1, the volumetric efficiency was calculated using the engine inlet (or more precisely the intercooler outlet) conditions. The table below summarizes the data of the three plots as well as an additional 6500 rpm data point.

Engine Speed	Volumetric Efficiency	
(rpm)	Original "Y"	Larger "Y"
5000	102 - 107%	114 - 124%
6000	103 - 105%	105 - 127%
6500	102 - 104%	116 - 122%
7000	96 - 107%	106 - 110%

In general, the larger "Y" section resulted in significant volumetric efficiency gains, especially at speeds below 7000 rpm. Also, it can be inferred from these data that the volumetric efficiency is more sensitive to speed than load.

Effects of Spark Ignition. The poor combustion pressure traces were believed to be due, at least in part, to the glow ignition carried over from the commercial engine. While this had been adequate at the lower speeds and loads of that engine, all of the testing to date on the single rotor rig engines have utilized spark ignition. During the second rebuild it was determined that these particular rotor housings were unique in that the required spark location could be achieved with available 14mm long reach spark plugs. This however also raises some concern that the glow plugs were installed "too deep" in the housing and were restricting flow in and out of the pilot cavity.

The switch to spark ignition resulted in measurable decrease in specific fuel consumption as can be seen in Figures 3.1.5-2 through 3.1.5-4. The observed improvement was as much as 4%.

Fuel Metering System Calibration. A post-test calibration of the fuel flow measurement system, performed after testing of the third build, revealed an offset of +5 lb/hr (2.3 kg/hr). The previous calibration was performed prior to testing of the second build. It cannot be determined when the change occurred.

For this reason, some portion of the specific fuel consumption values for the second and third build may be conservative. Therefore fuel consumption values of the second and third builds should not be compared with that of the first build. The data shown in the tables above is from the first build and as such is known to be accurate insofar as the pre- and post-test fuel flow calibrations were accurate. While the data shown in the comparison of glow and spark ignition may not be correct in an absolute sense, the trend is correct. If the offset occurred during the transition from glow to spark ignition, the magnitude of the resulting improvement would be significantly higher. It seems unlikely that this would be the case since all of the data used for the comparison was taken over a two day period.

3.1.6 Engine Failures. As mentioned in previous sections, a number of engine failures occurred during this testing. For the purpose of this report, the failures of the baseline and upgraded baseline are grouped together and discussed along with remedial action and progress in section 3.2.5.

3.2 - UPGRADED BASELINE ENGINE

3.2.1 Introduction. The intent of this effort was to introduce advanced components for evaluation as the hardware became available. Several improvements were made to the engine in a continued effort to advance the engine towards the program performance goals. Also, several failure modes were identified during the earlier baseline evaluation phase of this contract. Various hardware improvements were introduced during that phase which were monitored during this phase as well as were further improvements introduced during this Upgraded Baseline Engine phase.

The previous testing identified fuel system capacity, intercooler capacity and peak combustion pressure as the items limiting engine performance. Further detail may be found in section 3.1 and the "Baseline Engine Test Report" dated 08 November 1993.

The primary means selected for increasing engine output and reducing peak combustion pressure is to increase air flow by enlarging the intake and exhaust ports. Secondary improvements might be gained through selection of main nozzle spray pattern and turbocharger. Changing the port features to those required for the desired performance level could only be achieved by manufacturing new rotor housings. The lead time for new housings is such that they could not be incorporated into the Upgraded Baseline Engine as was originally planned. For this reason, the engine output was not expected to increase much beyond that demonstrated during the earlier testing since the engine would continue to be combustion-pressure-limited.

The upgraded baseline test was re-planned to gain experience at the rated speed of 8000 rpm and then assess improvements to the other limitations by evaluating an up-rated fuel injection pump and larger intercooler. Additional detail for the upgraded baseline engine may be found in the "Test Report: Upgraded Baseline Engine" dated 01 September 1994.

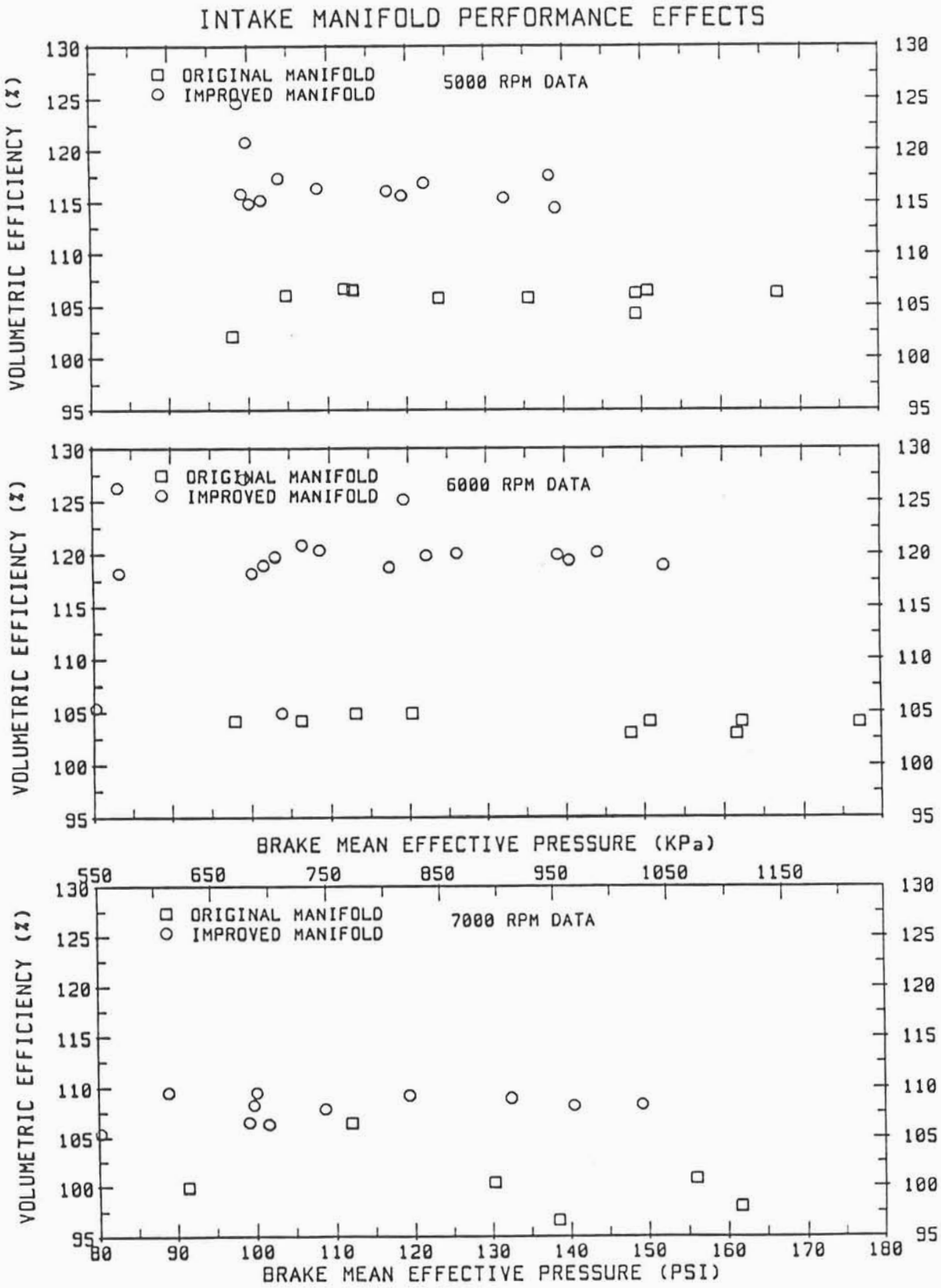

Figure 3.1.5-1 **Volumetric Efficiency Performance of Intake Manifold Configurations**

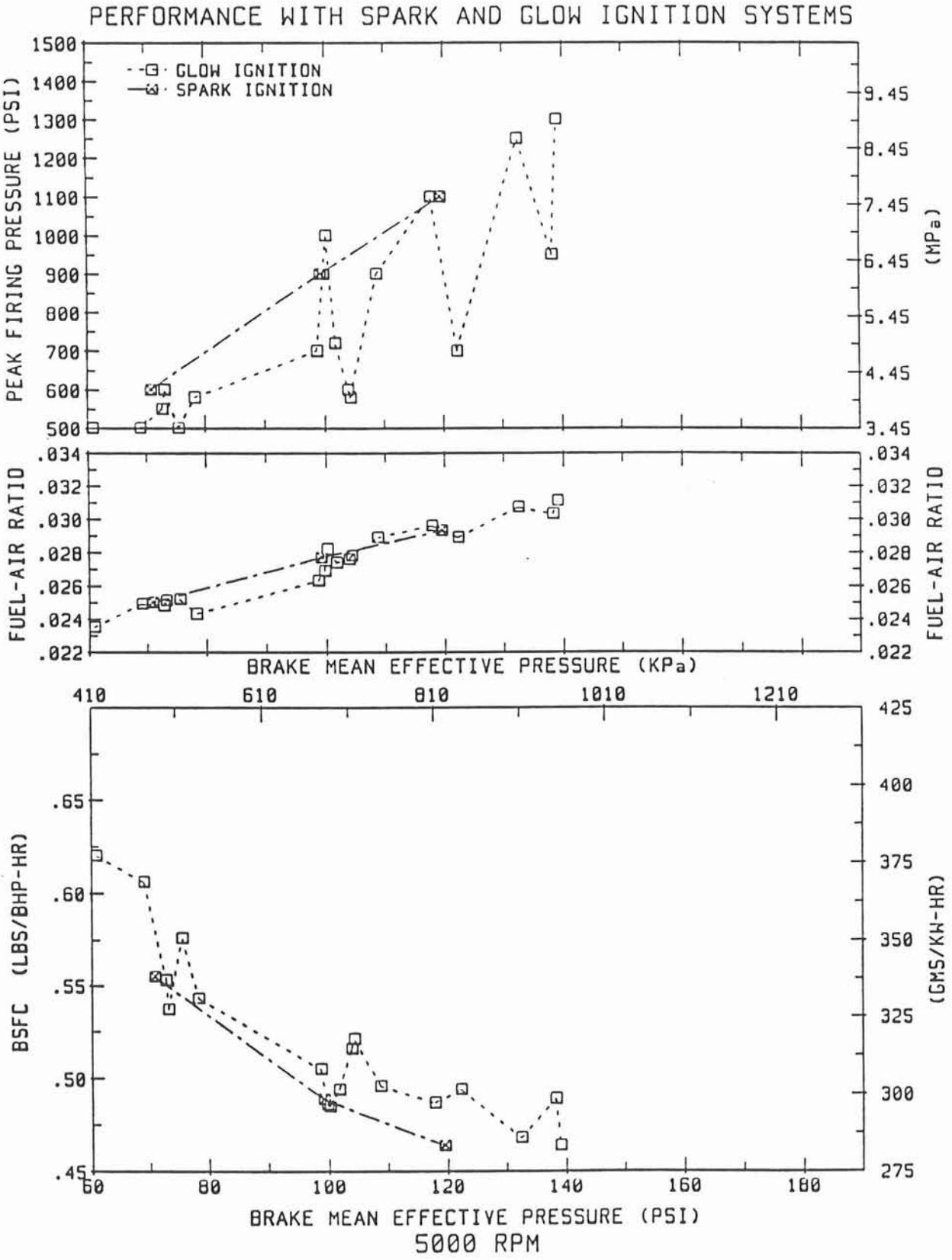

Figure 3.1.5-2 Performance Comparison of Ignition Systems (5000 rpm)

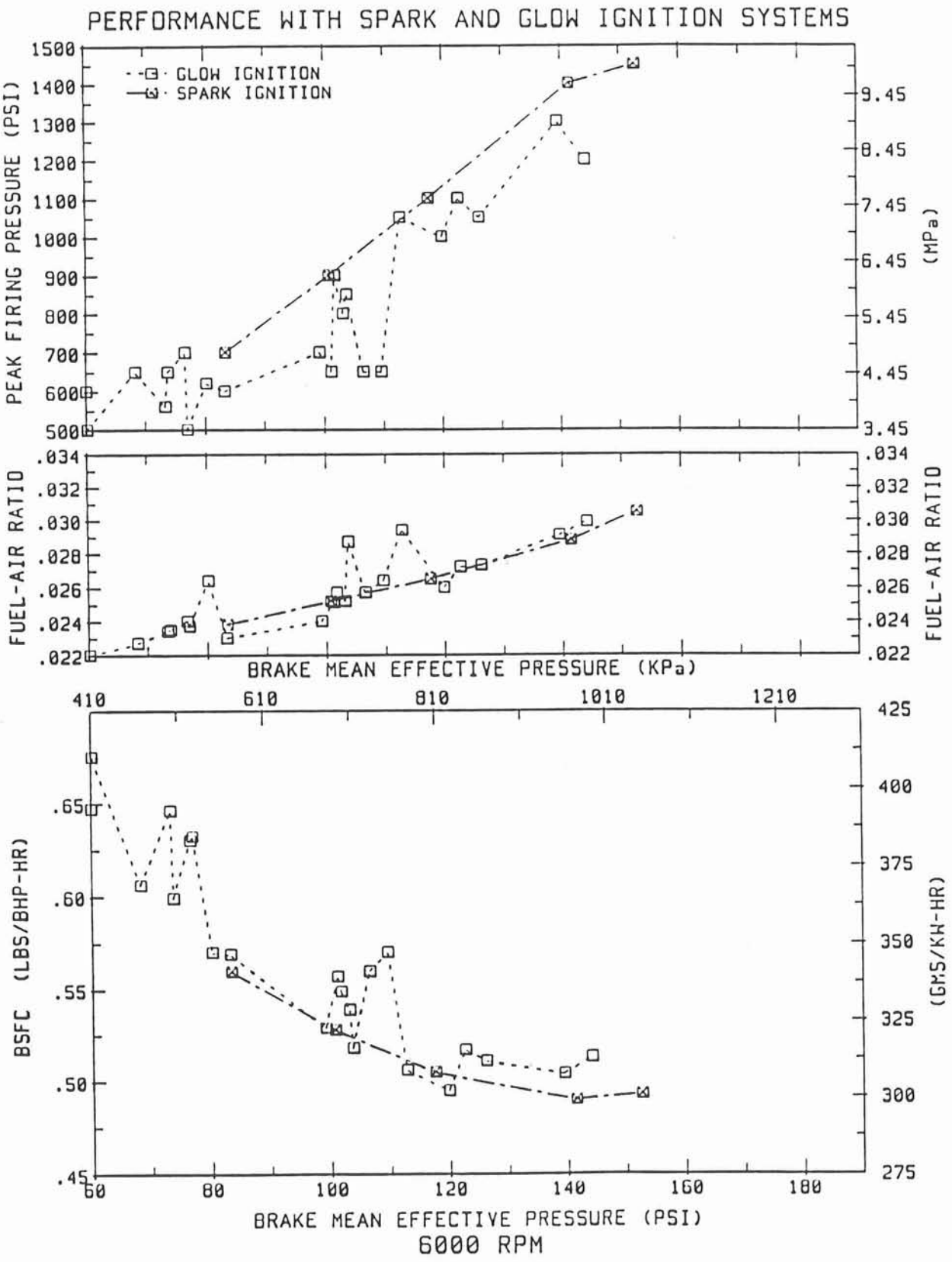

Figure 3.1.5-3 Performance Comparison of Ignition Systems (6000 rpm)

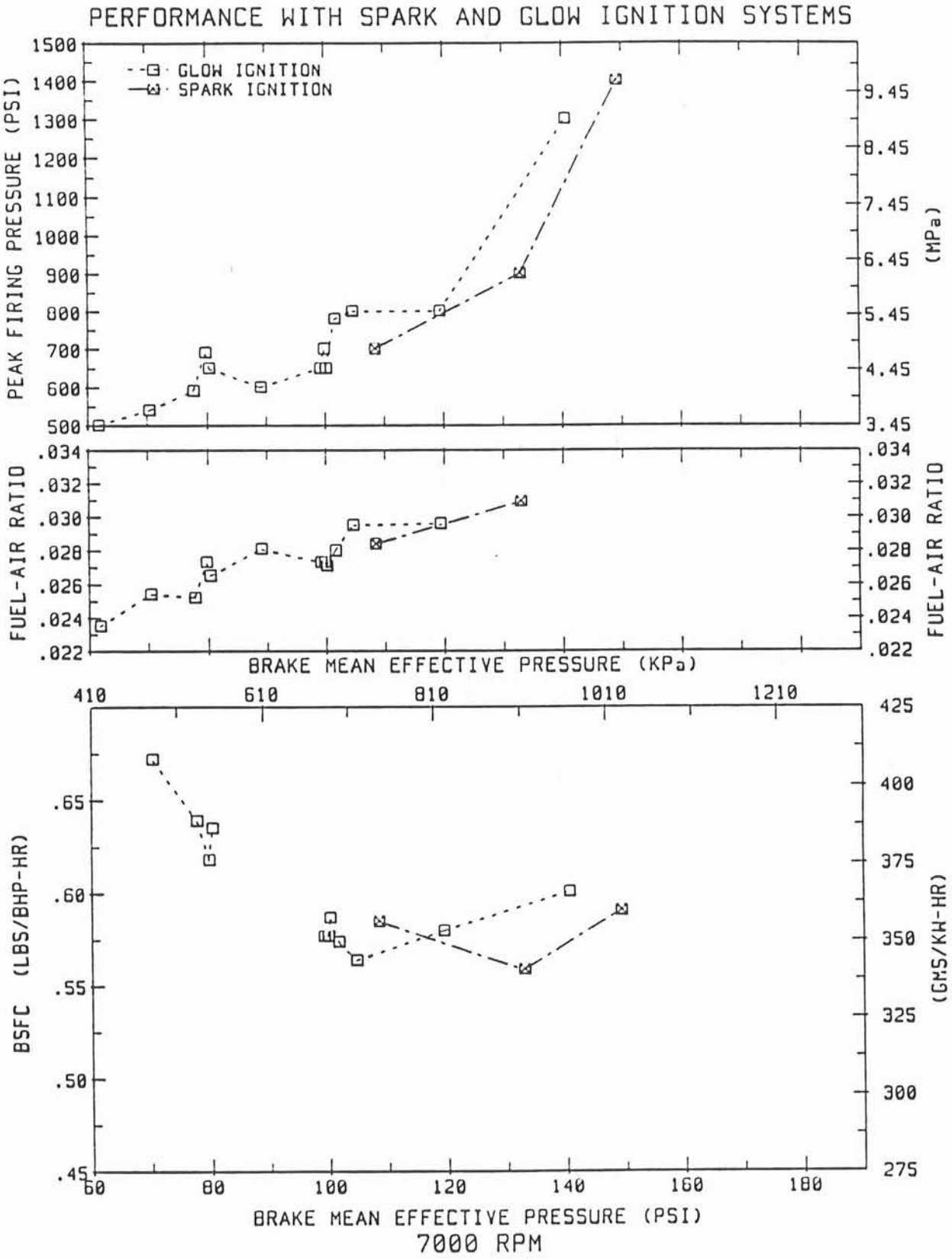

Figure 3.1.5-4 Performance Comparison of Ignition Systems (7000 rpm)

3.2.2 Engine Configuration. Due to the hardware availability problems mentioned above, the upgraded baseline engine was essentially equivalent to the baseline configuration with the following changes introduced during the course of this testing:

Reworked Rotor Gears. To address the two failures of the drive end rotor gear during the baseline test, the rotor gears were reworked to improve the safety factor and material properties of the mounting lug regions of the gear. A partial view of the rework drawing is shown in Figure 3.2.3-1.

Increased Intercooler Capacity. To address the continuing marginal air inlet temperature situation, a larger intercooler having approximately twice the capacity of the original, was adapted and installed into the test cell.

Spark Ignition Control Unit. An improved version of spark ignition control system, borrowed from another engine development program at RPI, was installed to provide the additional energy required to fire the spark plug reliably at the higher speeds and loads of this program.

Up-rated Fuel Injection Pump. During the baseline testing, the fuel injection pump was at its limit at an engine output somewhat less than the cruise rating. Any further increase in fuel rack resulted in pumping in the start-retard mode. An up-rated fuel injection pump was built and bench-tested to provide the additional fuel required for the ratings of this test.

3.2.3 Testing Performed.

Rated Speed Test. The engine configuration tested first was the baseline engine with the addition of the reworked rotor gears.
The engine was operated at speeds of 4000, 5000 and 6000 rpm. At speeds above 6000 rpm the ignition system was no longer able to fire the spark plug every engine revolution. The higher energy ignition control unit borrowed from another program at RPI was installed; this ignition control is generally referred to as the "FOE" system.

With the ignition system operating properly, the engine speed was increased to 8000 rpm. After approximately 25 minutes of operation at this speed and at moderate loads of 61 and 77 psi (4.2 and 5.3 bar) BMEP, the anti-drive end rotor bearing failed and the engine was removed from test. To address this failure, the engine was rebuilt with increased rotor bearing clearance.

Up-rated Fuel Injection Pump & Intercooler. The test cell intercooler was replaced with a unit having approximately twice the cooling capacity. The engine was installed and run-in with the baseline fuel injection pump for comparison purposes.

At approximately five hours into the test, the up-rated fuel injection pump was installed. To obtain proper injection event timings, the pilot plungers were re-shimmed and the main injection line size increased from 1.5 to 2.0mm ID. After resolving some test cell difficulties, the engine was operated at 7000 rpm and 130 psi (9.0 bar) BMEP for an output of 187 BHP (139 kW) at which point the chip detector alarmed. One of the drive end rotor gear attachment screws had failed.

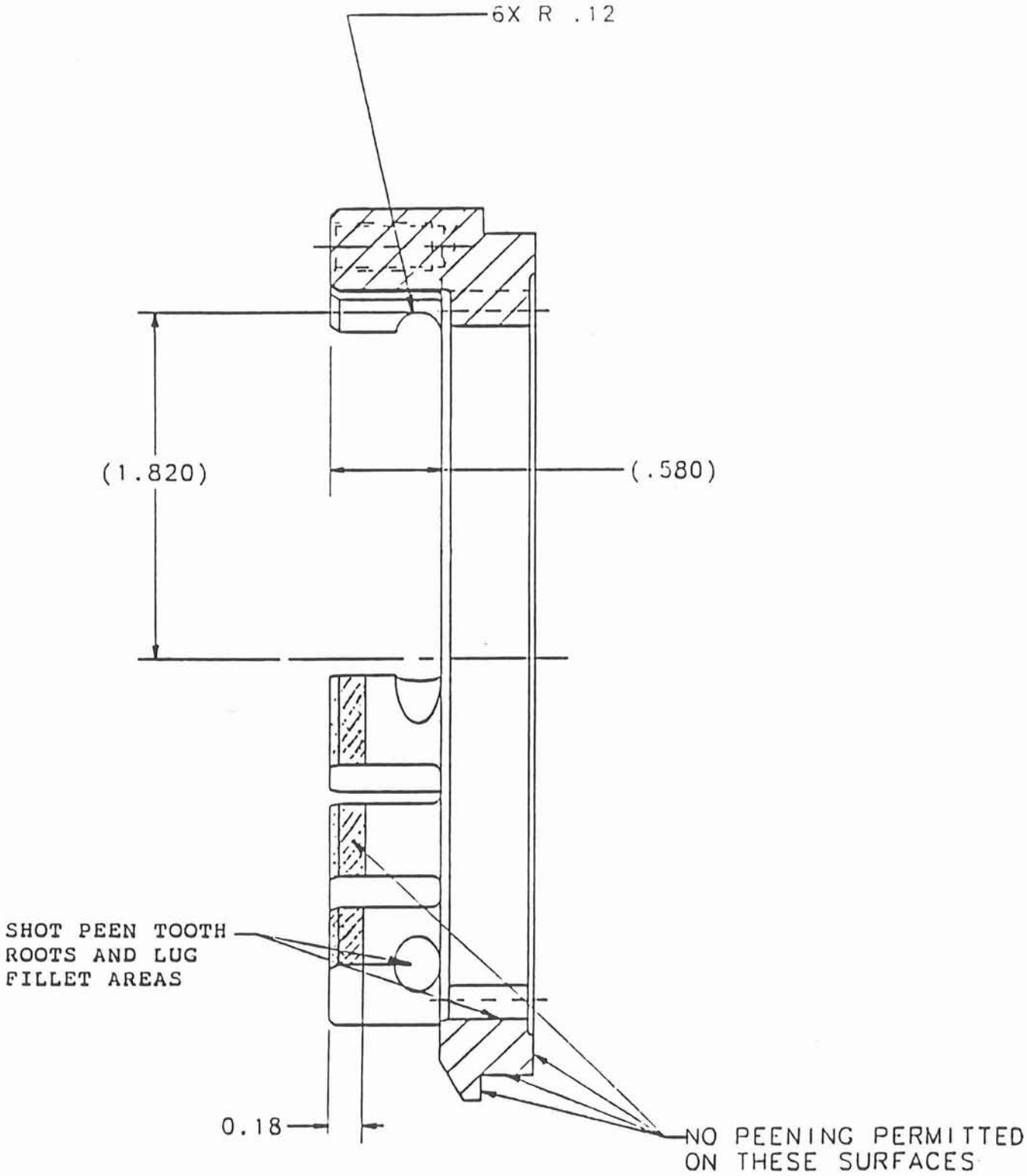

Figure 3.2.3-1 Rotor Gear Rework

3.2.4 Performance Results

Rated Speed Testing. The engine was operated at 8000 rpm at two loads, 61 and 77 psi (4.2 and 5.3 bar) BMEP. Prior to recording data at the higher load, the rotor bearing in the anti-drive end bank failed. This particular build was not operated at high loads. The table below illustrates the low load performance as it varies with speed. The 7000 rpm point, identified as run 5-17, is from the subsequent build and is included for completeness.

Run	Speed	Power	BMEP	BSFC	F/A
	rpm	BHP (kW)	psi (bar)	lb/hp-hr (g/kW-hr)	
4-7	8000	99 (74)	61 (4.2)	0.728 (443)	0.0253
5-17	7000	80 (60)	56 (3.9)	0.715 (435)	0.0230
4-3	6000	67 (50)	55 (3.8)	0.668 (406)	0.0215
4-2	5000	57 (43)	56 (3.9)	0.613 (373)	0.0232
4-1	4000	48 (36)	59 (4.1)	0.577 (351)	0.0264

Effects of Up-rated Fuel Injection Pump. The fuel consumption performance of the engine with the up-rated pump is essentially the same as that obtained using the baseline pump. The up-rated pump with increased diameter plungers would also be expected to increase injection pressures and rates somewhat and decrease injection duration. The injection duration decreased from 66° to 57° crankangle at 7000 rpm and 160 psi (11.03 bar) BMEP; a similar 9° to 10° decrease was observed over the 7000 rpm load range. The advantage of this pump was to provide increased fuel flow to allow operation to higher power levels. Figure 3.2.4-1 shows the fuel consumption, peak combustion pressure and fuel air ratio observed at 5000, 6000 and 7000 rpm. The high fuel consumption points at 7000 rpm are attributed to the calibration shift of the fuel flow meter described previously. The peak combustion pressure limitation of 1420 psi (98 bar), defined for maximum cruise continuous operation, continued to prevent engine output above 230 HP (172 kW) at 7000 rpm.

3.2.5 Failures Experienced, Corrective Actions and Results.

As mentioned in previous sections, a number of engine failures occurred during the testing of the baseline and upgraded baseline engines. These failures are described in more detail in the following paragraphs along with the changes made and their effectiveness in testing at the conclusion of the upgraded baseline phase.

Rotor Bearing. A small section of the anti-drive end rotor bearing liner was lost during the third build of the baseline engine. This particular bearing was manufactured by Glacier and had an aluminum-tin liner material (AS-15). While this was not the only such failure ever

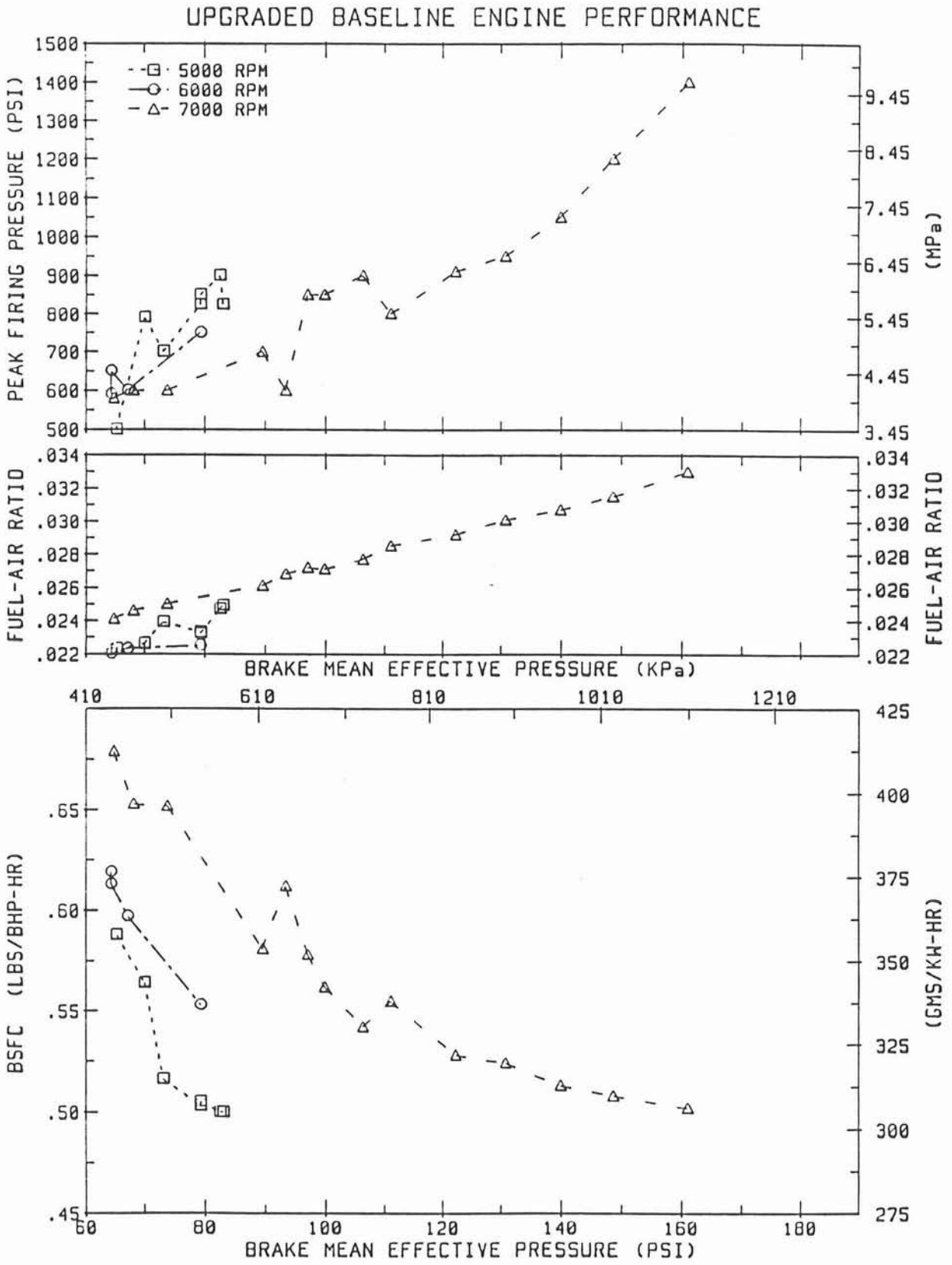

Figure 3.2.4-1 Upgraded Baseline Engine Performance

experienced, Glacier bearings have been used in a variety of rotary engine projects with generally excellent results. Also, there was evidence of a localized contact pattern on the bearing back which suggests that there was a high spot in the assembled bearing at the failure location. At this point the bearing was changed to evaluate an alternate Bohn MB-8 (aluminum) liner material which has a slightly higher fatigue life than the Glacier material.

The anti-drive end rotor bearing experienced a major failure during the first build of the upgraded engine while operating at 8000 rpm. The aluminum bearing liner had largely separated from the steel backing. This may have been a defect in the bearing manufacture, but the failure precipitated a design review of the original rotor bearing calculations. Several errors were found and corrected. Various bearing parameters were studied with the net result of increasing the bearing clearance specification from 0.0023"/0.0035" (0.058/0.089 mm) to 0.0035"/0.0045" (0.089/0.114 mm). The second build of the upgraded baseline engine incorporated the increased clearance and returned to the Glacier liner material. The rotor bearings were satisfactory upon disassembly of the engine at a total time of 26:20.

Rotor Bearing Rotation. Upon disassembly of the first build of the baseline engine, it was noted that the anti-drive end and drive end rotor bearings had rotated 5° and 180° respectively. The bearings did not move axially. Both were removed and the outside diameter examined. Apparently the steel shell received a tin flash plating as part of the manufacturing process which is believed to have contributed to bearing migration due to a reduced friction coefficient. These bearings were of a clinch-butt design which had not been tested at the speeds and loads of this program. Previous NASA programs utilized full round, welded-butt designs.

To address this issue, welded-butt bearings are now used exclusively on this program and any plating is removed from the outside diameter. Also, the range of interference fit was increased from 0.0050/0.0065" (0.127/0.165 mm) to 0.0060/0.0072" (0.152/0.183 mm). Approximately 64 hours have been accumulated on the welded-butt bearings with no indication of bearing rotation or movement. As a result of back-to-back tests run at the same interference fit, it has been concluded that the rotation problem was the result of the clinch-butt design and/or the tin flash plating.

Rotor Gear and Attachment Screw Failures. Drive end rotor gear failures were experienced on the first and third builds of the baseline engine. These were fatigue failures having origins in the area where one of the mounting lugs (bosses) meets the ring-shaped body of the gear, as shown in Figure 3.2.5-1.

A major revision to the rotor gear design was made which increased the critical tooth root and mounting lug radii and extended the case hardening to the mounting lug regions. Portions of this design are shown in Figure 3.2.5-2. The procurement of the NJ12484 Rev. C gears was initiated but due to the time required to manufacture such gears, the upgraded baseline engines used a rotor gear which was reworked. This rework consists of increasing/blending critical radii and shot-peening the region where the failures had occurred. This rework is more fully described on drawing 070X00341A, a portion of which is provided here as Figure 3.2.3-1. In spite of the increased safety factor and material

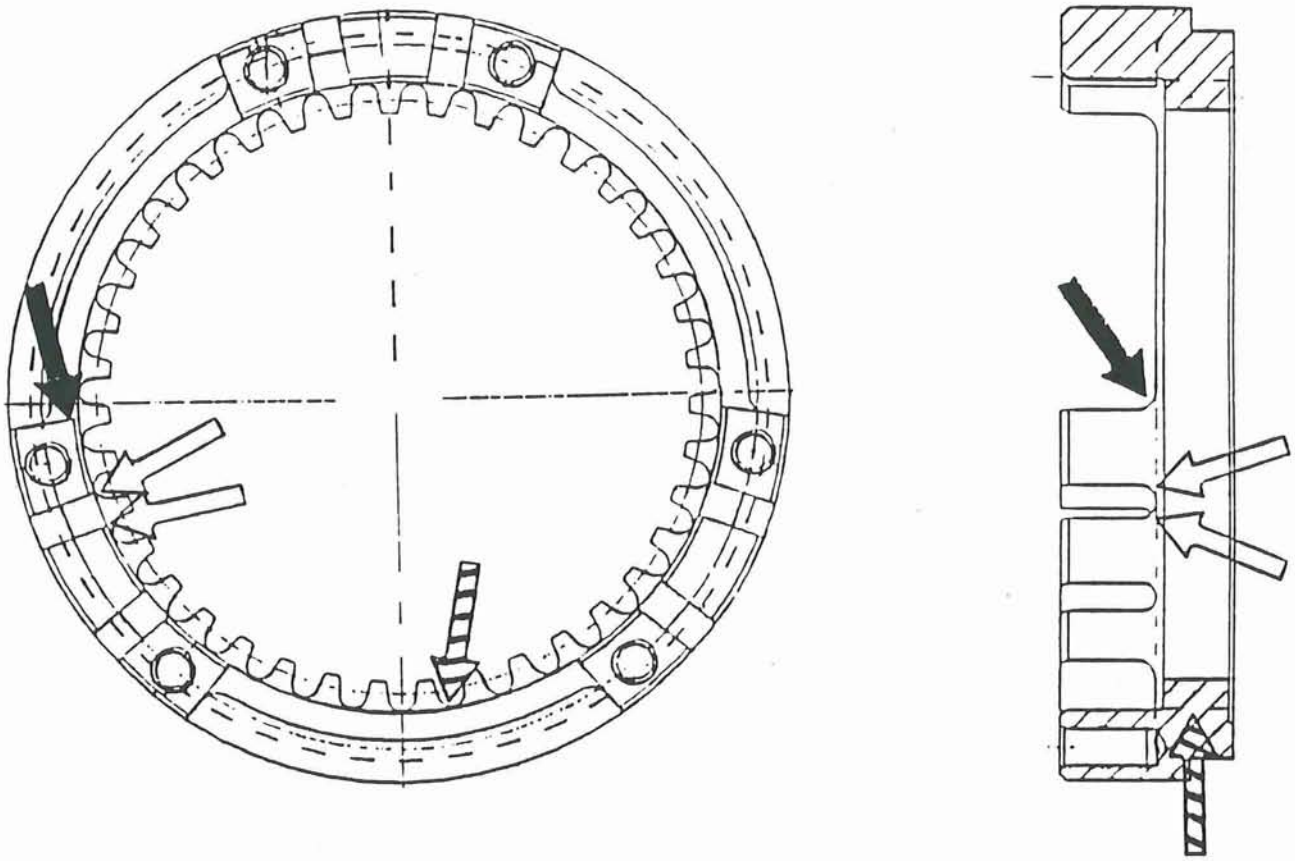

Legend:

Dark Arrow - Primary Failure @ Mounting Lug

Striped Arrow - Failure @ Tooth Root

Open Arrow - Failure @ Mounting Lug

Figure 3.2.5-1 Rotor Gear Failure Locations

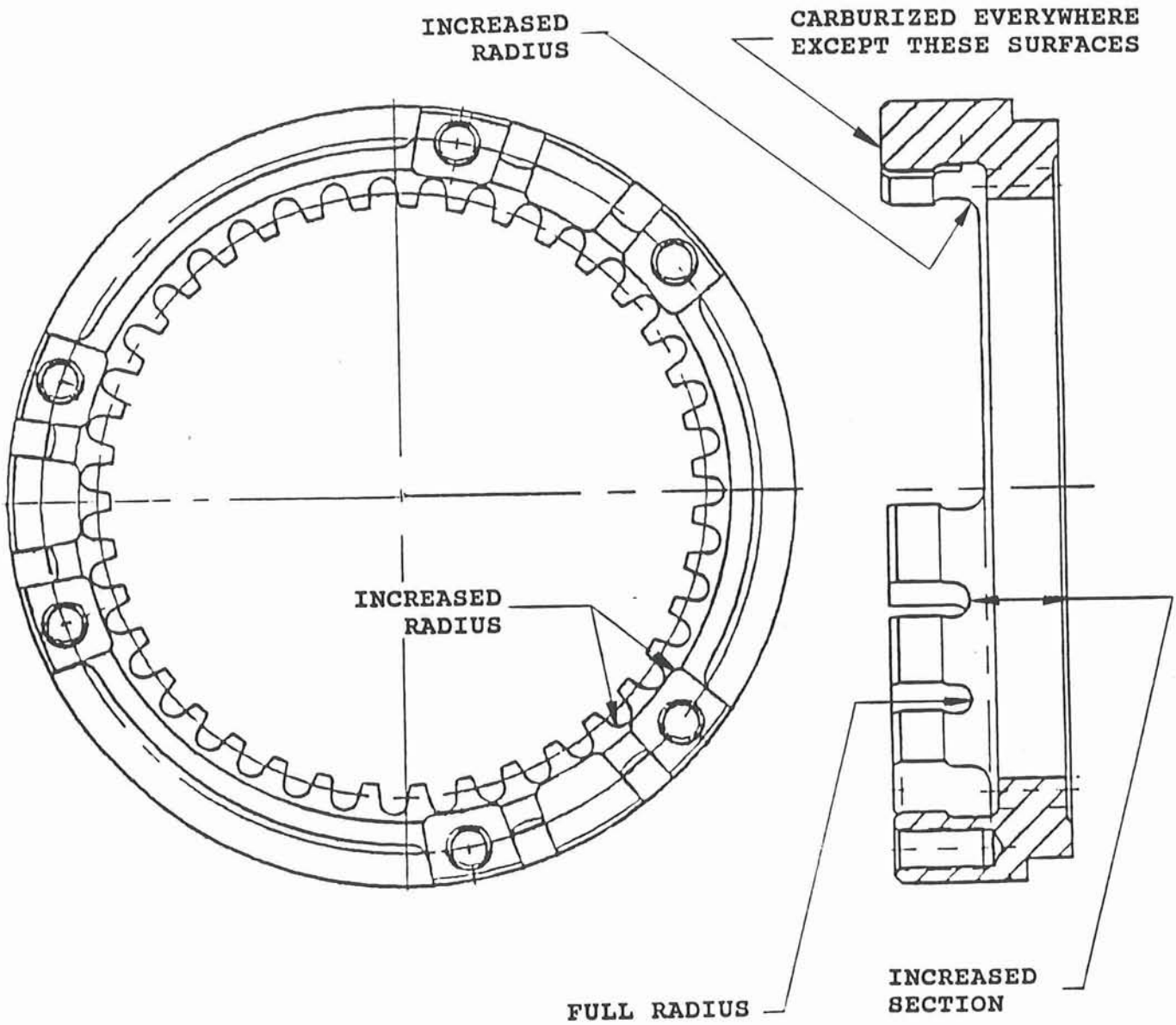

Figure 3.2.5-2 Improved Rotor Gear - NJ12484 Rev. C

properties of the reworked gear, the drive end rotor gear again failed in the second build of the upgraded baseline engine.

A related series of incidents concern the rotor gear attachment screws. During disassembly of the first baseline engine, it was noted that three of the six screws were loose. It is not known whether this was an engine incident or an assembly oversight. It should be noted that this first engine was assembled 2 years prior to the failure and, at that time, the rotor gear installation was performed by an outside supplier. There was a procedure in place and the supplier is considered reliable.

The corrective action addressed the installation of the attachment screws to ensure that they remained in place. The application of lubricant, a two-step torquing sequence and an increase in installation torque from 145-160 in-lb (16.38-18.08 N-m) to 155-170 in-lb (17.51-19.21 N-m) were used in the balance of the baseline and upgraded baseline engine builds. The rotor gear attachment screws are now installed in-house.

The third build of the baseline engine failed both the drive end rotor gear and stationary gear, however, all of the gear attachment screws were at the proper torque upon disassembly. One of the six drive end rotor gear attachment screws failed during the second build of the upgraded engine. (The rotor gear had failed as well.) The attachment screw was recovered in three pieces. While the screw could have loosened and then broken, the size of the pieces suggest that the screw failed at the plane of engagement and then again as it backed out of its hole. (See Figure 3.2.5-3)

The rotor gear and attachment screw failures are two symptoms of gear loading in excess of that which the gear is designed for. To provide further insight into these problems, structural and vibration analyses were initiated as is reported in Section 5.4.

Drive End Support Bearing. A failure of the drive end outboard support (outrigger) bearing caused the termination of test of the first engine. The bearing moved axially towards and into the flywheel. Examination and analysis of the hardware suggests that the bearing failed quickly while operating at the 231 BHP (172 kW) 7000 rpm condition.

The bearing itself had a flash plating of tin on the outside diameter of the shell which contributed to its ability to move. Unfortunately, the build records are incomplete and the as-built interference fit of the bearing into the support housing cannot be determined. However, based on examination of other bearings of the same lot, it is likely that the interference fit was at the lower limit (or below). The design limits for the fit were 0.0025" to 0.0045" (0.064 to 0.114 mm).

For the subsequent build, a bearing was selected which provided an interference fit of 0.0036" (0.091 mm). Also the tin plating, used as a preservative, was removed from the O.D. of the bearing shell. This bearing has been used since that time and upon completion of the upgraded baseline engine test had accumulated over 64 hours without incident.

Center Main Bearing Assembly. During disassembly of the first build of the baseline engine, three of the twelve center main bearing assembly bolts had failed. One failed in the threaded region at the interface of the nut plate and bearing support. Two bolts suffered low

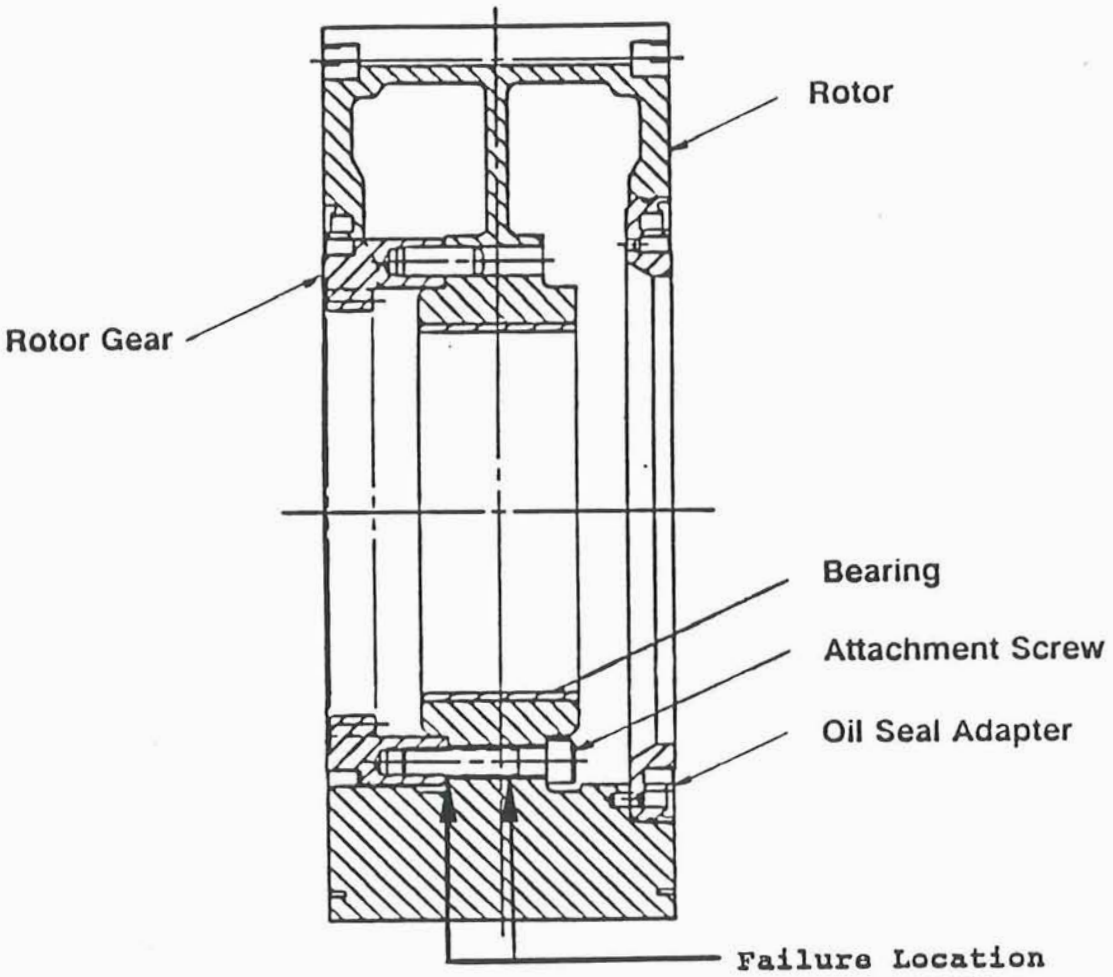

Figure 3.2.5-3 Failure of Rotor Gear Attachment Screw

cycle under-head failures. The surfaces of the bearing support and cone pieces had a relatively thick and uneven coating of dry lubricant. A view of the center main bearing assembly, Figure 3.2.5-4, is included here for reference.

It is postulated that the center main bearing assembly did not pull up tight which would result in the nut plate being at some angle other than 90° to the bolt axis. This would tend to impart a bending moment to the bolt at the threads. Also, such a "soft" assembly would allow the bolt to experience a variable loading.

As a result of several assembly trials, it was concluded that the dry film lubricant, when applied in a uniformly thin coating, is suitable. Also, to ensure that the bolts are in pure tension, special assembly-only nut plates are used to draw the cone pieces past the bearing support and the housing hub. The special nut plates are then removed and standard plates installed. Since the cones are proud of the surrounding parts, the nut plates contact the cones squarely, providing a solid steel-to-steel assembly and without imparting any bending moment to the bolts. The final installation torque simply stretches the bolt. This change to the assembly procedure has accumulated 64 hours of test time without incident.

Apex Seal. The testing of the second build of the engine was terminated when the apex seals of the anti-drive end rotor were inspected and found to have flatted. This flatting was due to poor combustion quality, e.g. excessively high combustion pressure and rate of pressure rise.

To prevent this problem in the subsequent build, the causes of the poor combustion were investigated and rectified. The primary problem was a jump (advance) in the timing of the main injection event when the rack was increased above 75% maximum. This was corrected by switching to zero-retraction-volume delivery valves. During the balance of the baseline and upgraded baseline testing, 47 hours have been accumulated on this type of apex seal with satisfactory wear.

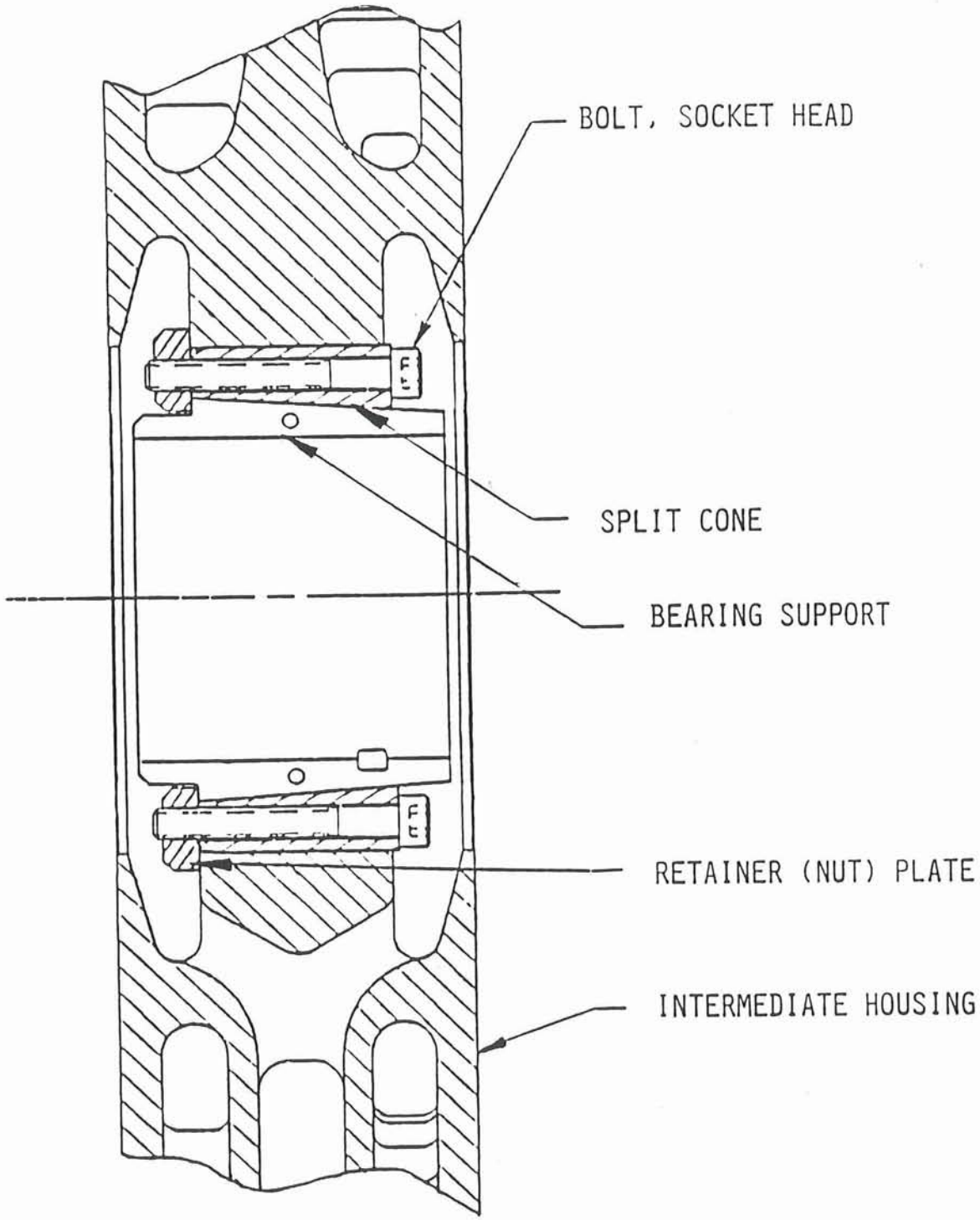

Figure 3.2.5-4 Center Main Bearing and Support Assembly

4.0 SUPPORTIVE SINGLE-ROTOR ENGINE COMPONENT EVALUATION

4.0 SUPPORTIVE SINGLE-ROTOR ENGINE COMPONENT EVALUATION

Single rotor rig engines are widely used at RPI to evaluate improvements to the power section of rotary engines. Combustion development is more straightforward due to the flexibility of independent and adjustable main and pilot fuel injection pumps as well as the absence of bank-to-bank imbalances. For these reasons, the single rotor rig engine was used to evaluate port area and timing, nozzle spray patterns and the advanced electronic high speed unit injector (HSUI) fuel system and, to a lesser extent, ignition and turbocharger systems.

4.1 PORTING AREA AND TIMING EVALUATION

4.1.1 Purpose of Test.

The focus of the porting/timing engine was to optimize the engine performance for the rating conditions of this program by selecting the area and location (timing) of the intake and exhaust ports. The area and timing of the ports are the primary parameters determining the mass of air trapped in the combustion chamber, all other things being equal. The takeoff rating and the fuel consumption at maximum cruise both suggest that the trapped air mass be maximized.

The configuration of the engine and the performance results are summarized below. For further detail, the reader is referred to "The Effects of Intake and Exhaust Porting and Timing on Engine Performance, Engine 65704-11 and -12" dated August 18, 1993.

4.1.2 Engine Configuration.

The rotor housing and porting inserts are the most significant engine features. The rotor housing is a unique casting to allow the use of port inserts. The interchangeable intake and exhaust port inserts are the key element enabling the porting/timing engine performance test. Each insert provides a specific and desired port opening and closing event while providing smooth transitions to the adjacent manifolds and trochoid penetrations.

A selection of three intake and three exhaust port inserts was provided for the test. These inserts range from the relatively small baseline ports to the largest port considered viable. Several of the features of this porting/timing rotor housing prevent its use on the two rotor engine; thus this particular test could only be accomplished using the single rotor rig engine.

4.1.3 Engine Performance Test Results.

With the baseline port inserts installed, the engine performance was mapped through 8000 rpm. The maximum output at 7000 rpm was 124 BHP (92 kW) and was limited by the peak combustion pressure of 1460 psi (99.3 bar). Operation at 8000 rpm was limited to 140

BHP (105 kW), also limited by the peak combustion pressure of 1600 psi (108 bar).

The engine porting was reconfigured to the largest available exhaust port, having a cross-section of 2.86 in^2 (1850 mm^2) and the designation NJ12354N6. With this change, the engine was operated at 7000 rpm and various loads. At 7000 rpm and 122 BHP (91 kW) the observed fuel consumption was 0.45 lb/hp-hr (274 g/kW-hr) as compared to 0.496 lb/hp-hr (302 g/kW-hr) achieved with the baseline exhaust port.

While repairs to the test cell were being made, the engine was removed to examine the rotor gear attachment bolts and rotor bearing due to failures of the same in the two rotor engine. The rotor gear attachment bolts had not lost any preload but the rotor bearing had rotated. The clinch-butt bearing was replaced with a welded-butt bearing, the engine reassembled and the designation changed to 65704-12.

Several combinations of intake port and exhaust port configurations were tested with the conclusion that the best performance was achieved with the largest, longest duration intake port (NJ12589) and the largest, longest duration exhaust port (NJ12354N6). This combination reduced fuel consumption to 0.45 lb/hp-hr (274 g/kW-hr) at the max cruise condition of 7000 rpm and 180 psi (12.4 bar) BMEP. These combinations, along with the data obtained later with the advanced engine rotor housing, are plotted in Figure 4.1.3-1. Also, the volumetric efficiency improved from 123.8% to 125.8%, although it should be noted that the volumetric efficiency does not discriminate between trapped and bypassed air flows.

Similar improvements were noted at 8000 rpm. In particular, at 8000 rpm and 150 psi (10.3 bar) BMEP the specific fuel consumption was reduced from 0.525 lb/hp-hr (319 g/kW-hr) to 0.475 lb/hp-hr (289 g/kW-hr). The large ports also permitted demonstration of the takeoff rating with a fuel consumption of 0.525 lb/hp-hr (319 g/kW-hr) observed at 8000 rpm and 208 psi (14.3 bar) BMEP for an output of 170 BHP (127 kW). Volumetric efficiency rose from 122.3% to 130.7%. In addition to improving the fuel consumption, the large port configuration also reduced the peak combustion pressures by a significant amount.

The engine was removed from test after having flatted and then failed the apex seals. It has been concluded that this testing simply exceeded the operational capabilities of the three piece FerroTic apex seal system. For this reason, the subsequent engines utilized apex seals of alternative materials and design.

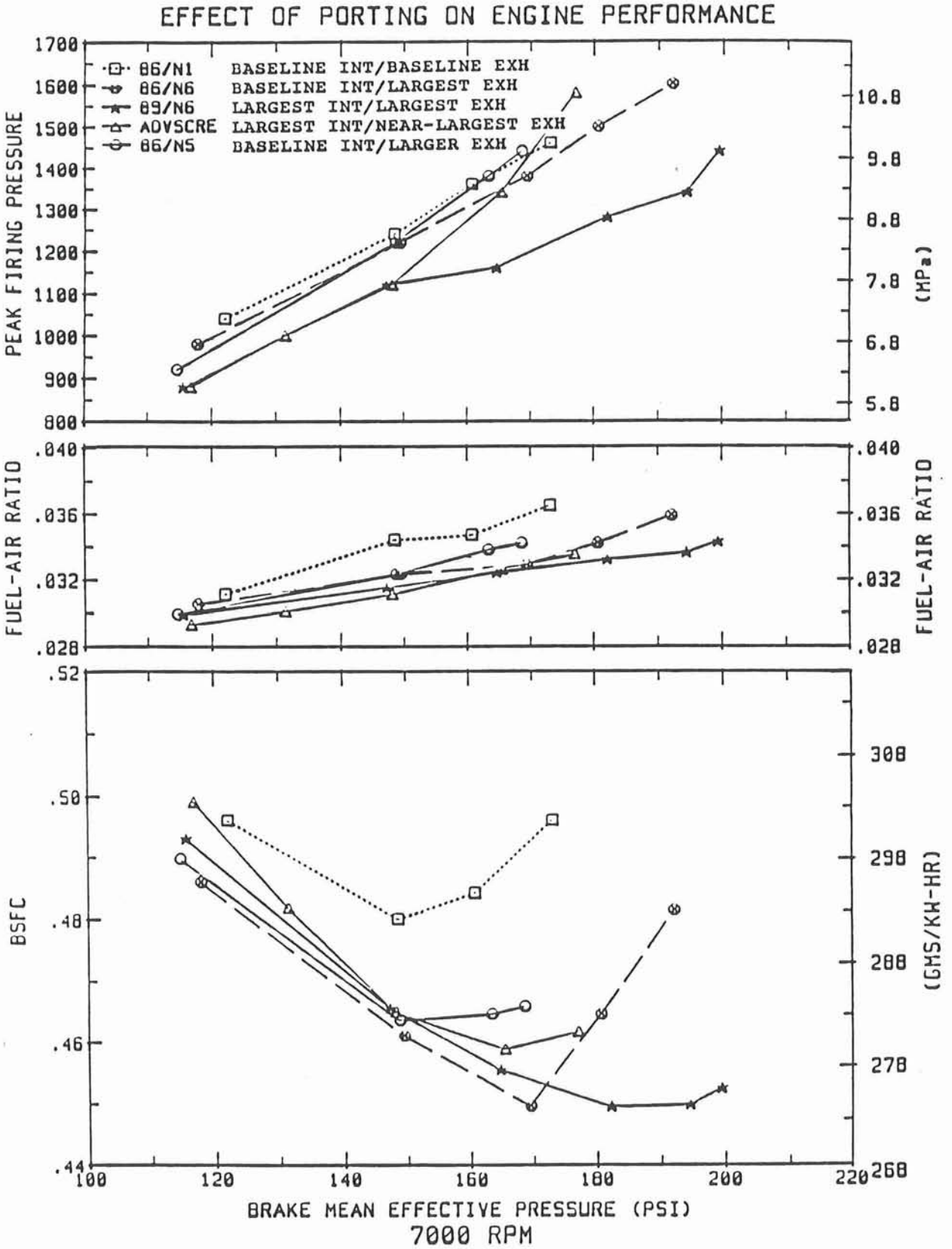

Figure 4.1.3-1 Port/Timing Engine Performance Results - Single Rotor Engine

4.2 TURBOCHARGER AND INJECTION NOZZLE PATTERN EVALUATION

4.2.1 Engine Configuration.

The rig engine was rebuilt using the second porting/timing rotor housing and the designation changed to 65704-13. This particular rotor housing had a casting breakthrough from the exhaust port to a coolant passage. The salvage rework consists of permanent, press-fit installation of one of the exhaust port inserts and resin impregnation of the housing. Due to secondary damage to the 8.4:1 compression ratio rotor used previously, an 8.0:1 rotor was used. To address the previous failure the apex seal material was changed to Gopalite which has proven successful on another program at RPI. The seal geometry was not changed.

4.2.2 Engine Performance Test Results.

Several nozzles and the turbocharger were replaced in order to achieve performance similar to that of the previous engine. A significant performance penalty was traced to a new exhaust system. This new system was installed in anticipation of demolition of a portion of the existing system by the facility owner. The original system consists of a simple 44 foot (13.4 m) run of 3 inch (0.076 m) diameter pipe without a muffler; the small pipe ran into a large vertical stack which provided some measure of silencing. The new system is of larger diameter and adds a large muffler.

The exhaust was temporarily returned to the original configuration and the engine demonstrated a bsfc of 0.455 lb/hp-hr (277 g/kW-hr) at 7000 rpm and 180 psi (12.4 bar) BMEP using an "N34" main nozzle (7F x .010) which is similar to that achieved during the porting/timing test using an "N15" (6A x .011) main nozzle. The peak combustion pressure was 1200 psi (83 bar) as compared to 1450 psi (100 bar) observed during the porting/timing test. This reduction may be due to the change in nozzle spray pattern, the reduction in compression ratio from 8.4:1 to 8.0:1 or, more likely, a combination of both.

The 0.96 A/R turbine housing, which provides a smaller flow area than the previously tested 1.14 A/R housing, was tested at cruise and take-off power ratings. Engine performance at cruise with the 0.96 A/R housing did not reduce the engine bsfc despite a substantial reduction in the fuel-air ratio, refer to Figure 4.2.2-1. The fuel-air ratio at cruise was reduced to .0307 from .0329 by substituting the .96 housing for the 1.14 housing, however, the bsfc remained constant at 0.458 lbs/hp-hr (279 g/kW-hr).

Testing of the 0.96 A/R turbine housing at the take-off rating indicated a similar increase in delivered airflow and boost. As can be seen in Figure 4.2.2-2, an increase rather than improvement in bsfc was observed at most tested loads at 8000 rpm relative to the 1.14 A/R housing. Test results to date appear to indicate that the 0.96 housing is too restrictive for the required engine airflows (ref. Figures 4.2.2-3 and 4.2.2-4). Portions of this data were provided to several turbocharger manufacturers for guidance in selecting turbomachinery for the two rotor engine. Subsequent testing was performed with the 1.14 A/R turbine housing.

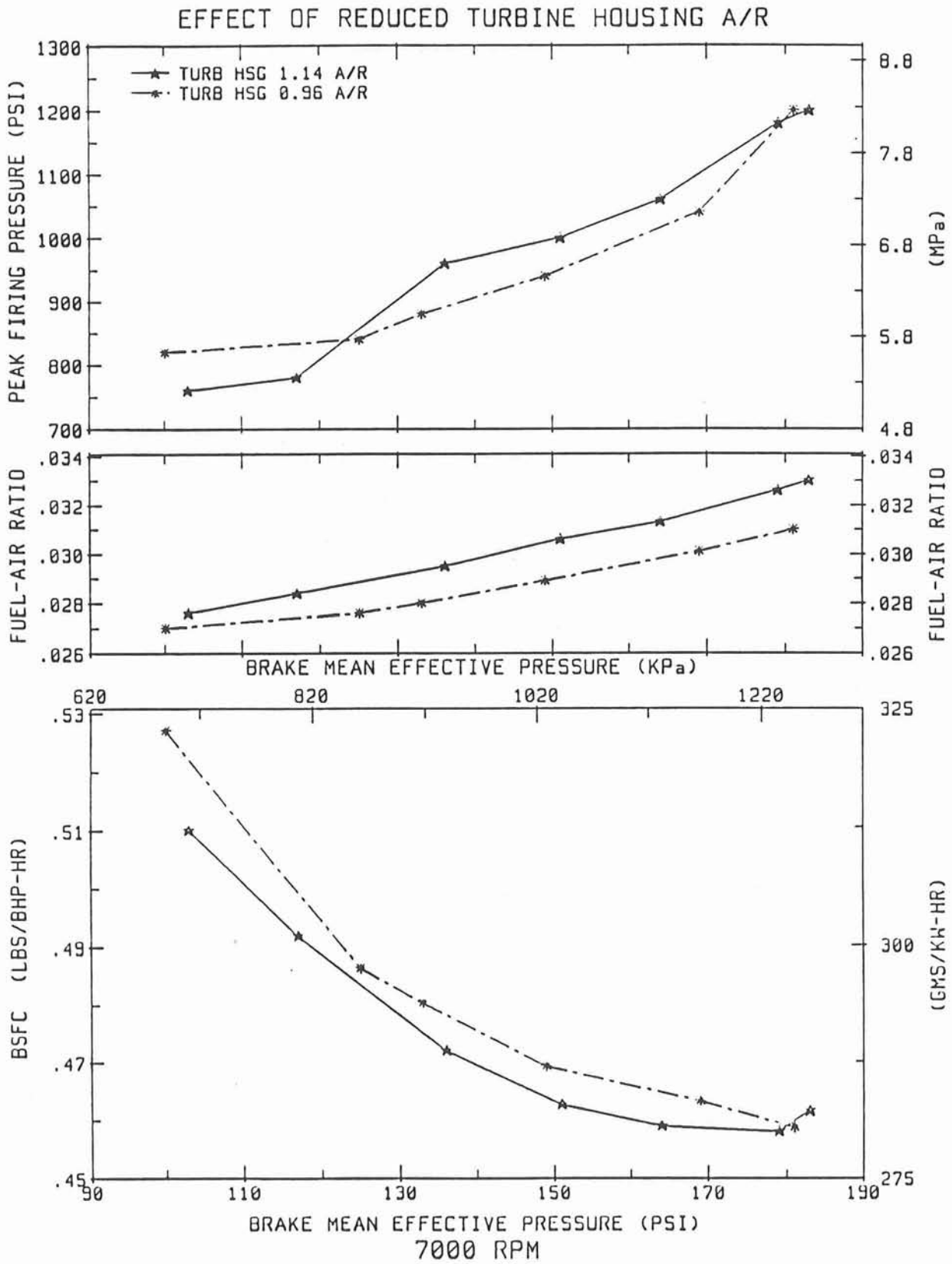

Figure 4.2.2-1 **Effect of Reduced Turbine Housing A/R on Single Rotor Engine Performance (7000 rpm)**

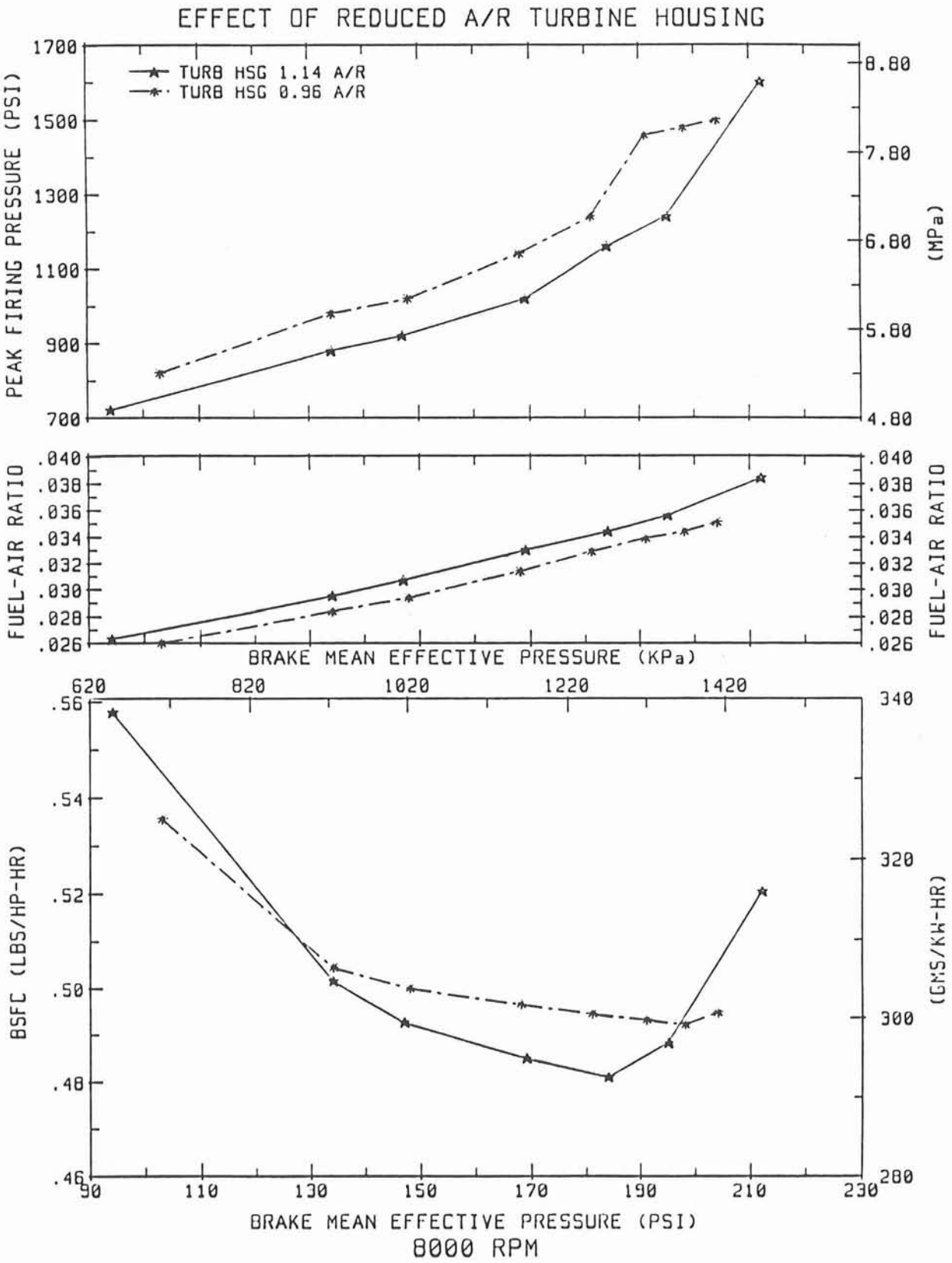

Figure 4.2.2-2 Effect of Reduced Turbine Housing A/R on Single Rotor Engine Performance (8000 rpm)

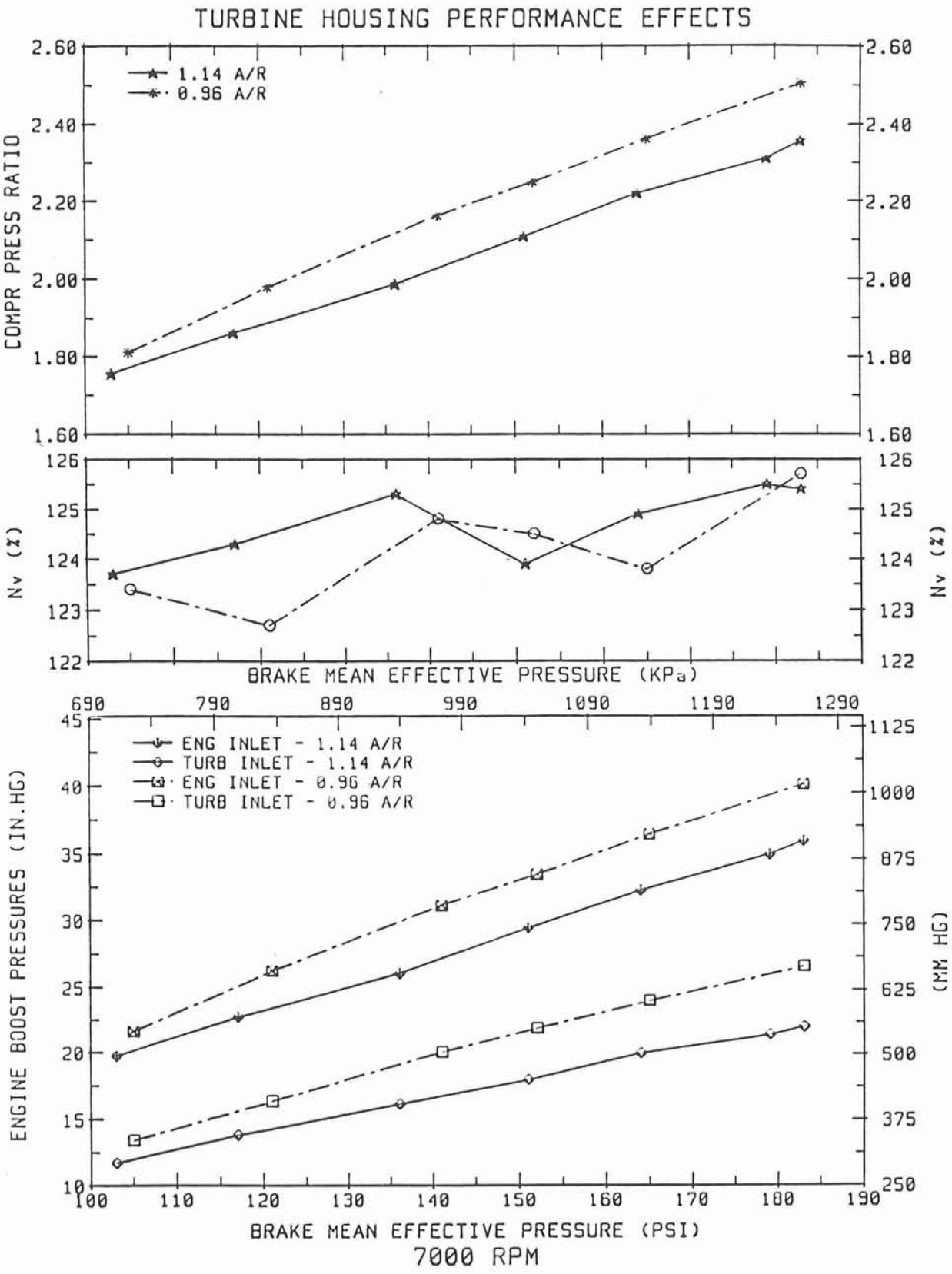

Figure 4.2.2-3 Turbocharger Performance (7000 rpm) - Single Rotor Engine

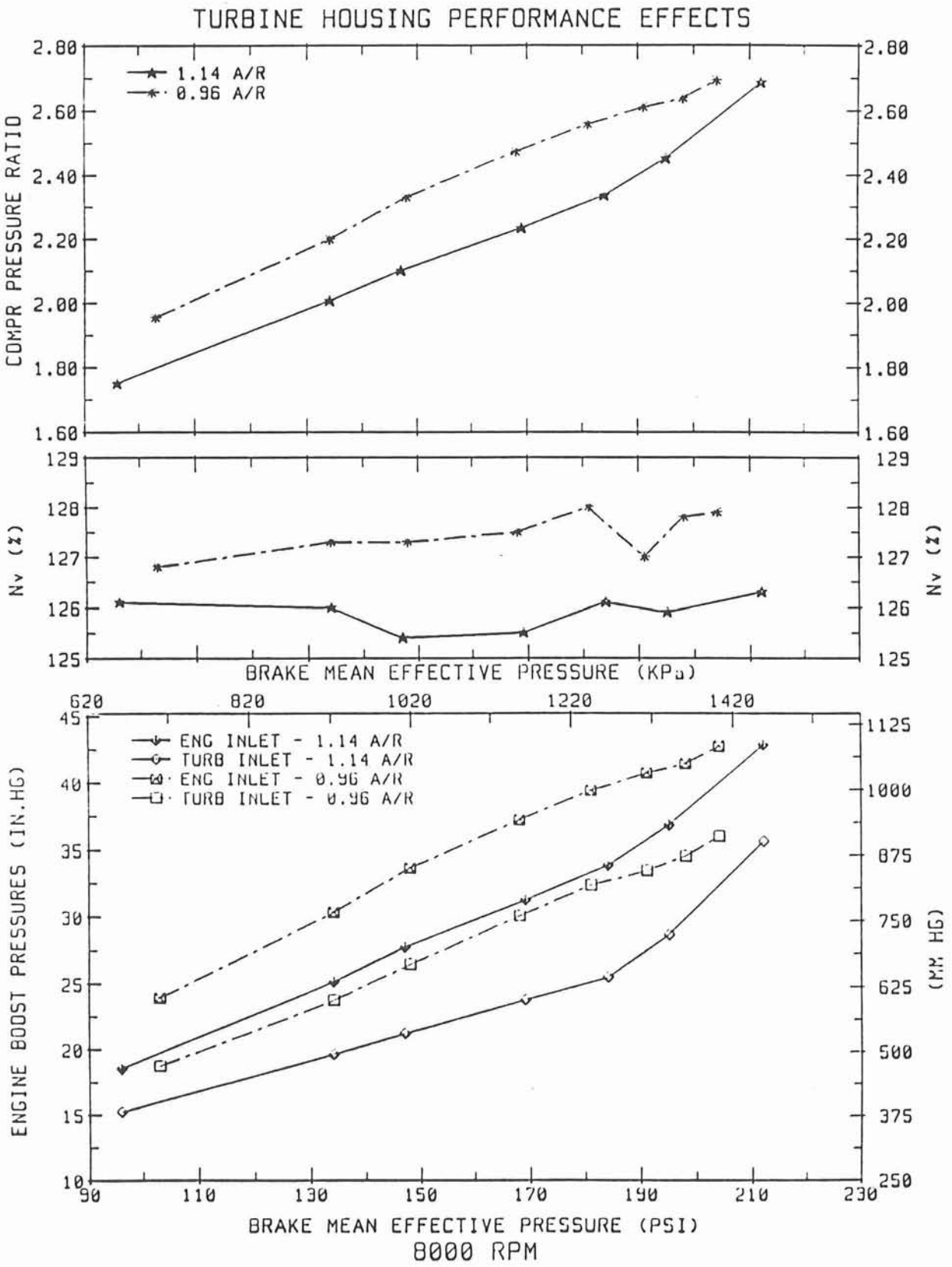

Figure 4.2.2-4 Turbocharger Performance (8000 rpm) - Single Rotor Engine

The effects of ignition timing and duration were tested at 4000 and 7000 rpm. A "D&V" ignition control was modified to provide variable control of the ignition start and duration. Testing indicates that an ignition duration of 35 crankangle degrees is required and that a delay of ignition start of up to 10 degrees crankangle from optimum appeared to be tolerated well.

Three new injection spray patterns were tested in this engine. The "N33" pattern (7E x 0.010) appears to provide the lowest bsfc, having demonstrated 0.458 lbs/hp-hr (279 g/kW-hr) at the max cruise operating point. The "N34" pattern (7F x 0.010) is closely comparable as can be seen in Figure 4.2.2-5. A third pattern, "N42" (7H x 0.011) was tested but the engine bsfc performance appears to be hindered at the max cruise rating by the larger orifice size of 0.011 inches (0.279 mm). A test with this nozzle hole pattern but with 0.010 inch (0.254 mm) diameter holes would be desirable but this combination was not included when the nozzle procurement matrix was decided.

The takeoff rating was demonstrated using both the "N33" (7E x .010) and the "N34" (7F x 0.010) main nozzles. With the "N34" nozzle, the observed fuel consumption was 0.50 lb/hp-hr (304 g/kW-hr) as compared to 0.52 lbs/hp-hr (316 g/kW-hr) observed with the "N33". The peak firing pressures were somewhat higher with the "N34" as can be seen in Figure 4.2.2-6. The engine was removed from test due to failure of the rotor bearing.

The engine was rebuilt using the first Advanced Engine rotor housing and the designation changed to 65704-14. Using the existing Nippondenso pump, AMBAC nozzles and an "N33" (7E x 0.010) main nozzle, the engine demonstrated a fuel consumption of 0.461 lb/hp-hr (280 g/kW-hr) at the max cruise operating point with an observed peak firing pressure of 1580 psi (109 bar). The "N34" pattern (7F x 0.010) was also tested and produced a max cruise bsfc of 0.458 lb/hp-hr (279 g/kW-hr) and peak firing pressure of 1560 psi (108 bar). These data are plotted as Figure 4.2.2-7. Allowing for the friction differences between the single and two rotor engines, the 0.435 lb/hp-hr (265 g/kW-hr) two rotor engine goal translates to a single rotor target of 0.448 lb/hp-hr (273 g/kW-hr). Thus the bsfc obtained with the single rotor engine was withing 2% of the goal. The fuel consumption performance of this engine is equivalent to that demonstrated by the earlier builds, however, the peak firing pressure is significantly higher than for the previous two builds - 1560 psi vs. 1180 psi (108 bar vs. 81 bar) for 704-13.

A thermocouple-instrumented spark plug test was performed at 7000 rpm using the "N33" main nozzle. The spark plug insulator temperature varied from 1640°F (893°C) at 100 psi (6.9 bar) BMEP to 2112°F (1156°C) at 175 psi (12.1 bar) BMEP for a constant pilot fuel flow rate of 4.0 lb/hr (1.8 kg/hr) equivalent to 5.5 mm^3/stroke. A further test indicated a very large change in temperature with pilot flow rate; for this reason the pilot flow rate is being kept low. Subsequent to this change there have been few problems with the spark plug.

The effect of pilot fuel flow on fuel consumption was also studied at 6000 and 7000 rpm. The pilot flow was varied from 3 mm^3/stroke to 9 mm^3/stroke while operating at 100 psi (6.9 bar) BMEP at both speeds. This variation in flow was found to have no significant effect on either fuel consumption or peak firing pressure at these operating conditions.

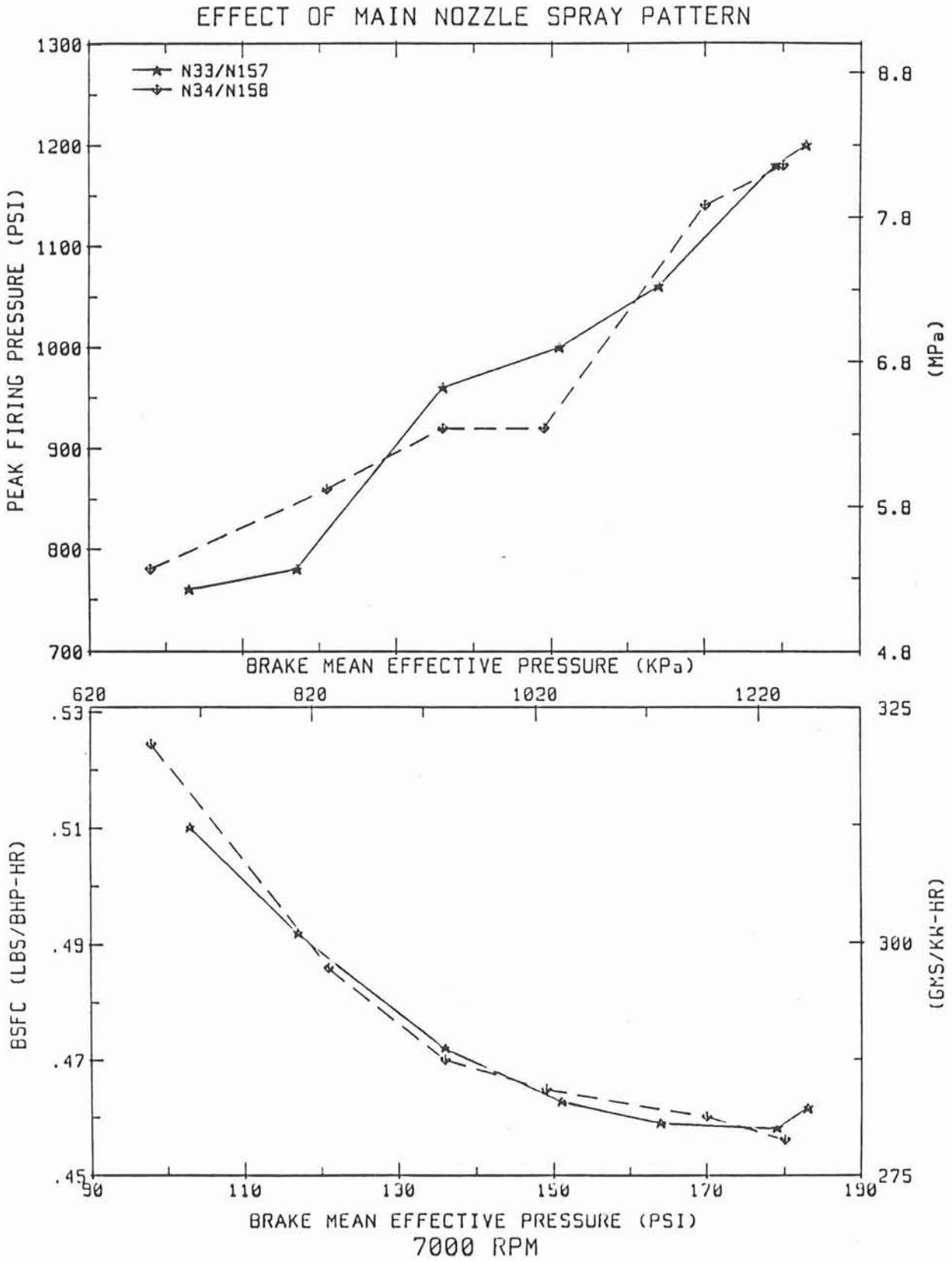

Figure 4.2.2-5 **Main Nozzle Spray Pattern Performance (7000 rpm) Single Rotor Engine**

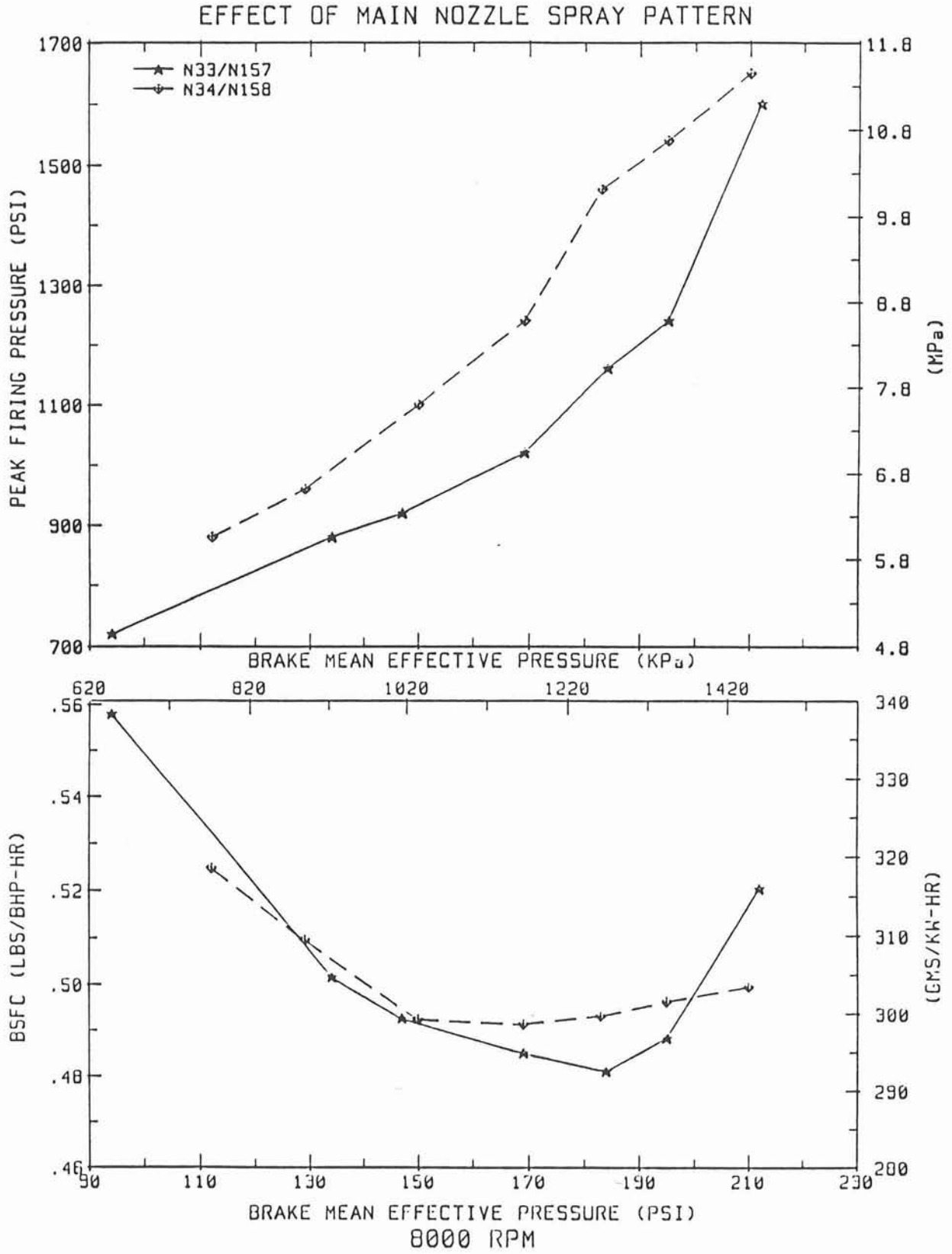

Figure 4.2.2-6 Main Nozzle Spray Pattern Performance (8000 rpm) Single Rotor Engine

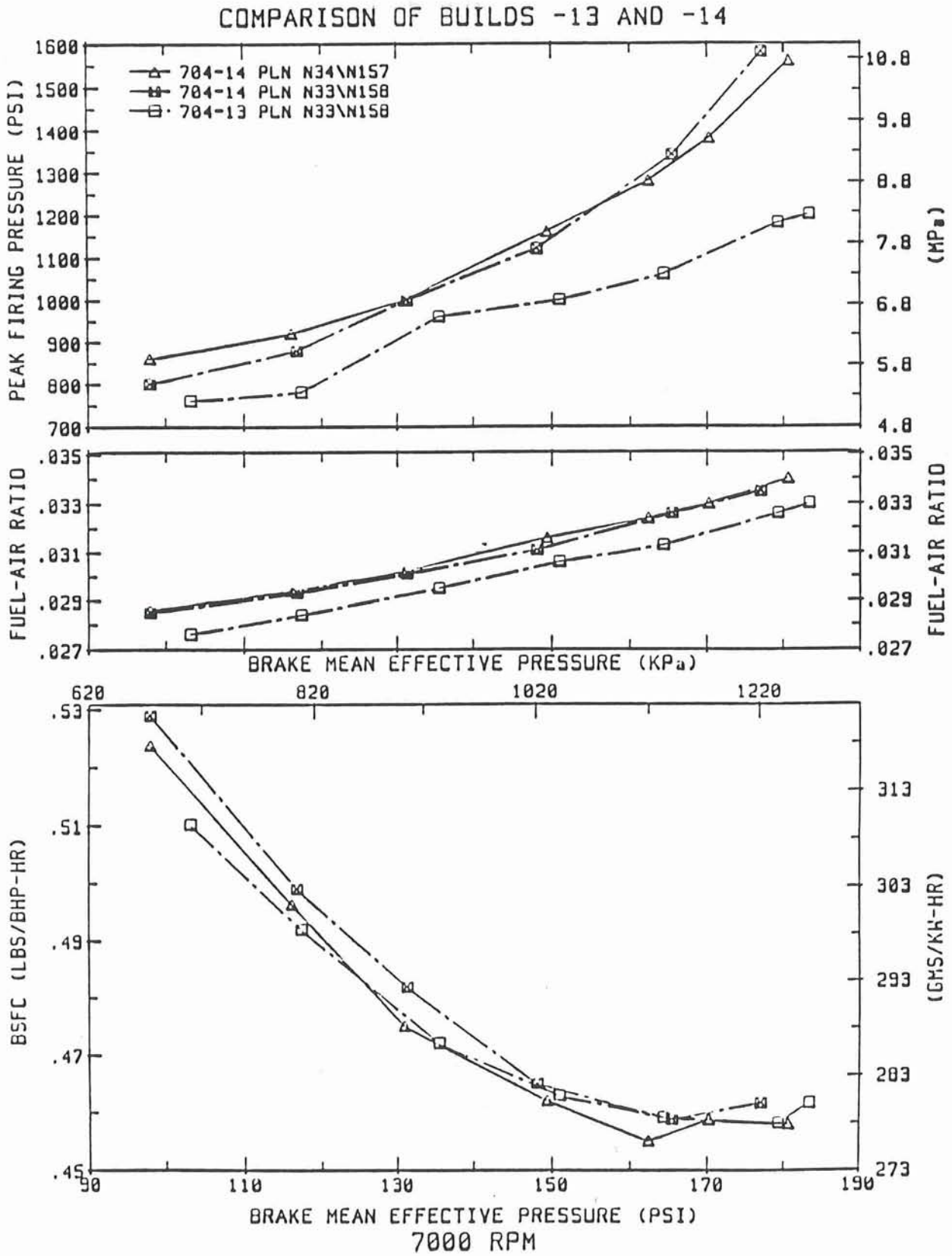

Figure 4.2.2-7 Single Rotor Engine Performance with the Advanced Rotor Housing

4.3 ADVANCED FUEL INJECTION SYSTEM (HSUI) EVALUATION

The electronic high speed unit injector (HSUI) fuel system was designed and developed for the unique requirements of the SCRE operating at the rating conditions of this program. Further information on the testing of this system on the single rotor engine can be found in Section 6 of this report as well as separate performance test report for the single rotor engine 65704-14.

4.3.1 Engine Configuration.

The HSUI system was installed on 65704-14 while the engine remained installed in the test cell. The power section configuration was unchanged from that described in section 4.2.1. Externally, the AMBAC nozzles were replaced with Ganser-Hydromag injectors and an accumulator/pressure relief valve/pressure transducer assembly installed. High pressure fuel was supplied by a single head AMBAC M100 pump which is a distributor-type fuel injection pump; in this application all of the outputs are ganged and delivered to the accumulator. The initial development testing was performed with the NR10540N34 (7F x 0.010) main nozzle and the NR10541N250 (2B x 0.007) pilot nozzle.

4.3.2 Engine Performance Test Results.

Testing proceeded smoothly and without significant incident up to 6000 rpm and 114 psi (7.9 bar) BMEP (70 BHP = 52 kW) at which point increased loads and speed produced significant engine misfires. These misfires, characterized by out-of-phase or missing fuel injection commands were traced to the control system misreading the speed. This was resolved by new control software which screens out the erroneous speed signals.

Performance testing continued up to and including the max cruise condition. The cruise power was demonstrated operating at three rail pressures of 7350 psi (500 bar), 8820 psi (600 bar) and 10000 psi (700 bar) with the results as shown in Figure 4.3.2-1. At 7000 rpm, operation with the 500 bar rail pressure demonstrated a poor bsfc of 0.503 lb/hp-hr at 122 BHP (306 g/kW-hr at 91 kW); operation with 600 bar rail pressure provided an improved characteristic in being easier to obtain cruise power and demonstrated an appreciably improved bsfc of 0.467 lb/hp-hr at 128 BHP (284 g/kW-hr at 95 kW). Operation at 700 bar rail pressure was not generally as good as with 600 bar and demonstrated a bsfc of 0.484 at 126 BHP (294 g/kW-hr at 94 kW). In all cases the fuel consumption increased with increasing load but was least sensitive at the 600 bar rail pressure.

The Ganser-Hydromag injectors provide for adjustment of the solenoid control orifice clearance which affects the nozzle opening rate. An increased orifice clearance reduced the fuel consumption sensitivity to rail pressure observed previously but no further reduction of engine fuel consumption was obtained. It was not possible to thoroughly explore this variable.

Four additional main nozzle configurations were evaluated. The observed performance at 7000 rpm is plotted as Figure 4.3.2-2. The "N30" is the same 7F pattern as originally tested, except the orifices are smaller (0.009" vs. 0.010"). The fuel consumption at the max

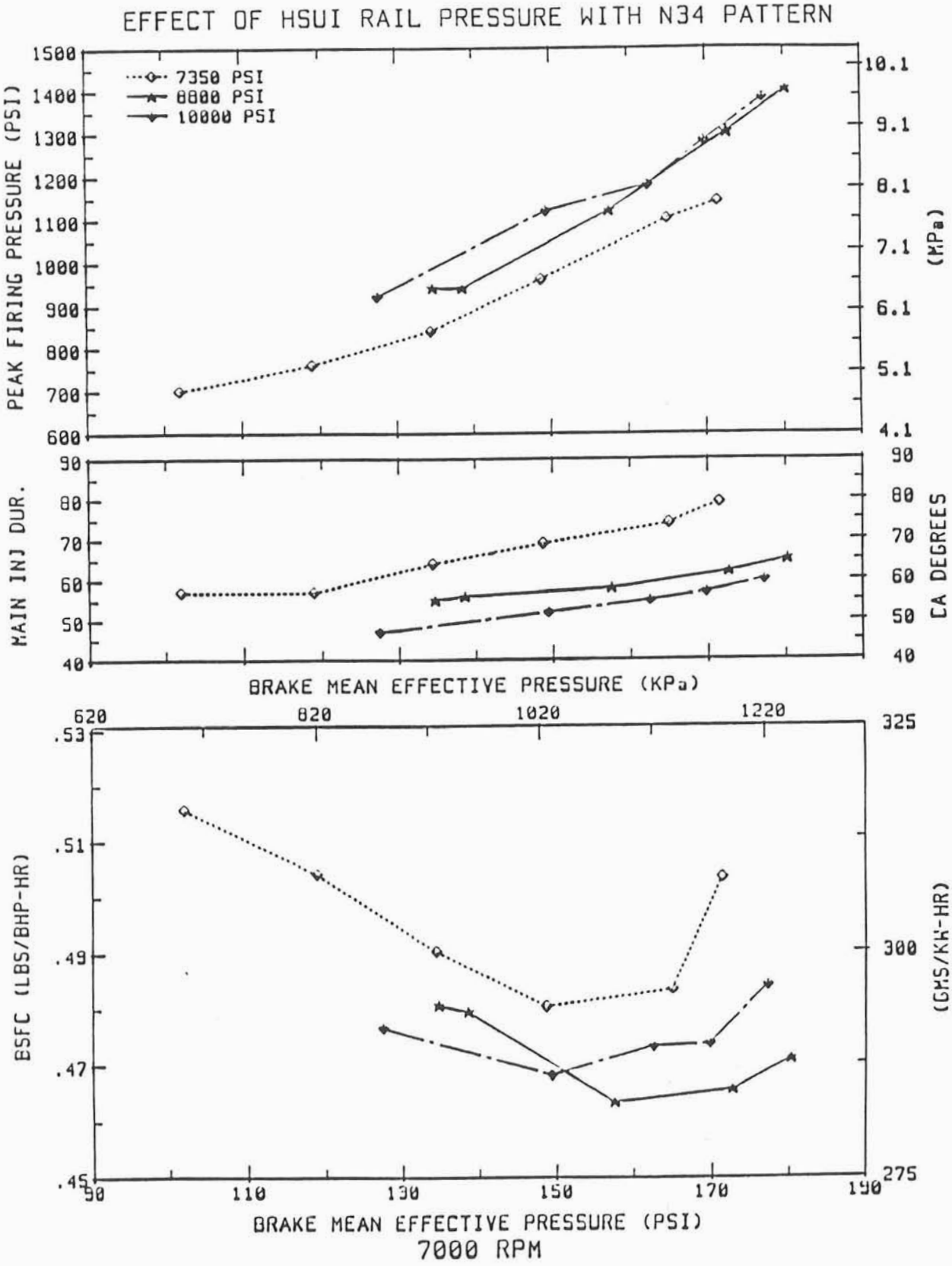

Figure 4.3.2-1 Performance Sensitivity to HSUI Rail/Accumulator Pressure - Single Rotor Engine

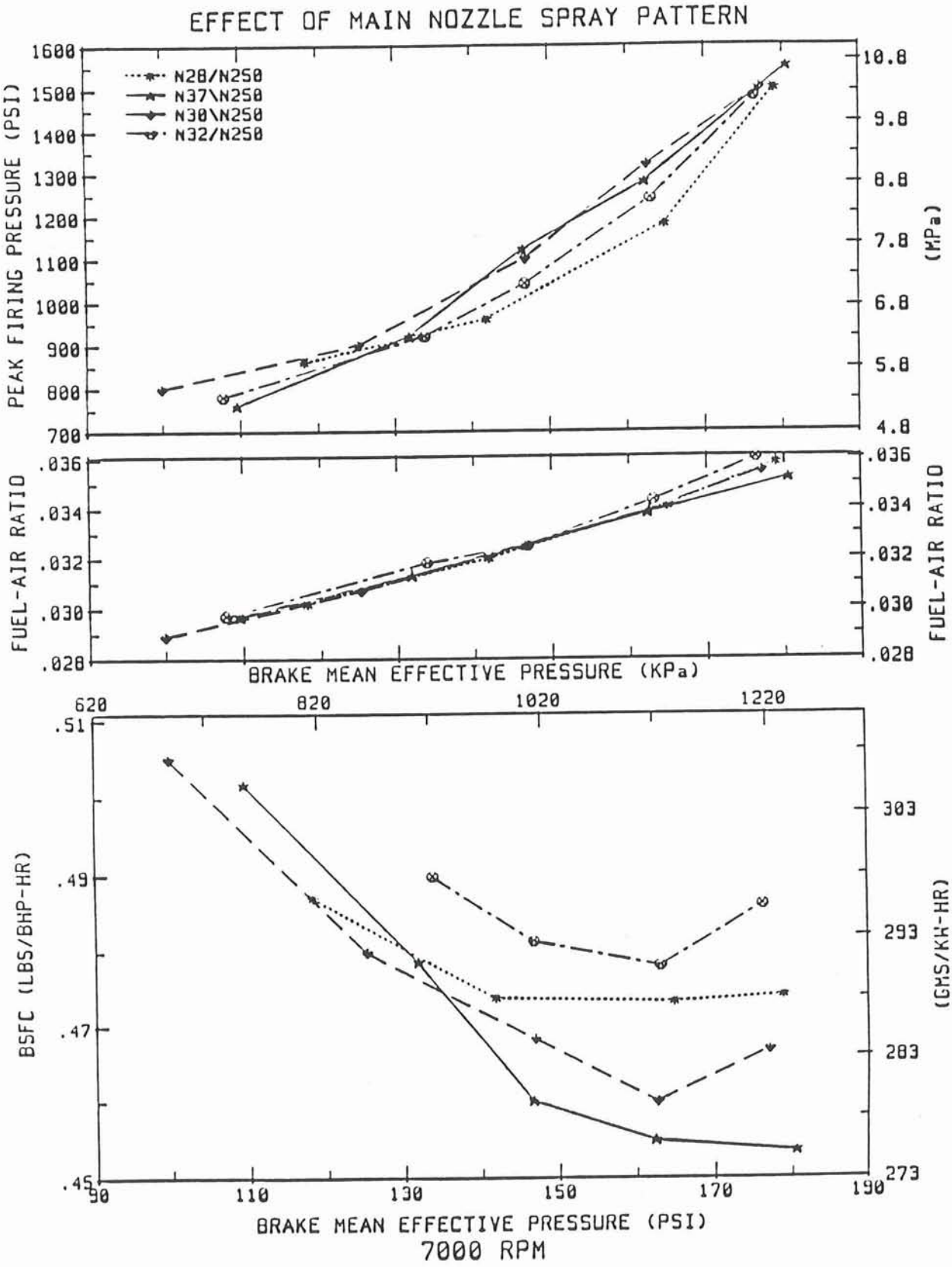

Figure 4.3.2-2 HSUI Main Nozzle Spray Pattern Performance - Single Rotor Engine

cruise condition was identical to that of the larger version - 0.467 lb/hp-hr (280 g/kW-hr). The "N37" (7G x .009) non-shadowing pattern demonstrated a significantly better max cruise bsfc of 0.454 lb/hp-hr (274 g/kW-hr). This nozzle shows very little sensitivity ot the accumulator/rail pressure as shown in Figure 4.3.2-3. The remaining two patterns, the "N28" (7E x .009) and the "N32" (7H x .009) did not match the fuel consumption performance of the other two. The "N28" pattern demonstrated some useful reduction of peak firing pressure while operating at 8000 rpm.

The test cell exhaust system was modified since the large vertical exhaust stack used to shroud the test cell exhaust pipe was removed by the facility owner. The exhaust system which had been installed previously was necessarily reinstalled (ref. section 4.2.2). This system includes a new exhaust pipe and transition, a 10 inch (.25 m) muffler and stack. The fuel consumption performance with this new exhaust system was poor - 0.47 lb/hp-hr (286 g/kW-hr) at 7000 rpm and 100 BHP (75 kW).

A brief test was performed using an alternate, unmuffled system consisting of a 3 foot (0.91 m) length of 4 inch (0.10 m) pipe. This restored most of the performance lost when the muffled system was installed. An exhaust system was designed which was tuned for operation at an engine speed of 7000 rpm. A 3 inch (0.076 m) inner diameter pipe was chosen to maintain high exhaust velocity. A length of 8.5 foot (2.59 m) was selected which corresponds to returning a rarefaction wave to the exhaust port 15° after exhaust port opening at 7000 rpm. This system uses the same 10 inch (0.25 m) muffler tested previously, which was installed downstream of the tuned length. With this exhaust system, the max cruise fuel consumption returned to the previous levels - a bsfc of 0.455 lb/hp-hr (278 g/kW-hr) was observed at 7000 rpm and 178 psi (12.3 bar) BMEP. Figure 4.3.2-4 indicates the engine performance observed using the various exhaust systems described above.

Engine testing of 65704-14 was terminated by failure of a rotor gear attachment screw.

4.4 EXTENDED TESTING AND EVALUATION

4.4.1 Purpose of Test

The Advanced Engine rotor housing exhaust port was somewhat smaller than that of the best of the porting/timing rotor housing exhaust ports due to the tie bolt configuration of the two rotor engine. A rework to the advanced rotor housing was identified to enlarge the exhaust port for the purpose of determining if some further fuel consumption improvement at the max cruise condition was possible and if the combustion pressures would be reduced.

4.4.2 Engine Configuration.

The rotor housing for 65704-15 was reworked to enlarge the exhaust port. This rework provided the timing events of the largest porting/timing test exhaust port but the port flow area was limited due to as-cast wall thicknesses.

The rotor from the previous build was found to have a short crack at one gear bolt boss but was judged acceptable for continued test. Engine 65704-15 was built using this rotor with a

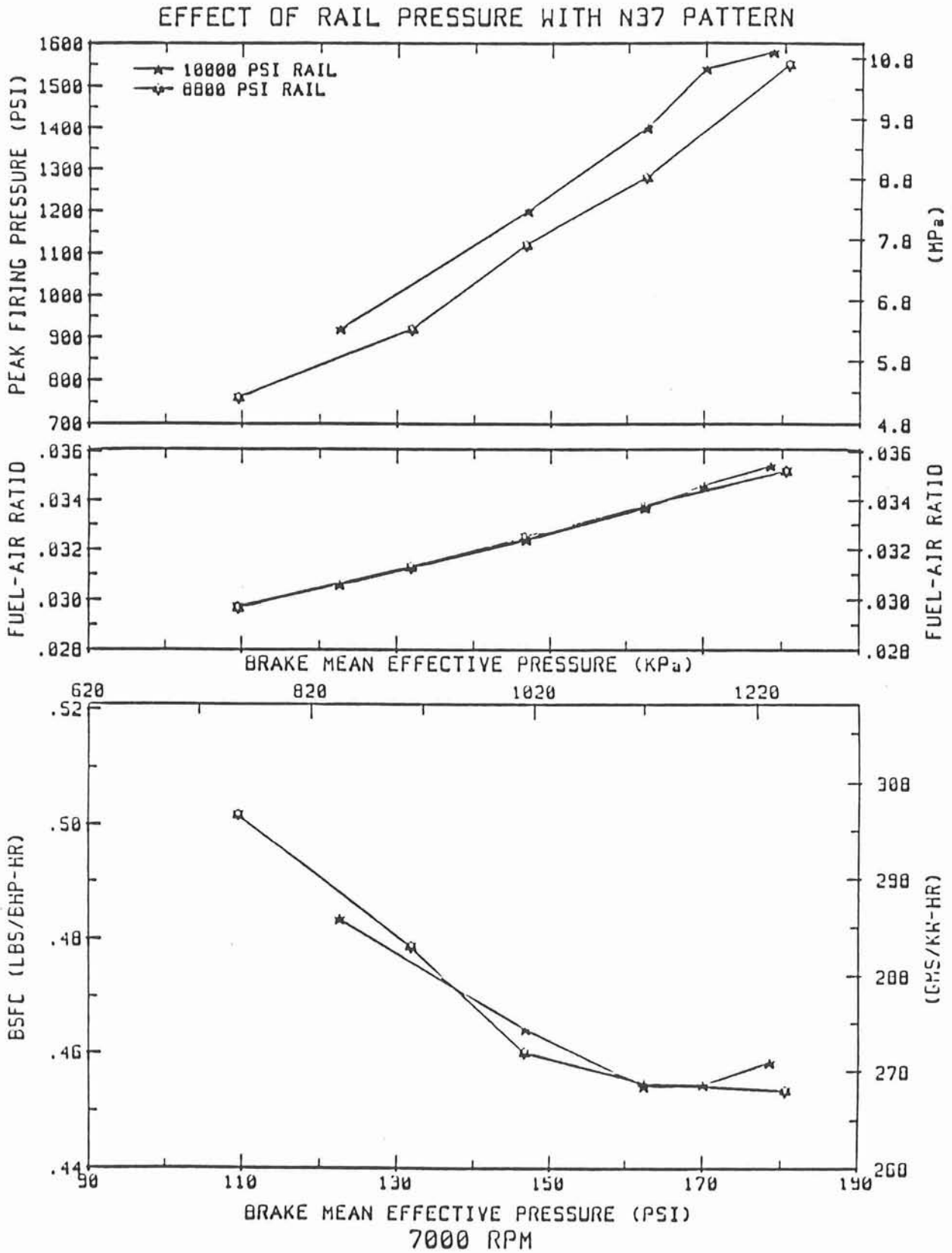

Figure 4.3.2-3 Performance Sensitivity to Rail Pressure with "N37" Main Nozzle Spray Pattern - Single Rotor Engine

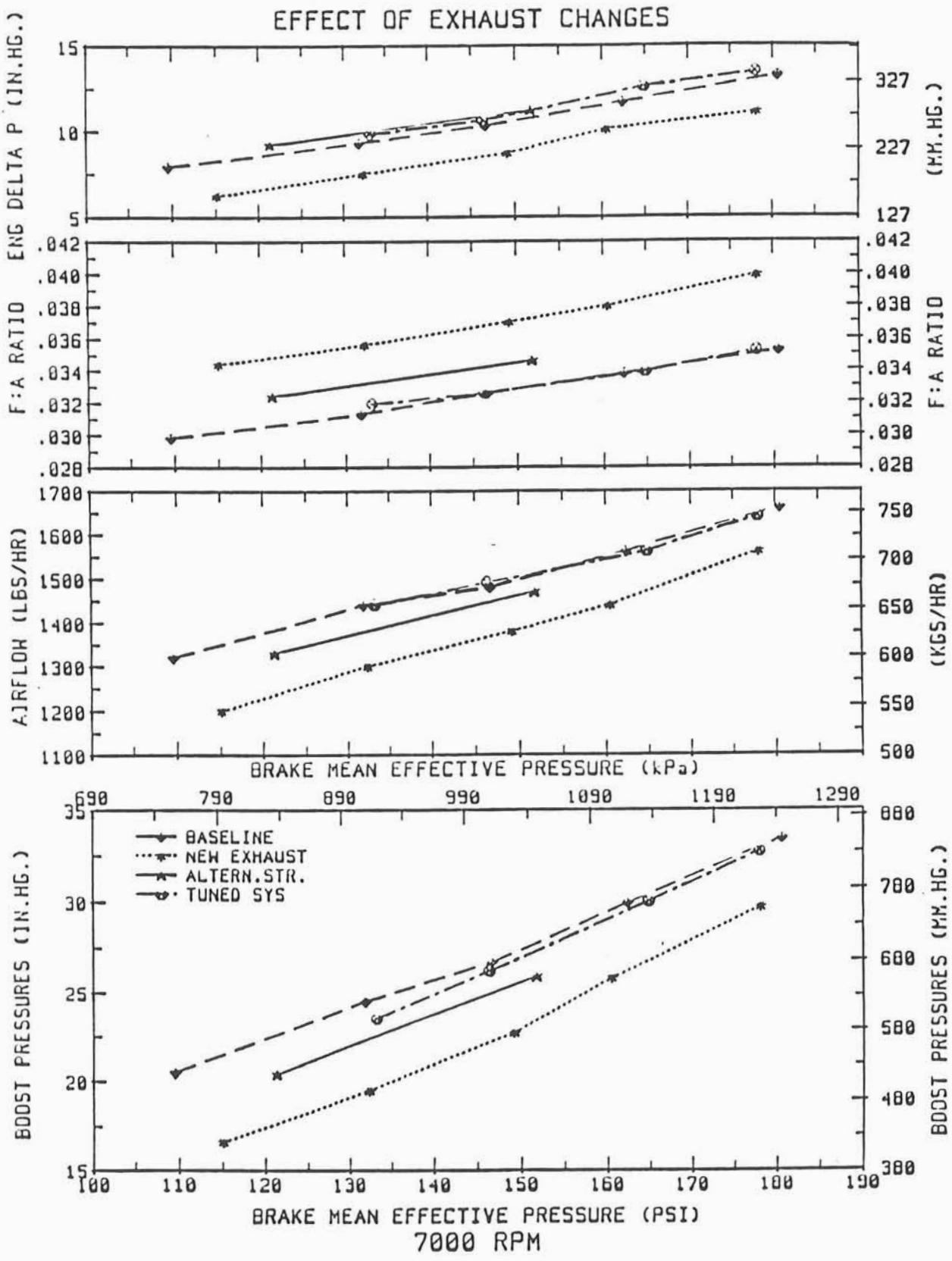

Figure 4.3.2-4 Performance Sensitivity to Exhaust System Configuration - Single Rotor Engine

new bearing and a new oil seal adapter to replace those damaged during the previous failure of the attachment screw.

To permit testing of the HSUI system on the two rotor engine, this build of the single rotor engine was run with the conventional pump-line-nozzle system used previously.

4.4.3 Engine Performance Test Results.

With the pump-line-nozzle fuel injection system, two main nozzle patterns were evaluated. The "N33" (7E x 0.010) demonstrated a fuel consumption of 0.471 lb/hp-hr (286 g/kW-hr) at the cruise condition. This somewhat inferior performance compared with an earlier build is not explained. The "N38" (7G x 0.010) pattern demonstrated an improvement to 0.454 lb/hp-hr (276 g/kW-hr) at the cruise condition. Also encouraging with the "N38" is the fact that the fuel consumption was nearly constant from 146 to 182 psi (10.1 to 12.5 bar) BMEP as compared with other patterns which typically show a best bsfc at lower loads. As indicated in Figure 4.4.3-1, the good fuel consumption did not exact a combustion pressure penalty; the observed peak firing pressure at the cruise condition was 1540 psi (106 bar).

Testing continued at 8000 rpm but the engine failed the rotor gear and oil seal adapter. At this point the evaluations intended by the single rotor engine as support to the advanced core engine were completed and testing of the 1007R was terminated.

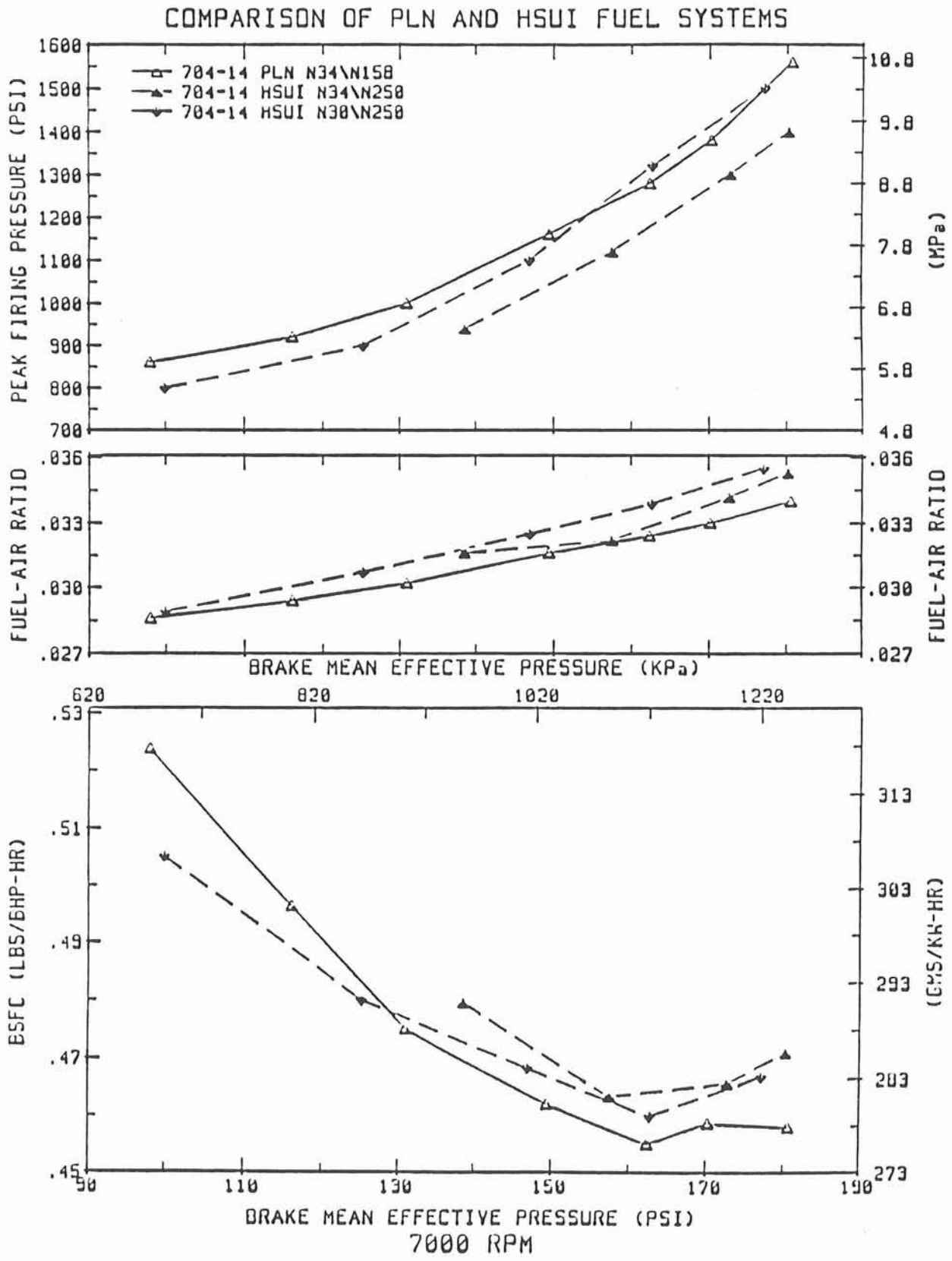

Figure 4.4.3-1 Performance Comparison of Pump-Line-Nozzle and HSUI Fuel Injection Systems - Single Rotor Engine

5.0 - ADVANCED CORE ENGINE EVALUATION

5.0 - ADVANCED CORE ENGINE EVALUATION

5.1 ENGINE DEFINITION

To achieve the performance goals of this program, several improvements to the baseline engine were required. At the outset of this program it was known that the increased power levels implied increased air and fuel flow. This is implemented in hardware by increasing the size of the intake and exhaust ports, selecting an appropriate turbocharger and upgrading the fuel injection system. The need for these changes were confirmed by the baseline two rotor engine testing while the specific sizing and timing of the new ports was determined largely as a result of the single rotor rig engine port/timing tests.

The porting changes were of such an extent that new rotor housings had to be manufactured. Changes were also made to the fuel injector bosses to accommodate the larger, Ganser-Hydromag electronic fuel injector nozzles or conventional AMBAC nozzles. To improve the life of the spark plugs, the spark plug boss was designed for the larger and more robust 14mm plugs. The spark plug installs directly into the aluminum housing for improved heat transfer as compared to the previous housing which utilized a steel threaded insert.

The revised ports and higher flow rates dictated new intake and exhaust manifolds. Turbochargers were selected to provide optimum compressor efficiency at the cruise condition. A Schwitzer S4DS and a special Mitsubishi TD09 were procured.

New rotors were designed with an increase in nominal compression ratio from 7.5:1 to 8.0:1. The advantage of increased compression ratio is improved thermodynamic efficiency and therefore reduced fuel consumption. This particular design provides sufficient material at the combustion pockets to allow machining to any compression ratio between 8.0:1 and 8.4:1 albeit with somewhat higher rotor mass at the higher ratio. For this program, rotors were cast in both 17-4PH stainless steel and 4140 steel.

As a result of numerous rotor gear failures in both the single rotor rig and baseline engine, new rotor gears were designed and manufactured. The primary changes were increased radii at the tooth roots, increased radii and improved blending at the base of the mounting/attachment lugs and extending the case hardening beyond the teeth and into the lug area. Also, the rotor feature which corresponds to the outside diameter of the gear was re-designed to provide a slight interference fit at room temperature. This was incorporated to limit radial motion of the gear and thus reduce the alternating bending stress on the gear mounting lug and attachment bolt.

The rotor apex seals used in the baseline engine were of a three piece symmetric design consisting of two corner seals and a FerroTiC center bar. The junction between the corner seals and center bar is at the trochoid. During the baseline testing, one case of apex seal flatting was experienced which was attributed to poor combustion quality. Based upon

single rotor testing, a change was made to a two piece system with one corner seal and an apex seal of Gopalite material. In this design, the junction between corner seal and apex seal is at the side housing.

The take-off rating of this engine poses a challenge to the fuel system. The primary difficulty is the speed - each rotor bank requires 8000 injections per minute. This is at or near the limit for the conventional diesel inline injection pumps used on the baseline engine. The fuel injection system designed for this engine during the current contractual effort is a high speed electronic unit injector system (HSUI) consisting of a special AMBAC tandem M100 pump, Ganser-Hydromag electronic injectors, an accumulator/pressure relief valve assembly, Computer Systems Technology control system and associated connecting hardware. This system, integrated by Beginnings Technology Inc, is more fully described in Section 6.1 of this report.

5.2 BUILDS, RESULTS AND PERFORMANCE

5.2.1 Build A1 The first build of the advanced engine was configured with new advanced rotor housings, intake and exhaust manifolds. The drive end rotor was an earlier casting machined to a compression ratio of 8.0:1. The anti-drive end rotor was of the new design and of the 4140 material. Unfortunately, the casting patterns had errors which resulted in undersized gear attachment and oil seal adapter attachment features. New high strength bolts were used to attach the gear in combination with special washers to compensate for the lack of material in certain locations. Figure 5.2.1-1 shows cross sections of the rotor depicting both the "blueprint" and the salvage rework assemblies.

The alternate pump-line-nozzle fuel injection system was used since the HSUI system was still under development on the fuel injection rig. This system consists of the upgraded baseline injection pump and AMBAC nozzles. Dual orifice pilot nozzles were used here for the first time on the two rotor engine. The Schwitzer S4DS turbocharger was selected for this build. To provide insight to the rotor gear failures, torsiograph wheels were added to both ends of the engine crankshaft.

The engine was run-in at moderate loads and speeds from 4000 to 7000 rpm. The combustion quality was poor and was traced to insufficient pilot injection duration. This resulted from the increase in orifice area when changing from the single orifice to the dual orifice pilot injector nozzles. At this point, the most expedient change was to reduce the nozzle orifice area which was accomplished by replacing the 2B X 0.008" nozzles with 2B X 0.007" nozzles.

With the pilots replaced, the combustion quality was improved and a torque curve at 6000 rpm was begun. While operating at 140 psi (9.65 bar) BMEP, the chip detector alarmed and the engine was shut down. Disassembly revealed that two of the ADE rotor gear attachment bolts had failed. The loose pieces of bolt had peened and chipped away portions of the rotor oil seal adapter, intermediate housing and center main bearing assembly.

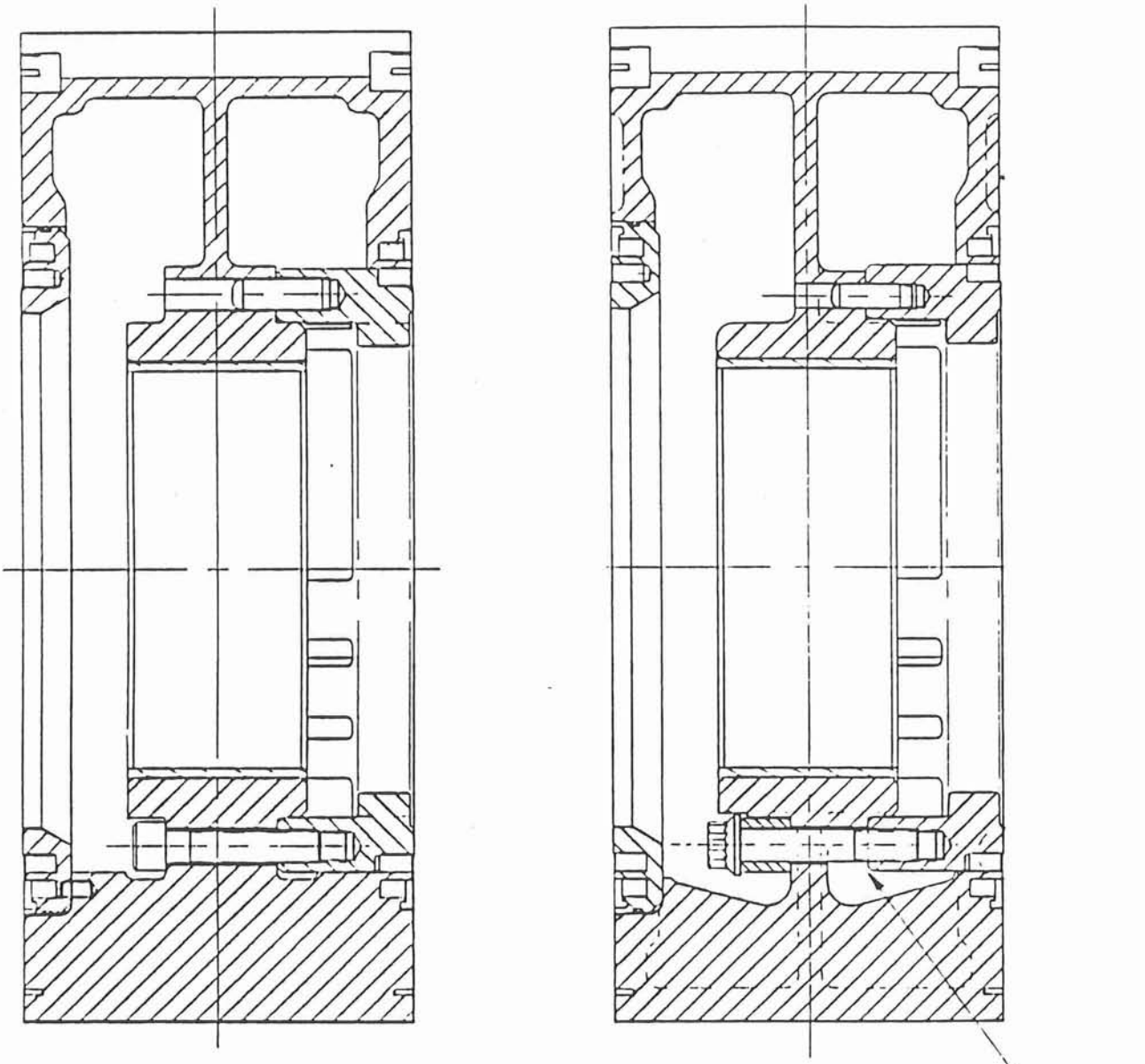

Figure 5.2.1-1 Rotor Assembly Cross-Sections

5.2.2 Build A2 To address the rotor gear attachment bolt failure experienced on build A1, several bolt/attachment bench tests were performed. The significant conclusions were as follows:

* the bolt stretch and thus the pre-load stress level where nearly double that expected for the specified torque (i.e. the actual coefficient of friction is significantly lower than that assumed)

* the stiffness of the salvage rework rotor bosses is approximately half that of the blueprint design which leads to significantly higher alternating stresses on the gear and its attachment hardware

* bolt installation in this critical an application must be performed by angle of twist or stretch and not by torque

To provide further information on gear loading, the stationary gears were reworked and strain gage instrumented. The gages were arranged and connected in such a manner as to be insensitive to radial loading and thus be sensitive only to torque.

Build A2 utilized the baseline 7.5:1 compression ratio rotors and seals since "blueprint" new-design rotors were still in the manufacturing process. To reduce the radial motion of the rotor gear, the ADE rotor was reworked to provide line-on-line fit at the outside diameter of the gear. The rotor feature was built up by flame spray and subsequently machined to match the gear. The actual hardware provided a slight interference fit of 0.0008" (0.02 mm). The high strength rotor gear attachment bolts were necked down for increased bolt stretch and reduced bending stress.

In addition to the instrumented stationary gears, the pulley at the anti-drive end of the engine was re-designed to accept a Vibratech viscous damper. The balance of the engine hardware was carried forward from the previous build.

After a brief run-in at 5000 and 6000 rpm, the damper was installed. The engine was then operated at 5000, 6000 and 7000 rpm at moderate load and then at 6000 rpm over the full load range. This combination was chosen to provide early sensitivities to speed and to load.

At this point, the ABB ignition system was installed and several runs to 5000 rpm were made but engine operation was poor. The original ignition system was re-installed and the engine operation improved somewhat. The difference is possibly due to an extra ten degrees spark duration available with the original system. It is expected that with further development, the ABB system could be made to perform as well as the original system.

The engine was operated at 7000 rpm at loads up to 158 psi (10.9 bar) BMEP. During subsequent operation the chip detector alarmed. A small amount of debris was found and removed, the oil system flushed and test resumed. The damper was removed and the engine

operated at 6000, 6600, 6800, 7000 and 7200 rpm at approximately 86 psi (5.9 bar) BMEP. During the 7200 rpm point the oil pressure dropped followed by the sounds associated with bearing failure. Upon disassembly it was determined that the outrigger bearing had failed in a manner similar to that of the first build of the baseline engine.

5.2.3 Build A3 To address the outrigger bearing failure experienced on build A2, a comparison was made with the other main bearings. The differentiating feature is that the outrigger bearing is installed directly into the aluminum housing while all other main bearings are installed into an intermediate steel gear or bearing support. A steel hub was designed and procured for this build.

The new design rotors were completed and available for this build as well. The 8.0:1 compression ratio was chosen as the peak combustion pressures for the 8.4:1 rotor were expected to be unacceptably high. As with build A1, the ADE rotor was of the 4140 steel material while the DE was of the 17-4PH stainless steel material. For both rotors, the rotor gears were installed with a nominal line-to-line fit. New two-piece apex seals were used as well.

With the damper installed the engine was operated at moderate load and speeds from 5000 to 7000 rpm at which point it was discovered that the pulley nut had backed off completely. The pulley/damper adapter was re-assembled and the engine operated at 7000 rpm at loads up to and including the 75% cruise condition.

Once again it was discovered that the pulley nut had backed off completely. It was re-installed using a thread locking compound and a ten percent higher installation torque. With the intent of improving the fuel consumption, the fuel injection pump timing was advanced approximately 6°. The engine was then operated at 6000, 7000 and 8000 rpm up to and including the 75% cruise and the takeoff ratings. While cooling down at approximately 7200 rpm and 138 ft-lb (187 N-m), the ADE strain gage signal disappeared and the oil pressure dropped. The engine was shutdown manually and removed from test. Disassembly revealed that the instrumented anti-drive end stationary gear had failed.

5.2.4 Build A4 The failure of the instrumented stationary gear was not entirely unexpected for two reasons. Firstly, the gear was compromised structurally to permit installation of the strain gages in such a manner as to have useable output signal. Also, the gear loads measured were several times greater than expected implying stresses beyond the capability of the material.

The engine was rebuilt with standard stationary gears. A new rotor housing and apex seals replaced those damaged when the instrumented stationary gear failed.

The engine was run-in briefly and a trim balance performed at 7000 rpm. The HSUI fuel system was then installed. A number of problems with the electrical/electronic hardware

and the software surfaced during the early part of this test. These are described in further detail in section 6.1.5.

The engine was operated at speeds up to 7000 rpm and moderate loads. At 7000 rpm the system was unable to maintain rail pressure when load exceeded 140 psi (9.6 bar) BMEP at 7000 rpm. It was determined that the #2 pump head had seized. The M100 head was replaced and the engine run at 7000 rpm in an attempt to reach cruise was made. The engine shutdown at 160 psi (11.3 bar) BMEP. Both of the M100 heads in the pump had failed. Since sufficient spares were not available, the pump was returned to AMBAC for failure analysis and rebuild.

To permit continued testing, a Nippondenso A-pump (NR10182), similar to that used on the baseline engine, was reconfigured by installing 10mm plunger sets at the main plunger locations. A standard Nippondenso electronic governor was reconfigured to interface with the HSUI control system. With the rail/accumulator pressure at a relatively low setting to preserve the pump, the maximum load possible at 7000 rpm was 150 psi (10.3 bar) BMEP. A further increase in load to the cruise rating of 180 psi (12.4 bar) BMEP brought the speed down to 6500. The pressure relief valve setting was increase to permit higher rail pressures. After warming up, the engine was operated at 7000 rpm and 93 psi (6.4 bar) BMEP at which point the engine shutdown. One of the fuel pump plungers had seized.

The Nippondenso fuel injection pump was rebuilt with 9mm plungers having smaller and simpler helix grooves with the expectation of reduced plunger side loading (which was the cause of the 10mm plunger failure). To improve the lubricity of the fuel a small amount of fuel injector treatment was added to the fuel. The engine was operated at 6000 rpm at moderate and full load and then at the 75% cruise condition of 7000 rpm and 180 psi (12.4 bar) BMEP. During the 75% cruise point, the engine shutdown due to a seized plunger in the fuel pump. Since the program no longer had the resources to continue, the testing was concluded at this point.

5.2.5 Engine Performance Results.

Takeoff Rating. Build A4 of the advanced engine demonstrated the takeoff rating of 340 HP (254 kW) @ 8000 rpm with the pump-line-nozzle fuel injection system installed. The fuel flow rate at that point exceeded the capability of the fuel metering system display (199.9 lb/hr = 90.7 kg/hr). Thus the optimistic fuel consumption would be 200/340 = 0.588 lb/hp-hr (358 g/kW-hr). The peak combustion pressure observed during this point was 1600 psi (110 bar) which is well below the limit established for the takeoff rating. The observed performance of the advanced engine with the pump-line-nozzle fuel injection system is shown in Figure 5.2.5-1.

The combustion quality was acceptable but the shape of the combustion pressure trace indicates that additional pilot fuel would have improved the initiation of combustion and smoothed the combustion pressure rise. Unfortunately, the pilot flow rate of the pump-line-

nozzle system is fixed. Also the main injection duration was quite long and had the expected characteristics of a long, late burn, i.e., increased exhaust gas temperatures and increased specific fuel consumption. Although not optimized, the engine operation at the takeoff rating is considered quite good as none of the operational limits were exceeded.

Further development of the fuel system and turbocharger would provide improved performance. Due to other constraints, largely due to the time required to bring the HSUI system to an operational condition, this effort remains for the future.

Cruise Rating. The engine was operated on three occasions at the max cruise condition of 7000 rpm and 180 psi (12.4 bar) BMEP. The best observed fuel consumption was 0.495 lb/hp-hr (301 g/kW-hr) achieved with the pump-line-nozzle fuel injection system. With the HSUI fuel system, the observed fuel consumption at cruise was 0.524 lb/hp-hr (319 g/kW-hr). This was achieved using a pump-limited rail pressure of 7500 psi (517 bar); from single rotor engine testing it is known that bsfc performance would have been improved if a higher rail pressure could have been maintained. Unfortunately repeated failures of the fuel pumps precluded any optimization at this point. Either system falls short of the 0.435 lb/hp-hr (265 g/kW-hr) goal. The 7000 rpm data for the advanced engine as well as the previous engines is shown in Figure 5.2.5-2.

Experience with the single rotor rig engine indicates that the fuel consumption is quite sensitive to the configuration of the exhaust system attached to the turbocharger turbine outlet. As reported in the single rotor test section, the engine with an appropriate (tuned) exhaust system demonstrating fuel consumption performance consistent with the goals of this program. For the two rotor engine, further enlargement of the exhaust port, improved turbocharger matching and exhaust pipe tuning would likely provide the greatest gains toward achieving the fuel consumption goal.

HSUI Fuel Injection System. The experience with the HSUI system to-date shows the benefits of such a flexible system. The injection timings and durations are easily and independently varied. It also provided an ability to start easily and operate at low speeds (2500 rpm) by turning the main injectors off and running pilot nozzles only.

The electronically controlled Ganser-Hydromag injectors performed well. The problems experienced were nuisance items such as fuel leaks at the return fittings and electrical penetrations as well as electrical leads which were not particularly robust. This could be resolve by minor revisions to the design.

The shortcoming of the system as it stands are that the AMBAC pump has unsatisfactory reliability. Since the pump has more than adequate capacity, design changes could be made which would trade some of this capacity for improved reliability.

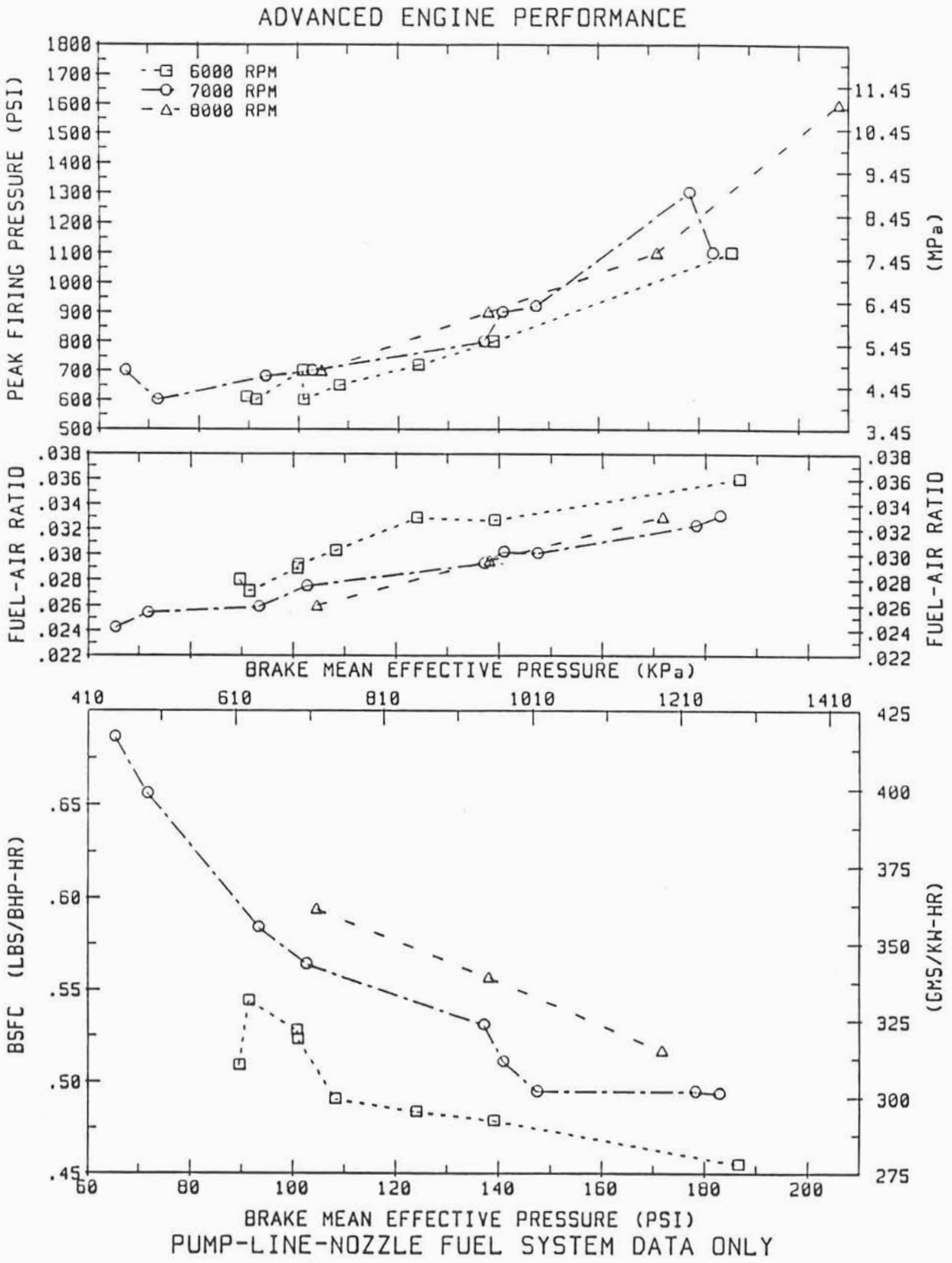

Figure 5.2.5-1 Advanced Engine Performance

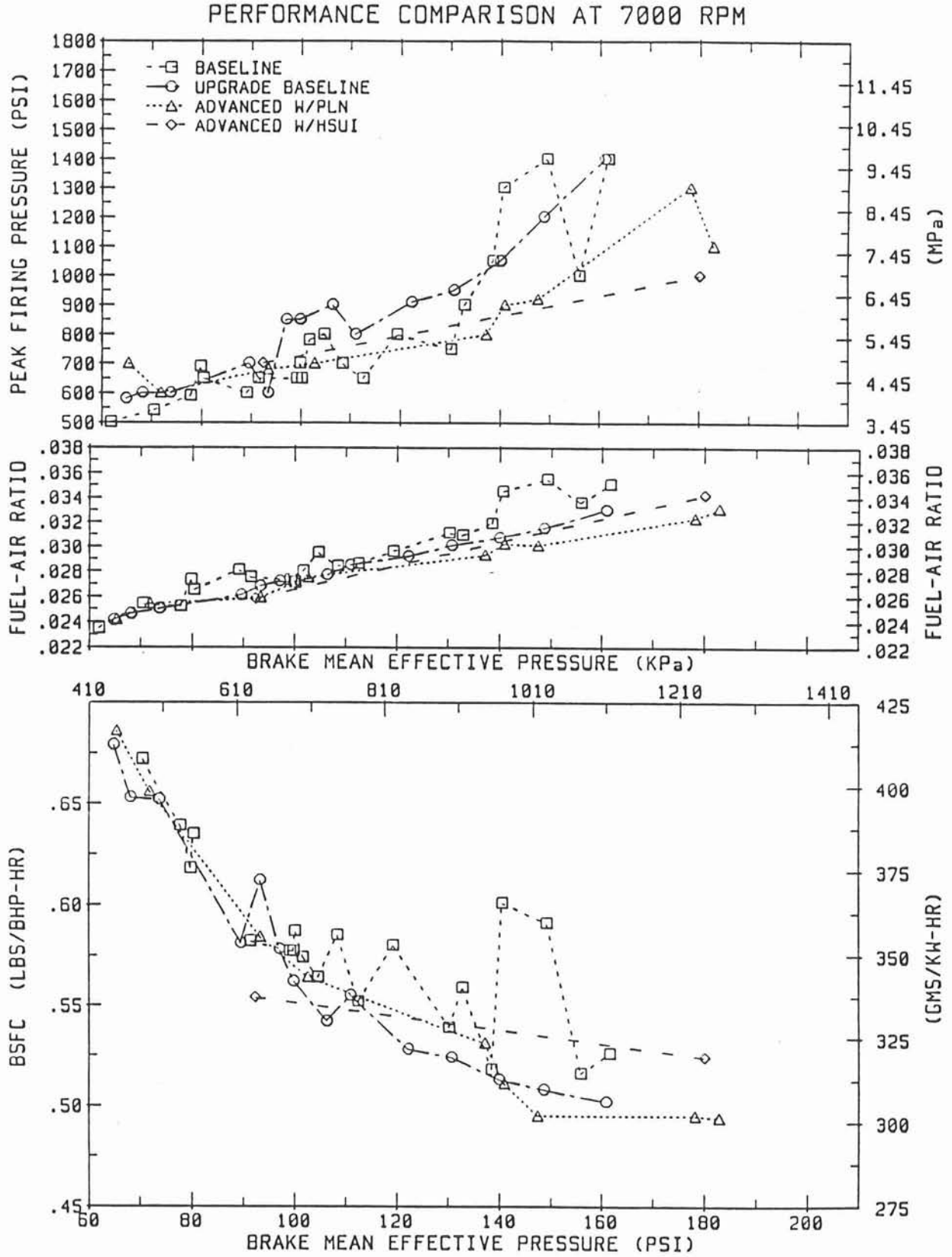

Figure 5.2.5-2 Two Rotor Engine Performance (7000 rpm)

5.3 MECHANICAL CORRECTIONS AND STATUS

The engine was operated for a total time of 23.5 hours and experienced three engine failures; rotor gear attachment bolts, outrigger bearing and an instrumented stationary gear. The fourth build of the engine did not fail.

5.3.1 Rotor Gear Attachment Screws For the advanced engine, special high strength bolts having a minimum ultimate tensile strength of 220000 psi (1500 MPa) were procured. Build A1 used SPS EWB22-4-14 bolts and experienced a failure which is attributed to the combination of a marginal joint design due to a rotor casting pattern error and excessive preload. As was noted, the casting pattern error resulted in the outboard half of the gear boss being unsupported. The subsequent builds of the advanced engine used necked-down SPS EWB TM9-4-12 bolts. These bolts were installed by measuring twist. The resulting preload, determined by test, is equal to the yield strength (assumed to be 80% of the minimum UTS). There have been no failures of this bolt in the 18:55 hours accumulated thus far. While this is encouraging, the low test time accumulated using this configuration demands cautious optimism.

5.3.2 Drive End Outboard Support Bearing A failure of the drive end outboard support (outrigger) bearing caused the termination of the test of the first baseline engine. At that time it was concluded that the bearing had insufficient interference fit. For the subsequent build, a bearing was selected which provided an interference fit as required by the blueprint. Also the tin plating, used as a preservative, was removed from the O.D. of the bearing shell. This bearing accumulated 72:35 hours at which point it failed in a similar manner during test of the advanced engine.

Since the other main bearings have been trouble-free for the 120 hours of this program, a comparison was made between those bearings and the outrigger bearing. The fits and clearances are similar. The remaining difference is that the outrigger is installed directly into the aluminum housing while the other main bearings are installed steel intermediate members. The steel hub provides additional support for the bearing, retains the room temperature interference fit at the operating temperature and provides an improved friction couple. For these reasons, a rework to the outrigger housing was designed which incorporates a steel hub. The initial results are encouraging though operating time with this new design is limited to 15 hours.

5.3.3 Instrumented Stationary Gear. The failure of the instrumented stationary gear was not entirely unexpected for two reasons. Firstly, the gear was compromised structurally by the circumferential groove ground into the outside diameter to permit installation of the strain gages in such a manner as to have useable output signal. Also, the gear loads measured were several times greater than the design load which implies stresses in excess of the fatigue limit of the material.

5.3.4 Rotor Gears As a result of earlier problems, the rotor gear was redesigned to include larger radii all around the base of the mounting lugs. To improve the material condition, the carburization previously limited to the gear teeth was extended include mounting lugs. The tooth root radius was also increased. The new design has two radii not smaller than .040" (1.0 mm) with a small, smoothly blended flat between. This is a considerable improvement over the approximately .020 (0.5 mm) radii in the failed gears. This design is identified as NJ12484 Rev. C.

Gears procured to the Rev. C design were introduced in the first build of the advanced engine and have not experienced any failures. While only 23:25 hours have been accumulated, the gears have been subjected to high power operation with high measured gear loading as well as gear attachment bolt failures and stationary gear failure without any indication of failure.

5.3.5 Rotor Bearings

Rotor Bearing Rotation. The first build of the baseline engine experienced rotation of both rotor bearings. The bearings which rotated were clinch-butt and had tin plating present on the outside diameter. All subsequent builds of the baseline, upgraded baseline and advanced engines have used welded-butt bearings. Since this change, 87 hours have been accumulated without any indication of rotor bearing rotation.

Rotor Bearing Failures. During this program one rotor bearing experienced a total failure of the liner; one other displayed, upon engine disassembly, a small area of surface fatigue. In the latter, a small section of the anti-drive end rotor bearing liner was lost during the third build of the baseline engine. This was attributed to a defect in the bearing and/or a high spot as indicated by a localized contact pattern on the bearing back.

During the first build of the upgraded engine, while operating at 8000 rpm, the anti-drive end rotor bearing experienced a more severe failure. The aluminum bearing liner had largely separated from the steel backing. A design review discovered an error in the bearing calculations which resulted in a revision which increased the bearing clearance. With the increased rotor bearing clearance, the engine has accumulated 50 hours without a repeat failure including operation at speeds and loads up to and including the 8000 rpm take-off rating.

5.3.6 Center Main Bearing Assembly

During disassembly of the first build of the baseline engine, three of the twelve center main bearing assembly bolts had failed. The assembly procedure was revised at that time and is more fully described in section 3.2.5 of this report. This procedure was followed during the advanced engine assembly and has proved to be trouble-free. At total of 87 hours have been accumulated without incident on center main bearings assembled using this new procedure.

5.3.7 Apex Seals

Testing of the second build of the baseline engine was terminated when the apex seals of the anti-drive end rotor were inspected and found to have flatted. This flatting was due to poor combustion quality, e.g. excessively high combustion pressure and rate of pressure rise. This problem was successfully resolved by rectifying the causes of the poor combustion, namely eliminating the injector timing jump (advance) at higher flows. During the subsequent baseline and upgraded baseline testing an additional 51 hours were accumulated with no signs of unusual wear with this three piece FerroTic apex seal system.

The advanced engine used an improved apex seal system. Both the geometry and the material were changed. This seal system is a two piece system with one corner seal and an apex seal of Gopalite material. The junction between corner seal and apex seal is at the side housing. Approximately 20 hours, including some very high power operation, have been accumulated without incident. (As should be expected at low hours, the seal wear is barely measurable and thus a seal wear rate calculation would be meaningless.)

5.4 - ROTOR GEAR DESIGN CONSIDERATIONS AND LOAD MEASUREMENTS

As has been noted in the various sections, several instances occurred of difficulties with the rotor gear and its attachment. This was an unexpected situation insofar as it had not appeared in previous testing with the single rotor engine which had run in prior programs to very high power levels, well above the scope of the current effort. However, during the current effort, the final single rotor engine of the previous contract was disassembled for observation and was found to have a broken gear. As also previously noted, the two rotor engine had been only briefly tested prior to this contract and never to speeds and power levels approaching the current goals.

Following attempts to improve existing gears by improving various radii between sections and shot-peening the sensitive areas, and attempts at improving the fastening, also not of large magnitude given the restraints of existing designs and hardware, it was determined that more drastic measures were required. First, new rotor gears were designed and procured. With the improvements in the various radii and in the carburizing of all the highly stressed areas it is estimated that the gear capability was increased in the order of a factor of two. In the limited amount of testing with these new gears there has been no failure. Another relevant factor is the change to provide a fit between the outer diameter of the gear and the rotor. The support thus provided substantially reduces the combined stresses in the rotor gear and reduces the variable load applied to the attachment bolts.

The design parameters were reviewed. It was reconfirmed that the original gear and attachment design was in conformance with the expected gear forces as predicted from prior rotary engine experience and also in accordance with gear loads as described in SAE paper No. 860562. In contrast, the failure experience was indicating that gear loads were higher than expected. To better understand the gear working environment, measurement of

the gear forces was initiated. Due to the difficulty of obtaining information from the moving rotor, the technique is to apply strain gages to the stationary gear in order to determine the forces which act equally on both gears. The gages are applied in a manner carefully constructed to be sensitive to only torque on the gear and not transverse forces.

All of the gear failures up to that time had occurred on the drive end rotor. To determine whether the forces were indeed different on the two different rotors in the engine, and gain insight into why, if so, both stationary gears were gaged. The gaged gears were run and measured in two different engine builds. This is the first time that data has been available from both ends of an engine: in fact most if not all prior data has been from single rotor engines. The instrumented stationary gears were statically calibrated and successfully installed into the engine for two different engine builds. Data was obtained throughout a range of engine loads from 6000 to 8000 RPM including measurements at the max cruise conditions and at take-off power.

Analysis of the recorded data confirmed higher than expected gear tooth forces. At times the gears in the opposite ends of the engine experienced unequal levels of forces but overall the maximum loadings of the two gears were approximately equivalent and it could not be concluded that the drive end was any more highly loaded than the anti-drive end. A resonance of sorts was observed in the gear load traces in the vicinity of 7000 RPM. No exact resonant speed was found and generally it was not a pure resonant condition although when attempting to correlate the crank-angle of gear load events with actual gear teeth it was found that the relative angle varied with different engine operating conditions which implies a phase change such as associated with resonant conditions. Thus no particular event was identified with any specific location on the gear.

The quasi-resonant condition was more a function of engine torque than of speed. At some speeds as engine load was increased the gear torque would go through an abrupt change in that it would become more regular or less regular and which would be associated with a change in force level. When this occurred, the forces could increase substantially on one of the gears and simultaneously decrease on the other. One example is shown of this in Figure 5.4-1. The resonant-like condition and the abrupt changes in recorded force pattern were not observed at 8000 RPM. The eventual failure of the instrumented anti-drive end stationary in the groove cut for the strain gages unfortunately resulted in a reduction of reliable data. The anti-drive end gear data is of suspect reliability for all of the 8000 RPM testing. The questionable anti-drive end gear indicated a continual increase in magnitude with increasing power at 8000 RPM whereas the drive end gear showed only a small increase in load with power, to the extent that at high power, the DE gear was less severely loaded at 8000 RPM than at 7000. It is possible that differences in gear loads (between banks or from load point to load point) result from differences in combustion characteristics of the two banks, which may obscure the test results, but in terms of simply the peak combustion pressures there was no evident correlation.

The test was run with and without a torsional vibration damper on the anti-drive end of the engine. No large differences in gear reaction were found with or without the damper.

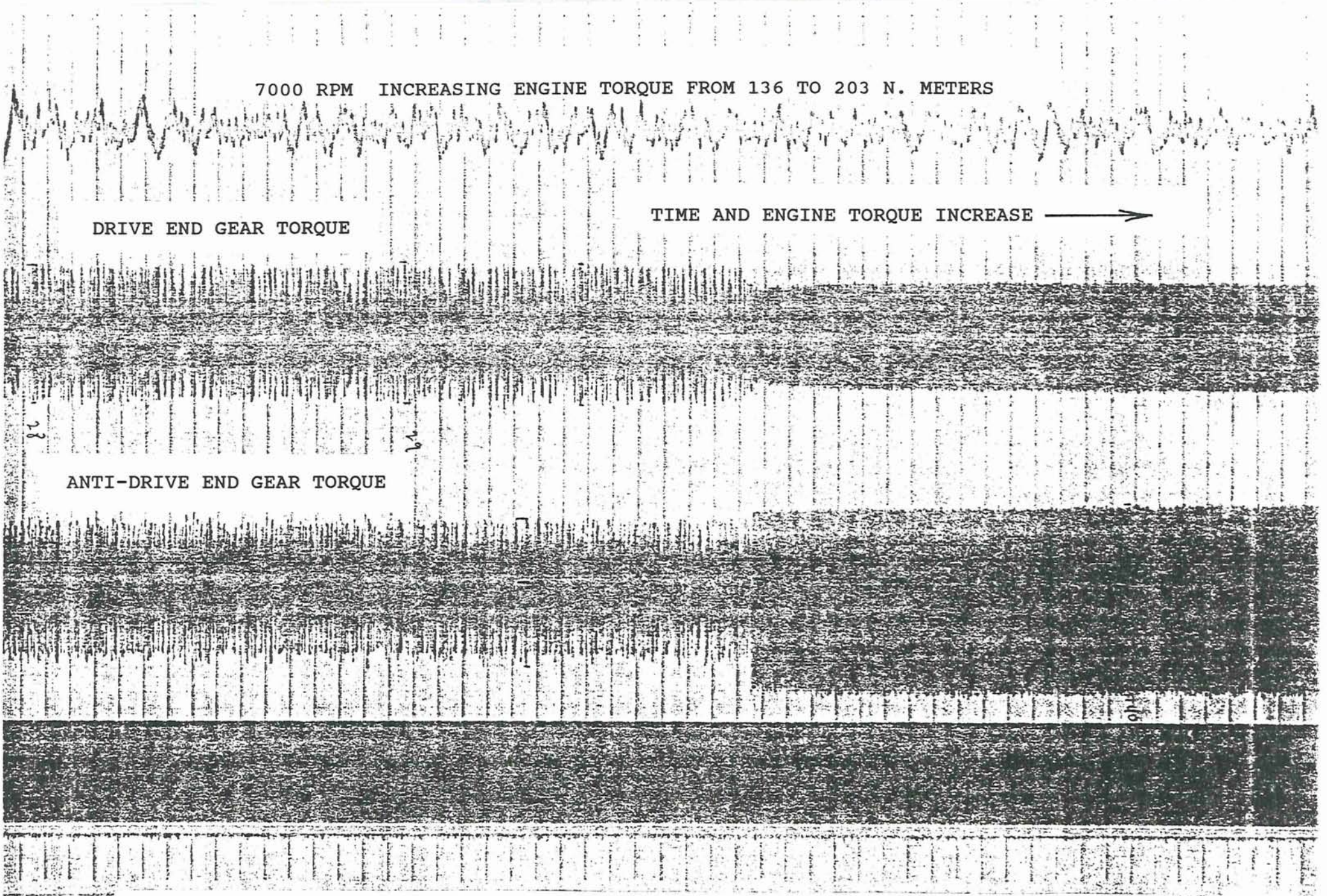

FIG. 5.4-1 MEASUREMENT OF FORCES ACTING ON THE STATIONARY GEARS

Also, and consistent with that result, no direct relationship was found between the gear loads and the crankshaft torsional motions.

The data collected has provided various guidance as to levels of load and trends with speed and load but it has proven dense in providing specific answers. The source of the gear forces was not determined nor were specific means of limiting or reducing the forces identified. Possibly continued study of the recorded wave forms would yield further insights but the scope of the current program could not support such an increase in the analytical activity. Based on the magnitude of the gear forces measured it appears necessary to introduce some improvement, preferably to reduce the forces, in future application of this engine at the higher speeds and power levels.

5.5 - TORSIONAL VIBRATION INVESTIGATIONS

5.5.1 Test Set-up

During the testing of engine 65202-3 a 60-tooth wheel was installed on the accessory end of the crankshaft for measurement of torsional motion, and on the drive end of the crankshaft the 117 tooth starter gear was utilized. Tooth counting was recorded during engine operation and was converted to torsional motion in the data analysis laboratory using an AE (Associate Engineering Developments Limited, Rugby, England) torsional motion analyzer. This unit synthesizes the torsional motion from the raw data of passage of the regularly spaced teeth past the pick-up. This output can be subjected to Fourier analysis to determine frequency and amplitude content.

The analyzer was calibrated against known, laboratory generated, torsional motion during the time period of the engine measurements. The calibration scanned a range of amplitudes to ±1.5° and frequency to 150 Hz, and confirmed reasonable accuracy of the instrument (significant errors were observed only at low amplitude). To check even further, a computer code was written in-house to also determine frequencies and components from the digitized tooth passage data. The two methodologies agreed in the initial engine data recorded after which the in-house program was not further utilized due to the resources required to acquire digitized data during test and the duplication of effort which would be entailed in continuing to perform the function in two ways. These latter considerations resulted in lack of a cross-check of the later data which indicated large torsional motions.

5.5.2 Test Results

The torsional motion data recorded during this test is shown in the chart which follows. The frequency response at 6000 RPM and 7000 RPM is almost pure first engine order. For the two locations, that is at both ends of the crankshaft, the torsional motions are in phase.

The large torsional motions (up to ± 9.0 degrees) measured on the engine flywheel were completely unexpected. This amplitude is considered erroneous in that the crankshaft could

not sustain the stresses that would arise from a repeated twisting of this magnitude. The amplitude of torsional motion measured on the anti-drive end of the engine is considered normal.

The chart also includes an estimate of the torsional motions that would be present at each of the two rotor locations if the amplitudes were accepted at face value. Knowing the torsional motion and frequency, the acceleration of the eccentrics and rotors can be calculated. The second chart lists the resulting stationary gear vibratory torques.

The largest calculated vibratory gear torque due to the torsional motions at the rotor locations occurs at the highest RPM and power setting, with a value of ±2018 in-lbs (228 NM). This is less than one third of the total torque measured on the instrumented gears, and as noted, is based on the measured but not accepted as valid high torsional motion measured at the flywheel. If it were assumed that the crankshaft torsional motion was everywhere equal to the motion measured on the opposite end of the crankshaft the resultant estimated gear stresses would be significantly less, by almost an order of magnitude, than shown in the chart for rotor No. 2. Under that unsubstantiated assumption the rotor gear stresses arising from the torsional motions are almost negligible.

During the final shutdown of the engine from 8000 RPM the stationary gear torque (of the one gear which remained intact with its gages) showed a sudden sharp increase as the engine speed passed down through the 7700 to 7000 RPM range. At that instant in time the concurrent torsional motion measurement showed no increase, tending to prove that the torsional motion is not the major contributor to stationary gear torque. This event also confirms that the sub-system resonance (rotor vibrating on the torsional spring of the stationary gear) is the major cause of the high vibratory torque measured on the stationary gear.

Additionally, as noted in the discussion of the gear torque measurements, the addition of a viscous damper to the accessory end of the engine did not have a large effect on the torsional amplitudes which also tends to confirm that the torsional vibration is not the most significant factor related to timing gear torques.

Analysis of the data recorded at low speeds during engine starts indicates that some sort of torsional resonance at 66 Hertz is present. The source of this resonance is unknown; the torsional analysis of the test cell drive-line does not show any natural frequency in this range.

5.5.3 Conclusions

1. Further study of torsional vibration data and measurement technique is necessary to understand and resolve the very large indicated motions at the engine flywheel and determine torsional motion data that can be accepted with confidence.

2. Although some of the torsional measurements are not understood at this time, it seems apparent that engine torsional vibratory motion is not the prime contributor to the large vibratory torques measured on the stationary gears.

3. The purpose of further study is that an understanding of the causes of the gear torques could lead to the determination of possible means to reduce their magnitude.

6.0 ACCESSORIES AND SYSTEMS - DETERMINATIONS AND EVALUATIONS

6.0 ACCESSORIES AND SYSTEMS - DETERMINATIONS AND EVALUATIONS

6.1 ADVANCED FUEL INJECTION SYSTEM

6.1.1 Selection and Design The stratified charge rotary engine (SCRE) achieves high power density by firing each combustion chamber one or more times per engine revolution. This places great demand on the fuel injection system. Figure 6.1.1-1 graphically shows the magnitude of the problem. The SCRE engine also requires pilot and main injection through separate injectors. Fuel must be able to flow from the pilot and main injectors simultaneously, so that the pilot and main injection events can overlap in time.

In addition to the speed and flow increases, the push for improved performance has driven a requirement for flexible and repeatable control of the injection timing and rate. Performance may be augmented by control over the flow rate at various times during the injection. A slow initial rate followed by a higher final rate seems to provide more consistent burn on a many engines.

Reliability and safety are important requirements for any engine. The HSEUI (High Speed Electronic Unit Injection) system was designed for use on an aircraft. For this application it is imperative that no failure mode can occur which completely shuts down the engine, since that would endanger the pilot and passengers in the airplane.

Concept selection

Several alternative fuel injection system configurations were considered in light of these design requirements, and the Electronically controlled high pressure common rail system was selected.

The system labeled Jerk Pump consisted of a conventional jerk pump coupled with a timing device.

The camshaft driven unit injector system was made up of electronically controlled unit injectors along with the two camshafts and the extra gear-train required to drive them in an engine of this configuration.

The Rotary Pump with Splitter Valve system considered an advanced rotary fuel injection pump with timing control coupled to a valve which split off a pilot injection into the injection nozzle.

The unit pump system considered unit pumps, the camshafts required to drive them, a timing device to provide timing, and individual control of the unit pump rack positions.

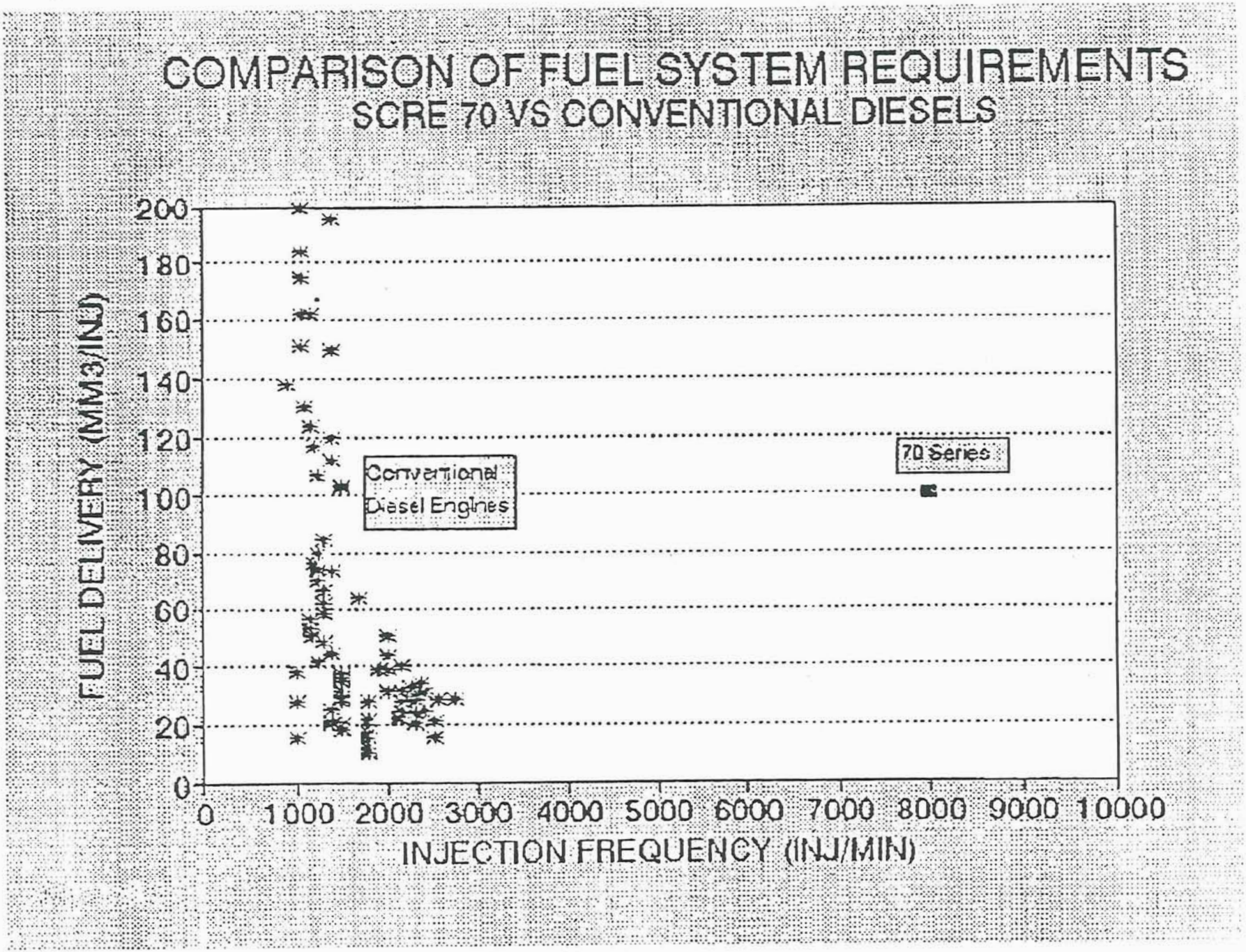

Figure 6.1.1-1 Fuel System Delivery Requirements Comparison

The high pressure common rail system consisted of two separate and separately driven high pressure supply pumps pumping into a common accumulator, appropriate check valves, and solenoid servo valve controlled injectors.

The intermediate pressure common rail system was the same as the high pressure common rail system except for a larger, lower pressure supply pump, accumulator, and all piping, and the addition of a hydraulic amplifier to the nozzle.

The systems were rated for safety, reliability, weight, timing control flexibility, and injection rate control flexibility. The results are shown below in Table 1.

Table 1: Fuel Injection System Evaluation

	Safety	Reliability	Weight	Timing	Rate
Jerk Pump	4	9	2	2	3
Camshaft driven unit injectors	5	10	9	6	3
Rotary Pump with Splitter Valve	3	5	10	4	3
Unit Pumps	9	8	3	2	3
Intermediate Pressure Common Rail System	9	5	8	10	5
High Pressure Common Rail System	10	7	10	10	5

Safety: the system safety was ranked based upon the likelihood of a single failure causing the engine to become uncontrollable. For the Jerk pump, any failure of the pump control rack, failure of any plunger, or failure of any component of the drive train would cause loss of control of the engine. The camshaft driven unit injectors would suffer loss of control from any failure of either of the two drive trains required on the rotary engine. Failure of any component of the pumping system would cause loss of control with the rotary pump system. The unit pump system could be designed so that only failures of the drive line would cause loss of control of the engine. If two separate drive lines were used, then no

single failure would cause loss of control of the entire engine, but the weight of the system would increase dramatically. For both the High Pressure common rail and the Intermediate Pressure common rail system, the potential weak point is the accumulator. The accumulator is a thick walled steel vessel with no moving parts. Chances of the accumulator failing are virtually nil.

Reliability: Reliability estimates are based on the number of parts and the robustness of parts. The rail systems rank below the jerk pump system in reliability because of the increased complexity of the injection nozzle and because of the added reliability concerns due to the electronic control system. The advantage of the high pressure rail system configuration is that the system can be designed to compensate for the failure of either supply pump without a loss of performance or with a preselected, limited power loss depending upon the design compromises chosen. Other failures can be compensated for in part by adaptive controls.

Weight: The system weight ranged to nearly 15kg while the best systems were around 10 kg.

Timing: A value of two implies timing control with about 15 degrees of engine rotation. The pilot and main timings can be varied together but not separately. Four implies some independent variability between the pilot and main injection timings over a limited range of approximately 20 engine degrees. Six implies independent pilot and main timing variability, with a somewhat larger range of timings. The only systems which provide completely independent pilot and main timing ranges were the rail systems.

Injection rate: All the camshaft driven systems were given the same rating for control over the injection rate shape. The reason for the low rating is that any significant change to the injection rate requires a change of hardware, such as changing a plunger or a camshaft. With the pump-line-nozzle systems, minor changes to rate and rate shape can be made by changing delivery valves or injection lines. The rail system were judged somewhat better, since the overall pressure and hence the average injection rate can be changed or continuously varied without stopping the engine. The injection rate shape can be changed by mechanical adjustments which modify the rate at which the injector opens. As with the pump line nozzle systems, changes to the injection rate shape can be accomplished by tuning the inlet tube from the accumulator to the injector.

System Design

Figure 6.1.1-2 is a schematic of the HSUI system. Two high pressure variable displacement pumps provide fuel through check valves into the accumulator. Solenoid controlled injectors meter the high pressure fuel from the accumulator into the engine. Pressure, speed, and timing sensors provide inputs to the Electronic Control Unit (ECU) which provides control signals to drive the pump displacement actuators and the Injectors.

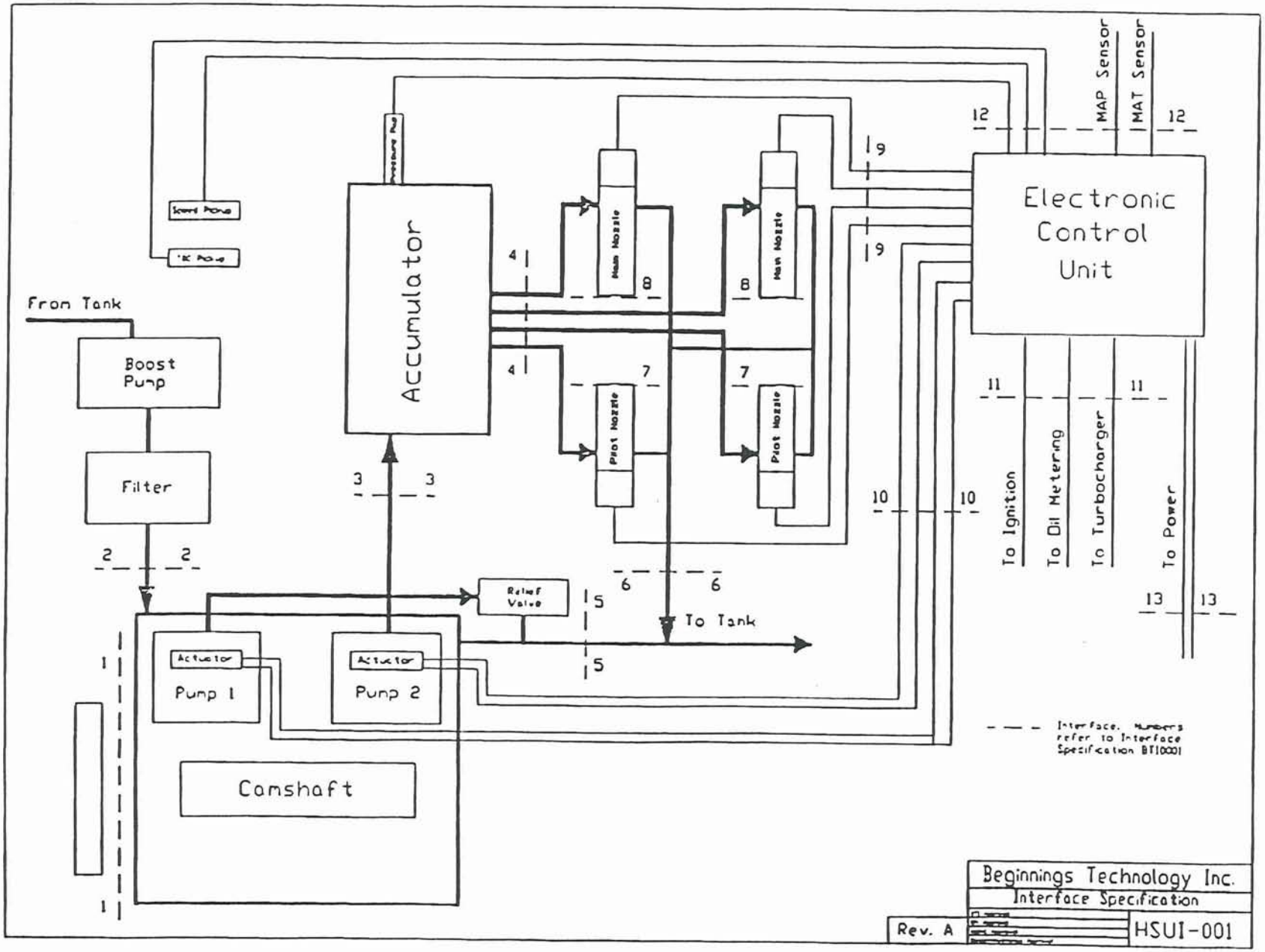

Figure 6.1.1-2 HSUI System Schematic

Injectors

The injectors are solenoid controlled servo powered devices designed and built by Ganser-Hydromag in Zurich Switzerland. The injectors are designed to accept "P" type injection nozzles. The nozzles for the rotary engine were extended in order to provide clearance for cooling passages and to prevent interference with the spark plug. The main and pilot injectors were identical except for the nozzle. This involved some compromise in pilot injector performance, limiting the minimum pilot injector flow to approximately 8 mm^3/ injection at 10000 psi rail pressure.

The injectors require some high pressure fuel to drive the servo mechanism which opens and closes the injection nozzle. The initial system design provided for a high pressure fuel loss rate which was 60% of the injected flow. As will be seen later, this rate is conservative.

Accumulator

The accumulator provides damping of the pressure pulses generated by the injection pumps and the injectors. It also provides part of the hydraulic pathway between the main and pilot injectors. Accumulator volume was approximately 60 cm^3. The accumulator volume was selected to limit the pressure pulses inside the accumulator to 7% of the rail pressure. This 7% variation is acceptable to the injectors as long as the pulses occur periodically with the engine rotation. The ratio of the accumulator volume to pump output at cranking speed is critical, since it determines how quickly the system will be at pressure and ready to fire the engine. In order to bridge the distance between the main and pilot injectors, the accumulator had to be approximately 15 cm long.

The accumulator was stepped, with a section 1.6" long made at .75" diameter and a section 3.5" long made at 1.25" diameter. This was to improve the damping of pressure waves which reached the accumulator and to prevent standing waves from building up in the accumulator when the engine passed through resonant speeds. Figure 6.1.1-3 compares the damping between a stepped and a single diameter accumulator.

High Pressure Pump

The high pressure pumps selected were AMBAC M50 hydraulic heads. These are sleeve metered distributor style fuel injection pumps. A distributor style pump was selected because it provides a large overall volume of fuel output for each pumping element. The M50 was selected as a result of AMBAC's experience operating this head with a variety of fuels, including gasoline, and because it is capable of operating at up to 12000 psi injection pressure. The need for safety dictates that an aircraft engine will have two independent supply pumps with separate drives. Since only dynamometer testing was to be performed, a single two headed injection pump which could be retrofit into the existing fuel injection

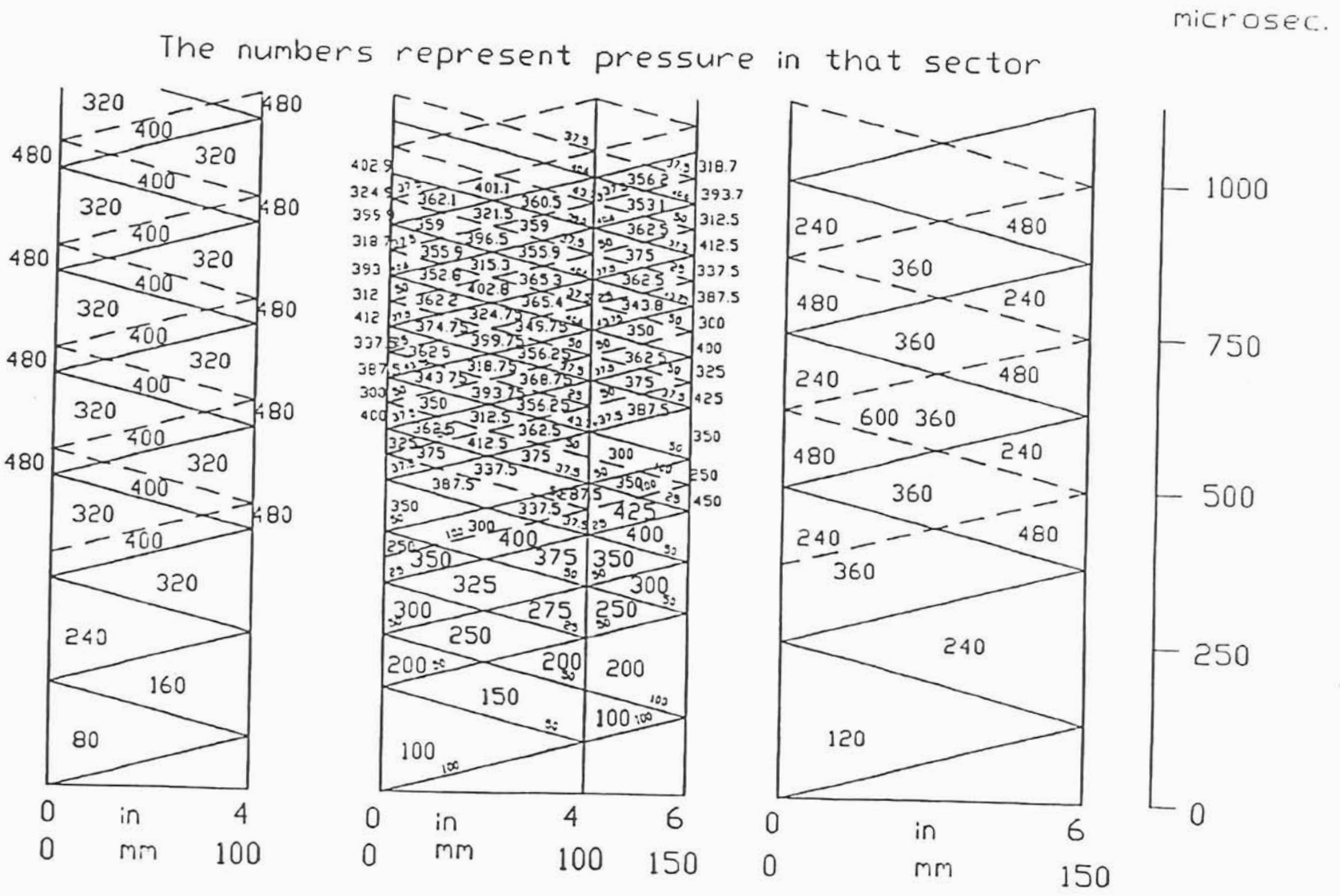

Figure 6.1.1-3 Comparison of Three Accumulator Designs

pump drive pad was designed. The hydraulic heads were independently controlled, but were driven from a common driveline.

In order to fit the existing engine and facilitate testing, the two M50 heads were installed in a cambox, making essentially a two headed M100 injection pump. This removed some of the difficulties which are inherent in developing a new accessory drive line and facilitated development of the fuel system and the engine.

Control System

The control system was based on an IBM 486 compatible PC operating at 66 MHZ. Two DA cards were used, one driving each bank of the engine. A counter timer card was used to input the speed and timing signals, and to output pulse width signals to the high pressure pump displacement actuators.

Interface boxes were designed which provided the high current (15 amps peak) required to power the fuel injectors and (3 amps peak) required to drive the pump rack control actuators. An interface box was added to protect the counter timer card by conditioning the input signals.

Software was developed to provide control of the fuel injection system and engine. The on-board memory of the DA cards was loaded with the desired output voltage as a function of engine angle. These output voltages were triggered from the engine timing sensor, so that bank two output waveforms were the same as bank one except for a 180 degree delay.

Initially a large number of data points was used, so that the resolution of the output signal was better than .1 degree. It was found that this precision was not necessary, and loading all those data points created a number of misfires. The final configuration had 720 data points and provided half degree resolution. Finer control of the injector duration was achieved by varying the voltage of the terminating data point.

The timing trigger signal from the engine was fed into the counter timer card, where it provided an interrupt. When this interrupt occurred, all four channels of DA output were set to the beginning of the on card memory, the engine speed was read from another channel of the counter-timer card, and the clock rate of the DA cards was set to provide two data points per engine degree of rotation. There was some difficulty learning how to reset and trigger the DA cards.

A second software task reads the accumulator pressure and adjusts the pulse width to the injection pump rack drivers using a PID control strategy This task operates independently of the injector driver task.

6.1.2 Preliminary/Enablement Testing

Due to the complex nature of the electronic high speed unit injector system, a thorough bench test was planned to evaluate the various subsystems as well as the complete system including a test with an operating ignition system to determine the interactions and sensitivities to the type of electrical noise expected on the engine.

The system was assembled in the RPI fuel lab using a Hartridge fuel injection pump stand. The first test was planned to characterize the AMBAC tandem M100 head pump as well as the ability of the control system to maintain a desired rail (accumulator) pressure. The system configuration for this test also included the accumulator/pressure relief valve/pressure transducer assembly and a single injector as well as the computer control system and associated driver circuits.

The system was first tested through the point of achieving electronic actuation of the injector at system pressures up to 6000 psi (nom. 400 bar). (Ref: Design operating pressure is 10,000 psi / 700 bar, testing to this pressure followed.) The needle lift instrumentation worked well as did the pressure feedback, rack feed back and accumulator.

The rack actuators on the AMBAC pump were "sticky": difficult to move and not smooth in operation. The pump rack moved easily but there was binding with the actuators assembled to the pump. Actuation was successful when the actuators were assembled loosely. Due to this difficulty, testing of the full control loop was not possible at this time. The pump was returned to AMBAC for correction.

A number of problems were experienced with the controller but have all been corrected by the supplier, including rework to the rack driver that had failed due to large voltage spikes returning from the rack control coils. Although not the sole cause, the "stickiness" in the actuators accentuated the voltage spikes. Extra protection circuitry and additional control software features were added.

Bench testing continued with a single head AMBAC pump intended for use with the single rotor rig engine. Initial operation of the pressure control showed severe pressure over- and under-shoots. It was determined that some of the parameters had been set as constants to inappropriate values. This required revision to the software.

One of the unknowns when designing the system was the effect of pumping into a constant high pressure rail. The M100 pump is designed to pump approximately 100 mm^3/injection through an injection line and a nozzle. Normally, the pump outlet is at minimal pressure at the beginning of the injection event. The pumping cycle involves bringing the system up to pressure, injecting fuel, and retracting some fuel from the system to rapidly drop the system pressure and prevent secondary injections. The only time there is significant pressure in the tube outside the pump is during pumping. The pumping duration is short, so there is little time for fuel to leak through the sealing surfaces internal to the pump.

With the HSUI system, accumulator pressure is applied to the pump continuously. The time available for leakage to occur is increased 10 to 20 times. While there are reasons to believe that little leakage will occur between pumping cycles, the effect of the high external pressure was unknown. A test was run with an existing M100 pump. The results are shown in Figure 6.1.2-1. The output at low pressures is 170mm^3/inj. instead of 100mm^3/inj. because the delivery valve retraction of 55mm^3 was removed. If the fuel were pressurized by a perfect process, the maximum output would drop from 170 mm^3/inj. to about 160mm^3/inj. due to the compressibility of the fuel. The results show that there is some 30 or 40 mm^3 of fuel delivery loss when pressure is applied to the M100 outlet. It is clear that a single M100 hydraulic head is capable of delivering over 120 mm^3/inj. in this application.

Figure 6.1.2-2 shows the flow efficiency of the main injector. About 20 percent of the high pressure fuel was required to drive the servo valve which opened and closed the injector needle. The data points were recorded while the fuel system was run throughout the speed and load range. The flow efficiency varied little with speed and load. The flow efficiency was considerably better than was assumed when the system was designed.

The pump was operated through the speed range; orifices were made and installed to provide the injection line with effective termination to damp reflected pressure waves. Unfortunately, the pumping rate of this pump has been found to be too high, more like a familiar "jerk" pump than a pressure supply pump as is required for proper operation of this type of system. It is believed that this is the cause of the 5000 psi (340 bar) pressure pulses observed in the injection line at high speed. Concern of over-pressure failure of the pump due to these pulses prevented testing of the accumulator to the 10000 psi (700 bar) target at this time.

A small accumulator was designed to be installed directly onto the pump outlet which reduces these pulses to 2500 psi (170 bar) or less which is expected to be adequate to operate throughout the desired range. These accumulators are also required on the tandem head pump intended for the two rotor engine.

The system was reconfigured to that required for operation of the single rotor rig engine by the addition of a second (pilot) injector. During testing it was found that the pilot injection trace was varying from injection to injection. This was determined to be the result of improper grounding in the control system. The power grounds and the signal grounds were run together, and during times of high current draw the signal ground was elevated, reducing power output to the injector. When this problem was solved, the injectors operated very consistently from injection to injection.

At this point, a difficulty with pilot sensitivity at low flow was noted. This was a consequence of requiring that the pilot and main injectors be of the same design except for the orifices drilled in the nozzle tip. This was improved somewhat by reducing the solenoid valve lift on the pilot injectors. Also, the resolution of the control system output was increased to gain some further control over the pilot injection. In combination, these

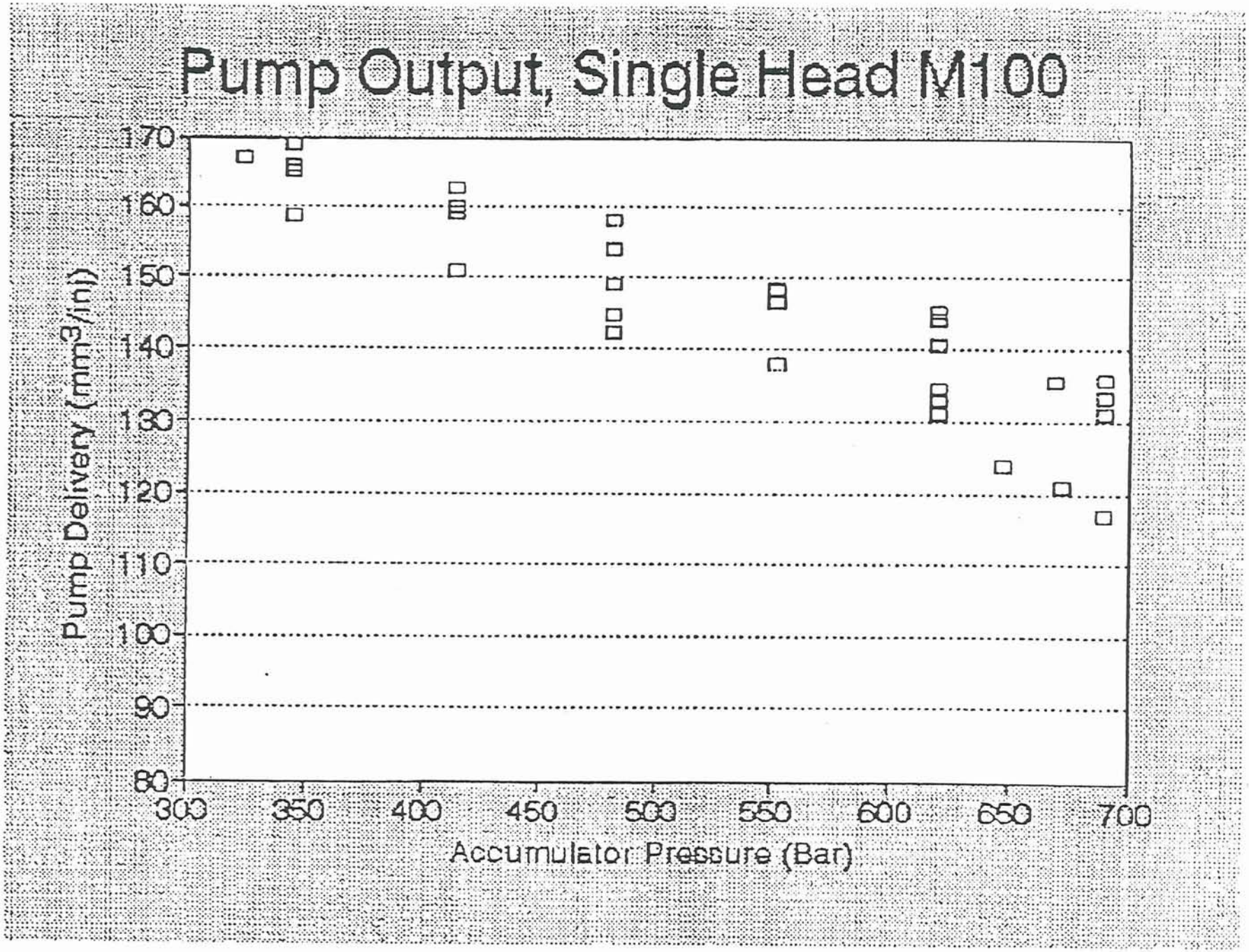

Figure 6.1.2-1 Single Head M100 Pump Delivery Into Accumulator

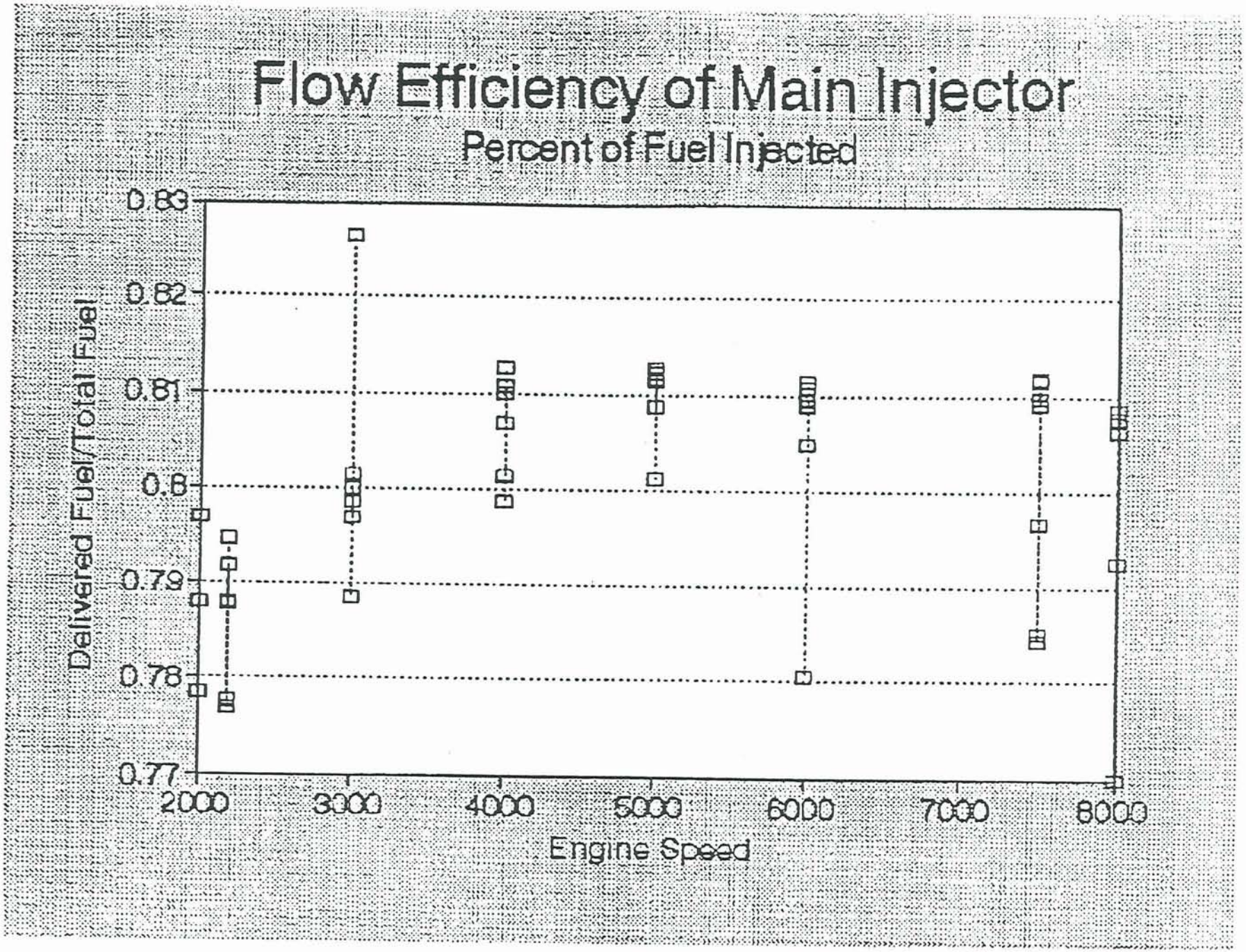

Figure 6.1.2-2 Flow Efficiency of Unit Injector - Configured with Main Nozzle

One very interesting conclusion which may be drawn from Figure 6.1.2-3 is that the power consumption is a much stronger function of speed than it is of load. This can be explained by the fact that the inefficiencies in the fuel injection pump occur at the beginning and the end of pumping, where the fuel is bleeding through orifices. The power consumption of this system could be improved by lowering the pumping frequency and increasing the quantity of fuel delivered in each stroke. By changing from a four lobed cam to a three lobed cam on the fuel pump, the power consumption could be reduced by approximately 1 Hp (.7KW). Further improvements might be obtained by optimizing the beginning and end of the injection stroke using such values as port area and plunger velocity.

6.1.3 Initial Engine Testing and Evaluation

Engine testing of the HSUI system was begun in March 1994 on the single rotor rig engine 65704-14. The system as installed included a fuel accumulator/pressure relief valve/pressure transducer assembly, an M100 single head AMBAC fuel injection pump, two Ganser-Hydromag electronic unit injectors and a control system developed jointly by Computer Systems Technology (CST) and Beginnings Technology Inc. (BTI). The initial nozzle spray patterns selected were the NR10540N34 (7F x .010") main and NR10541N250 (2B x .007") pilot.

Installation of the fuel system encountered no mechanical interferences but required modification of the test cell wiring harness as the nozzle control proved sensitive to the length of the control signal leads. Testing proceeded smoothly and without significant incident up to 6000 rpm and 114 psi (7.9 bar) BMEP (70 BHP = 52 kW). Operation at increased loads and speed produced significant engine misfires. These misfires, characterized by out-of-phase or missing fuel injection commands were traced to the control system misreading the speed. This was resolved by new control software which screens out the erroneous speed signals.

Performance testing continued up to and including the 75% cruise condition. The cruise power was demonstrated operating at three rail pressures of 7350 psi (500 bar), 8820 psi (600 bar) and 10000 psi (700 bar). At 7000 rpm, operation with the 500 bar rail pressure demonstrated a poor bsfc of 0.503 lb/hp-hr at 122 BHP (306 g/kW-hr at 91 kW); operation with 600 bar rail pressure provided an improved characteristic in being easier to obtain cruise power and demonstrated an appreciably improved bsfc of 0.467 lb/hp-hr at 128 BHP (284 g/kW-hr at 95 kW). Operation at 700 bar rail pressure was not generally as good as with 600 bar and demonstrated a best bsfc of 0.468 lb/hp-hr at 107 BHP (285 g/kW-hr at 80 kW) which rose to 0.484 at 126 BHP (294 g/kW-hr at 94 kW). In all cases the fuel consumption increased with increasing load but was least sensitive at the 600 bar rail pressure.

After approximately 25 hours of engine testing, the delivery valve in the fuel pump failed. It was replaced with an in-house spare and the testing resumed.

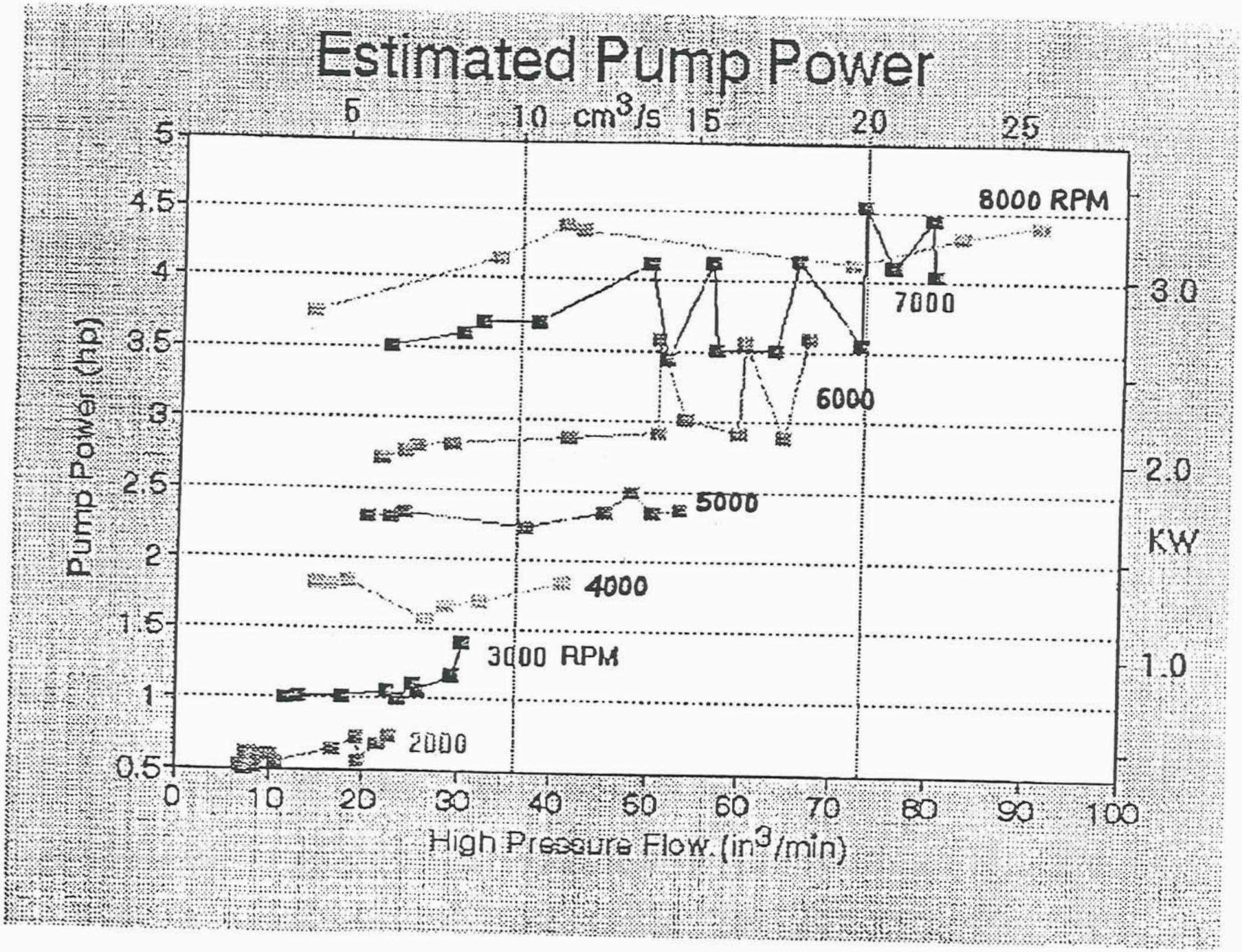

Figure 6.1.2-3 Estimated Pump-Drive Power - Tandem Head M100 Pump

The Ganser-Hydromag injectors provide for adjustment of the solenoid control orifice clearance. Increased clearance allows more rapid flow of fuel through the orifice which has the effect of increase the rate at which the nozzle needle lifts. Such an increased orifice clearance reduced the fuel consumption sensitivity to rail pressure observed previously. No further reduction of engine fuel consumption was obtained.

Four additional main nozzle configurations were evaluated. The first was the "N30" which the same 7F pattern as originally tested, except the orifices are smaller (0.009" vs. 0.010"). The fuel consumption at near-cruise condition was 0.460 lb/hp-hr (280 g/kW-hr) as compared to 0.466 lb/hp-hr (283 g/kW-hr) achieved with the original nozzle. The "N37" non-shadowing pattern (7G x .009) demonstrated the best fuel consumption performance achieved with this engine: 0.450 lb/hp-hr (274 g/kW-hr) at 7000 rpm and from 160 to 180 psi (11.0 to 12.4 bar) BMEP for an output of 114 to 129 BHP (85 to 96 kW). The remaining two patterns, the "N28" (7E x .009) and the "N32" (7H x .009) did not match the fuel consumption performance of the other two. The "N28" pattern demonstrated some useful reduction of peak firing pressure while operating at 8000 rpm. (Refer to Figure 4.3.2-2)

6.1.5 Two Rotor Testing

After a brief run-in of the engine the HSUI fuel system was installed on the fourth build of the advanced two rotor engine. A higher-than-expected number of electrical/electronic and software problems were encountered; these types of problems were believed to have been fixed during the considerable bench testing and single rotor rig engine testing. Changes made included adding a separate battery for the HSUI to eliminate problems associated with the large, periodic current draw of the ignition system. The sensor interface box failed. The control system computer timer/counter card failed; circuitry was added to the sensor interface box to protect the output stage of the timer/counter card. The system grounds were revised on several occasions to reduce the effects of ignition noise.

With those problems resolved, the engine was operated at speeds up to 5000 rpm and at moderate loads. The remaining problem was occasional major "drop-outs" and one instance where the control lost track of engine speed resulting in improperly timed main injections and multiple injections on bank #1. This problem was largely resolved by an upgrade to the software. The upgrade incorporated a feature to recover from glitches - usually extremely large indicated speed changes - within approximately 10 revolutions. At this point, it is probable that not all of the features developed during the single rotor engine test had yet been incorporated into the two rotor software.

The engine was now operating well. At 7000 rpm the system was unable to maintain rail pressure when load exceeded 140 psi (9.6 bar) BMEP at 7000 rpm. After determining that the main accumulator leakage was acceptably small, it was found that the #2 pump head had seized. A spare M100 head was reworked and installed in the pump in-situ. The engine was again run at 7000 rpm and an attempt to reach cruise was made. The engine shutdown

at 160 psi (11.3 bar) BMEP. It was determined that both M100 pump heads had failed. Since sufficient spares were not available, the pump was returned to AMBAC for failure analysis and rebuild.

A Nippondenso A-pump (NR10182), similar to that used on the baseline engine, was reconfigured by installing 10mm plunger sets at the main plunger locations and removing and plugging the pilot plunger locations. A standard Nippondenso electronic governor was reconfigured to interface with the HSUI control system. The engine was run briefly to determine control settings required for rail pressure stability. Some modifications to the system grounds, elimination of the speed signal to the governor and additions to the sensor conditioning circuits were also required. The pump mounted primary accumulators leaked; this leakage has been essentially eliminated by replacing the copper sealing washers with o-rings and backup washers.

With the rail/accumulator pressure at a relatively low setting to preserve the pump, the maximum load possible at 7000 rpm was 150 psi (10.3 bar) BMEP. A further increase in load to the cruise rating of 180 psi (12.4 bar) BMEP brought the speed down to 6500 rpm. The pressure relief valve setting was increase to permit higher rail pressures. After warming up, the engine was operated at 7000 rpm and 93 psi (6.4 bar) BMEP at which point the engine shutdown. One of the fuel pump plungers had seized.

The fuel injection pump was rebuilt with 9mm plungers having smaller and simpler helix grooves. This should reduce the pressure-induced side loading which caused the failure of the 10mm plunger. To improve the lubricity of the fuel a small amount of fuel injector treatment was added to the fuel. The engine was operated at 6000 rpm at moderate and full load and then at the 75% cruise condition of 7000 rpm and 180 psi (12.4 bar) BMEP during which the engine shutdown. The fuel pump had again seized a plunger. Since the program no longer had the resources to continue, the testing was concluded at this point.

6.2 - IGNITION SYSTEM

6.2.1 Definition and Selection

The specifications for a spark ignition system were prepared based on RPI's 70 series and 580 series Stratified Charge Omnivorous Rotary Engines (SCORE) which initiates combustion by igniting a small pilot charge which in turn ignites the air and fuel mixture in the combustion chamber. The major parameters for the ignition system effecting the combustion were identified as following.

Spark Duration	:	40°CA Desired for 150 to 10000 RPM.
Spark Energy	:	5000 mJ @ 150 RPM and 50 mJ @ 10000 RPM. Varying linearly between 150 and 10000 RPM as spark duration remains constant.
Spark Voltage	:	35 kV for spark gap of 0.070" at combustion pressure of 300 PSI.

Four different ignition systems listed below were considered for 70 series NASA engine development.

1. FOE (P/N 6305340) continuous spark ignition system developed by Autotronic for RPI's 580 series SCORE.

2. MSD 7, capacitive multiple spark discharge ignition by Autotronic.

3. HiFire inductive single spark ignition system by Mallory.

4. Continuous spark ignition by Plasmachine Inc.

6.2.2 Bench Test Performance

The FOE, MSD 7 and HiFire ignition systems were bench tested at RPI. The results are summarized in the table below. The Plasmachine ignition system was considered too expensive to buy for the bench test.

Ignition System	**RPM**	**Spark Duration °CA**	**Spark Energy mJ**	**Spark Volt kV**
FOE	150	80	6900	41
	10000	40	50	41
MSD 7	150	28	280	35
	10000	28	40	35
HiFire	150	1.8 (2mS)	200	35
	10000	72 (1.2mS)	110	35

The FOE ignition system was set to decrease the spark duration from 80°CA to 40°CA for speeds higher than 600 rpm but has capability of keeping the spark duration of 80°CA over the speed range of 150 to 12500 rpm.

As a result of bench testing, the FOE ignition system was selected for this contractual effort. ABB Process Analytics were awarded a sub-contract to build two ignition systems based on FOE ignition design. The ABB manufactured ignition systems (P/N NJ 13081)

were extensively bench tested, including spending considerable time for troubleshooting. Following are the results for comparison with the FOE ignition system.

Ignition System	RPM	Spark Duration °CA	Spark Energy mJ	Spark Volt kV
FOE	150	80	6900	41
	10000	40	50	41
ABB	150	78	6700	38
	10000	36	44	38

For the ABB ignition system the spark duration and energy were slightly lower than FOE ignition. No effort was made towards increasing the spark duration which would have also resulted in increased spark energy. The spark voltage difference may be a result of variation in simulated combustion pressure as set in the test pressure vessel as the two tests were performed at significantly different time intervals.

6.2.3 Engine Test

The first spark ignition system tested was a D&V (predecessor of FOE) ignition system. This system was tested on engine 65201-3 to improve the combustion process compared to the glow plug ignition system. The D&V spark ignition system helped to improve the BSFC and speed variation but was not capable of firing the engine above 6500 RPM. An FOE ignition system was then installed which eliminated the problem for firing the engine from start to 8000 RPM.

6.2.3.1 Optimum Spark Timing And Minimum Spark Duration Test. This test was conducted using the FOE ignition system on the single rotor rig engine 65704-13 for the purpose of determining the optimum spark timing and minimum required spark duration. The test data are recorded in the tables 1,2 and 3 below:

A. Test for optimum ignition timing at 4000 RPM, 60 PSI BMEP

Point No	Engine Speed RPM	DYNO LOAD lb	POWER[!] BHP	BSFC Lb/ BHP-HR	SPARK DURATION Start °CA	SPARK DURATION End °CA	PILOT INJECTION Start °CA	PILOT INJECTION End °CA	MAIN INJECTION Start °CA	MAIN INJECTION End °CA	MISFIRE OBSERVED PCPA/1000[@] Cycle, %	MISFIRE OBSERVED Oscilloscope Signal
178	4002	54.56	36.39	.5133	-56 2	-10	-49	-33	-39	-16	10.62	
179	4000	53.36	35.57	.5252	-51	-5	-49	-33	-39	-16	6.34	
180	4001	52.94	35.30	.5292	-46	0 3	-49	-33	-39	-16	5.56	
181	4007	52.49	35.05	.5330	-41	+5	-49	-33	-39	-16	4.5	
182	4008	51.34	34.29	.5448	-36	+10	-49	-32	-39	-16	5.44	
183	4002	51.02	34.03	.5489	-31 1	+15	-49	-31	-39	-16	7.51	
184	4000	50.78	33.85	.5518	-26	+20	-49	-30	-39	-16	11.19	*, *1
185	4004	50.34	33.59	.5561	-24	+18	-50	-32	-37	-15	12.22	*
186	4003	54.72	36.50	.5118	-60	-16	-50	-31	-39	-16	11.95	

*1 Misfire started for the spark starting at -30°CA and ending at +14°CA.

B. Test for minimum spark duration at 4000 RPM, 60 PSI BMEP

187	4003	54.03	36.04	.5183	-55	-15	-50	-31	-39	-14	9.05	
188	4001	54.09	36.06	.5180	-55	-20	-49	-30	-39	-15	7.81	
189	4006	54.10	36.07	.5179	-55	-25	-49	-30	-39	-14	9.12	
190	4000	54.23	36.15	.5167	-55	-30	-48	-30	-38	-15	9.26	
191	4003	54.05	36.03	.5185	-55 2	-35	-49	-30	-38	-14	9.04	
192	4009	53.80	35.87	.5208	-55	-40	-49	-30	-38	-14	8.96	
193	4004	53.76	35.84	.5212	-55	-45	-49	-31	-39	-14	8.62	*
194	3997	53.39	35.59	.5249	-50 1	-35	-49	-30	-38	-13	6.60	
195	4010	52.05	34.70	.5383	-45	-30	-49	-30	-38	-14	7.74	*
196	4008	51.13	34.09	.5480	-40	-25	-49	-30	-38	-14	6.77	*
197	4005	49.75	33.17	.5632	-35	-20	-49	-30	-38	-14	7.47	*

Table 1

! Power = Dyno Load x Engine RPM/ K_L, Where Load Constant K_L = 6000

* Combustion Pressure Signal on oscilloscope indicating misfire.

@ PCPA is RPI's peak combustion pressure analyzer which averages the combustion pressure over 1000 cycles and calculates misfire percentage.

1 Able to run without misfire.

2 Optimum ignition timing and minimum required spark duration.

3 + (plus) reflects °CAATC, - (minus) reflects °CABTC referenced to 0°CA as TC.

4 Pilot was advanced to reduce misfires for higher load at 7000 RPM.

5 Loss of load compared to previous test A in table 3 is due to reduced test cell fuel flow.

A. Test for optimum ignition timing at 7000 RPM, 65 PSI BMEP

Point No	Engine Speed RPM	DYNO LOAD lb	POWER[1] BHP	BSFC Lb/ BHP-HR	SPARK DURATION Start °CA	SPARK DURATION End °CA	PILOT INJECTION Start °CA	PILOT INJECTION End °CA	MAIN INJECTION Start °CA	MAIN INJECTION End °CA	MISFIRE OBSERVED Oscilloscope Signal
198	7002	40.08	46.76	.6328	-56	-10	-50	-22	-36	-2	
199	7005	39.72	46.34	.6385	-51 [1,2]	-5	-50	-22	-36	-3	
200	6999	38.90	45.38	.6520	-46	0 [3]	-50	-22	-36	-2	*, *[2]
201	6999	38.85	45.32	.6529	-41	+5	-50	-22	-36	-1	*
202	7003	37.70	43.98	.6728	-36	+10	-50	-22	-35	0	*
203	6996	36.29	42.30	.6995	-31	+15	-50	-22	-35	0	*

*[2] Misfire started for the spark starting at -49°CA and ending at -3°CA.

B. Test for minimum spark duration at 7000 RPM, 63 PSI BMEP

205	6999	38.83	45.30	.6532	-55	-15	-50	-22	-35	0 [3]	
206	6998	38.62	45.06	.6567	-55	-20	-50	-22	-35	0	*
207	6998	38.07	44.42	.6661	-50 [2]	-15	-50	-22	-35	0	

Table 2

A. Test for optimum ignition timing at 7000 RPM, 101 PSI BMEP

208	7000	62.03	72.37	.5274	-56	-10	-55 [4]	-29	-35	+4	
209	6994	62.26	72.64	.5255	-51 [2]	-5	-55	-30	-35	+4	
210	7002	60.18	70.21	.5437	-46	0	-55	-29	-35	+4	
211	7003	59.94	69.93	.5458	-41	+5	-55	-29	-35	+4	*
212	7002	59.40	69.30	.5508	-36	+10	-55	-30	-35	+4	*
213	7002	59.06	68.83	.5546	-31	+15	-55	-30	-35	+4	*

B. Test for minimum spark duration at 7000 RPM, 98 PSI BMEP

214	7001	60.20 [5]	70.23	.6191	-56	-15	-55	-30	-35	+4	
215	7001	60.02	70.02	.5327	-56	-10	-55	-30	-35	+4	
216	7001	59.99	69.99	.5329	-56	-20	-55	-30	-35	+4	
217	7001	59.81	69.78	.5345	-56 [2]	-25	-55	-30	-36	+4	
218	6999	59.39	69.29	.5383	-56	-30	-55	-30	-35	+4	*

Table 3

6.2.3.1.1 Summary - Spark Timing and Duration

A. Test data from table 1 A. shows that at 4000 RPM, the engine was able to run without noticeable misfires with ignition timing as late as 31°BTC for the pilot injection start timing of 49°BTC. Engine load loss (7.5%) and higher (6.9%) Brake Specific Fuel Consumption (BSFC) at ignition timing of 31°BTC were observed compared to 56°BTC ignition timing for same spark duration (46°CA) and fuel pump rack position.

B. Test data from table 1 B. shows that the engine was able to run without noticeable misfire with minimum spark duration of 15 crank angle degrees (CA) from 50°BTC to 35°BTC (15°CA) for the pilot injection duration from 49°BTC to 30°BTC (19°CA). Engine load loss (1.18%) and higher BSFC (1.27%) were observed for the spark duration of 15°CA (50° to 35°BTC) compared to 20°CA (55° to 35°BTC) and 40°CA (55° to 15° BTC) spark durations for the same pilot injection duration and fuel pump rack position.

C. Since the data observed on RPI's Peak Combustion Pressure Analyzer (PCPA) was not a reliable indicator of misfire compared to the combustion pressure signal observed on oscilloscope for the 4000 RPM test, we did not use PCPA for the 7000 RPM test.

D. Test data from table 2 A. shows that the engine did not tolerate any spark duration start time (ignition timing) later than pilot injection start timing at 7000 RPM and light load. Test data from table 2 B. shows that minimum required spark duration to minimize misfire was from 50° to 15°BTC (35°CA) for the pilot injection duration from 50° to 22°BTC (28°CA). This indicates that spark duration should cover the pilot injection duration completely at 7000 RPM and light load.

E. Test data from table 3 A. shows that the engine was able to run at the spark duration of 46° to 0°BTC (46°CA) without noticeable misfire but with significant load loss and higher BSFC compared to the spark duration of 51° to 5°BTC (46°CA) for the same pilot injection duration of 55° to 30°BTC (25°CA) and fuel rack position. Test data from table 3 B. shows that minimum required spark duration was from 56° to 25°BTC (31°CA) for the pilot injection duration of 55° to 30°BTC (25°CA).

F. Highest pilot injection duration was observed of 28°CA at 7000 RPM and light load. For such a case the minimum required spark duration was 35°CA (0.84 milliseconds). Coincidentally, the minimum required spark duration of 20°CA for the pilot injection duration of 19°CA at 4000 RPM reflects 0.84 milliseconds time wise. This condition may not be true for different engine speed and load as the pilot injection duration in terms of °CA and pilot fuel flow may not vary significantly with engine speed and load.

6.2.3.1.2 Conclusion of requirements based on the single rotor testing.

A. The ignition system should be capable of supplying minimum spark duration of 35°CA for a maximum pilot injection duration of 28°CA. This reflects a spark duration of 39 milliseconds for the starting speed of 150 RPM.

B. Optimum ignition timing is the start of the pilot injection.

C. The off-the-shelf inductive ignition system has a maximum spark duration of 2 millisecond and spark energy of 200 millijoules (Mallory Promaster coil and Hifire ignition control) and may not be able to start the engine at 150 RPM but may be able to start at 2500 RPM as 2 millisecond reflects 1.8°CA at 150 RPM and 30°CA at 2500 RPM.

6.2.3.2 Mallory inductive ignition test on engine 65704-13

Based on the data acquired from the previous test (6.2.3.1) Mallory HiFire ignition control and Promaster coil were tested on engine 65704-13. The Mallory ignition system is capable of providing fixed 2 millisecond (30°CA at 2500 RPM) of spark duration below 6000 RPM and fixed 1.2 millisecond (43°CA at 6000 RPM) of spark duration. This ignition system was not able to keep fixed ignition timing at the starting speed of 2500 on dynamometer test. The engine seemed to be firing inconsistently at several occasions. The ignition triggering signal from the Hall effect sensor observed on oscilloscope was neither following the target profile of 50% dwell angle nor was able to keep the timing constant. This may have occurred due to HiFire ignition control loading the trigger sensor. The test was concluded at this point. Further effort to correct the trigger signal is necessary. However Mallory ignition system may not be adequate to start the engine at lower than 2500 RPM.

6.2.3.3 ABB Ignition (P/N NJ 13081) test on Engine 65202-2

The ABB ignition was tested on the advanced core engine 65202-2. The engine was not running well at 5000 RPM with ABB ignition. There was slight improvement in engine operating condition with FOE ignition (P/N 6305340) system installed. The ABB ignition had spark duration of 36°CA as opposed to 40°CA for FOE ignition system. Further attempt was not performed to increase the spark duration and energy for ABB ignition system so as to not interfere with continuation of the gear load test. This test is not conclusive as the engine ran poorly at 5000 RPM with the FOE ignition system also. The ABB ignition was not further tested and the balance of the test program was completed using the FOE ignition system.

Because the ABB ignition is essentially equivalent to the FOE ignition it is believed that it could be made a satisfactory unit for this engine. Possibly the duration needs to be increased by the approximately 4°CA by which it differs from the FOE unit. Increase in the

duration concurrently increases the spark energy in proportion. The increase is a simple matter of signal voltage increase for the duration control. It is expected that the unit is capable of the energy increase.

6.2.3.3.1 Conclusion

Engine operation with the ABB ignition system was demonstrated although not to total satisfaction in the little time made available. The results indicate that the system can be easily modified to perform equally to the satisfactory FOE unit. Thus an alternate ignition unit has been identified and the technical specifications to duplicate it are available.

Also the inductive ignition system was shown to have significant capability and is a possible alternative candidate with the reservation that it may be incapable of starting the engine below 2500 RPM.

6.3 - TURBOCHARGER SYSTEM

The turbocharger for the baseline engine was a Mitsubishi TD08H-23K-33cm^2. It was determined early in the program that this hardware would not suffice at the higher flow rates required by the engine when operating at the 340 BHP (254 kW) @ 8000 rpm takeoff rating. Available data for the single rotor rig engine was reduced and extrapolated to the cruise and takeoff ratings and adjusted for the two rotor engine. Several turbocharger manufacturers were approached with this data and asked to recommend a suitable turbocharger for this application.

Schwitzer recommended and RPI procured a model S4DS006 turbocharger. Schwitzer did not perform an in-depth analysis but made the recommendation on the basis that the compressor matched the expected flows and that the turbine section was suitably large.

Allied Signal (Garrett) was contacted but offered no assistance or guidance of any type.

Mitsubishi analyzed the data and offered an experimental TD09 turbocharger with a recirculating compressor cover and an alternate turbine housing with the stipulation that the hardware would not be used on a vehicle of any type. The recommended hardware was procured.

The advanced engine was tested with the Schwitzer S4DS installed. With this turbocharger, the airflow observed at the cruise condition was 3900 lb/hr (1770 kg/hr) which is approximately ten percent above that predicted. A similar situation occurred at the takeoff rating where the observed airflow was 4700 lb/hr (2130 kg/hr).

The performance of this turbocharger was satisfactory for this test. According to the compressor map, the flow observed at the takeoff rating is essentially the maximum

available with this particular model. Should the engine require additional airflow, a model with a higher flow compressor should be selected.

Due to limited resources and brief test period of the advanced engine, the alternate (Mitsubishi) turbocharger was not evaluated.

7.0 SUPPLEMENTARY STUDIES - WEAR TESTING

7.0 SUPPLEMENTARY STUDIES - WEAR TESTING

7.1 Purpose of Wear Test Program

Cast 17-4PH steel had been the material utilized in the rotors for high performance testing in the previous NASA contract. The 17-4PH material was selected primarily because of high strength property requirements and its castability is comparable with other cast steels. This material is, however, highly susceptible to fretting, galling and material transfer in high contact stress and relative motion situations such as is experienced in the apex seal to rotor slot environment. As a consequence, compatibility of apex seals with the rotor slots has been of concern. Requirements of this application include to maintain a low coefficient of friction and to avoid excessive wear. To achieve seal/slot compatibility prior testing of the 17-4PH rotor has been with a low friction electroless Nickel-Thallium-Boron coating (Ni-Bron) applied to the apex seal slot walls. The slots thus coated have been moderately successful but some fretting and some apparent loss of the coating had been observed after long term engine tests.

7.2 Plan

In the current program it was concluded in the initial evaluation and planning to address to this concern which could potentially be critical to sustained operation at the high power levels planned. The directions chosen were to change the rotor to a material considered more compatible for the friction/wear couple. 4140 steel was the chosen alternative, based on comparable strength properties and as a commonly cast material. It was found that with careful planning and procurement some examples of each material rotor could be utilized and evaluated in the program at little added expense. Unknown was whether the 4140 would prove to be compatible with the apex seals.

A wear rig test program was initiated to evaluate the relative compatibilities of 29 current and alternative rotor and apex seal materials and various coatings or other surface treatments that could be identified as applicable. This would provide guidance as to the acceptability of bare 4140 slots and provide for an appropriate coating in the event that there would be a compatibility problem. Alternative coatings would be applicable to either rotor material.

7.3 Test Procedure and Results

The testing consisted of evaluating a large combination of materials utilizing a LFW-1 ring-on block wear tester which has shown to be a fairly reliable screening device for determining wear/compatibility of material combinations. The testing was supplemented by prior results and with essentially simultaneous similar effort for the USMC contract. Complementary testing was achieved to benefit both contracts without duplication of effort.

A total of 42 separate ring-on-block tests were run with the 29 different material combinations. Some of the tests served as "baseline" representing current rotor and apex seal materials for comparison; some tests were run in duplicate or for longer test periods to confirm results of promising couples, and a few tests were declared invalid because of apparent failure to achieve the control test conditions. Based on the results of the LFW-1 wear rig testing the material couples which were not previously engine tested and that would be recommended for engine evaluation are as given in the following table.

Material couples not previously engine tested which should be considered for evaluation on engine hardware:

ROTOR SLOT TREATMENT/COATING	APEX SEAL
Lube-Lok 7000	Gopalite/Ion Gopalite
Enplate NI-428	Gopalite/Ion Gopalite
Enplate 9095	Gopalite/Ion Gopalite
17-4 PH Bare	CIW-15
4140 Bare	CIW-15
17-4 PH Bare	Gopalite/Ion Gopalite

A material developed by NASA, PM-212CM, was considered during this activity. It had been wear-rig tested in a previous program with encouraging results and recommended for engine testing against three trochoid surface candidates including Tungsten-Carbide Cobalt which was current at that time. This is a powder metallurgy composite with self lubricating properties, comprised of 70 wgt % chromium carbide, 15% silver and 15% calcium fluoride/borium fluoride eutectic. In the current program it was considered beyond the practical scope to introduce another apex seal material in consideration of the inability to dedicate a special engine build or to achieve reliable back-to-back performance comparisons. The material, in the PM-212PS form, was a top candidate for slot coating as the encouraging wear results for use as a seal also apply to its probable suitability as a slot coating. However, as a sprayed material it was concluded by consultation with potential suppliers of sprayed coatings that it could not be applied to a satisfactory depth into the narrow rotor slots.

A more complete description and discussion of the wear testing, including a chart of the results of all tests and supplemented by comments on some engine testing in the USMC program, is provided in the appendix.

The net result for the current program was to cast doubt on the suitability of bare 4140 and thus it was not engine tested. Both 4140 and 17-4PH rotors were tested in the program as planned but in both cases the NiBron plating was utilized. In spite of initial reservations

the coated slots were satisfactory in all regards. For future consideration, engine testing in the USMC program has resulted in encouraging results with some apex seal materials in un-coated slots, as can be seen in the report appended.

8.0 CONCLUSIONS

8.0 CONCLUSIONS

8.1 Engine Performance Status. During the course of this program, the output of the two rotor engine was raised from the baseline rating of 200 BHP (149 kW) @ 6000 rpm to the advanced engine rating of 340 BHP (254 kW) @ 8000 rpm, thereby achieving one of the primary objectives of the program.

The specific fuel consumption of the two rotor engine observed at the 75% maximum cruise condition was 0.495 lb/hp-hr (301 g/kW-hr) which fell short of the 0.435 lb/hp-hr (265 g/kW-hr) goal. The most recent testing of the single rotor rig engine indicates measurable sensitivity of the fuel consumption to the configuration of the exhaust pipe downstream of the turbocharger. At the cruise condition, the fuel consumption of the single rotor engine varied from 0.49 to 0.46 lb/hp-hr (300 to 280 g/kW-hr) for the exhaust pipes tested. Unfortunately this was determined too late in the program to "tune" the exhaust pipe or experiment with the exhaust manifold configuration for the two rotor engine.

8.2 Engine Mechanical Status. During the course of this program a significant number of new failure modes (for this engine) were identified. Corrections were introduced for every item and the majority of these corrections have been proven. The most persistent and challenging of these are the rotor gear and rotor gear attachment failures. Stationary gear torque and torsiograph data were obtained throughout the operating range. The analysis of this data shows gear loads several times higher than expected based on earlier single rotor rig testing (1985).

The factors causing the high gear loads are difficult to resolve from the data. The contributing factors are the torsional vibration of the crankshaft, rotor/rotor gear/stationary gear subsystem resonance and possibly pressure gradients which may exist on the combustion face of the rotor. Torsional vibration is typically addressed by a damper. The viscous damper tested on the second and third build of the advanced engine reduced the magnitude of the gear load only slightly and there was not good correlation between gear loads and torsional vibration. A second variation of damper with reduced viscosity has been procured but not tested.

The possible contributors to high gear loads were not resolved during this program. The pressure gradient on the combustion face of the rotor is believed to be minimal and would be further reduced as the combustion is improved through the course of development. Several changes to the stationary gear and rotor gear have been contemplated as means to changing the subsystem but would require manufacture of new gears which is beyond the time frame of this program. Complete and satisfactory resolution of the rotor gear problem remains to be completed.

During the baseline and upgraded baseline testing, two rotor bearings failed and two rotated. The rotation problem was resolved by changing from clinch-butt to welded-butt

design and by removing any coating from the outer diameter of the steel bearing shell. The liner failures experienced have apparently been resolved by the increase in bearing clearance. The advanced engine was operated over a very wide speed and load range and experienced no rotor bearing problems. For the future, the performance margin that the longer, original rotor bearing would provide makes a strong case for its inclusion in any new hardware.

The outrigger bearing failure has been addressed in the advanced engine by the addition of a steel hub as an intermediate structure between the bearing and the aluminum housing. This mimics the other (trouble-free) main bearings and was successful during the limited testing of the third and fourth builds of the advanced engine.

The center main bearing support assembly screw failures were addressed by additional controls during the assembly process to assure that the components are installed as intended by the design. This problem has not repeated during the 87 hours and three disassemble/assemble cycles since the failure and appears to have been fully eliminated.

8.3 Accessories System Status.

Ignition Systems. During the course of this contract, several ignition systems were tested. The initial testing with glow plugs showed poor combustion quality. The engine was converted to spark ignition using a control system developed for another engine program at RPI. This system, designed and manufactured by Autotronic Controls Corp (ACC), is generally referred to as the D&V system. At speeds above 6500 rpm, the ignition system was unable to fire the spark plug every revolution of the crankshaft. The problem was that the energy required exceeded the capability of the ignition control. It was replaced with an improved control, also designed and manufactured by ACC, referred to as the FOE system. The FOE system was able to operate over the speed and load range without any problems.

For this program, Asea-Brown-Broveri Process Controls Subcontracting (ABB) manufactured two ignition systems based on the FOE design. Upon receipt at RPI, the systems were throughly bench tested. The system required the addition of a cooling plate. This was engineered at RPI and the system performance is satisfactory. When tested on the engine, the combustion performance was slightly worse than that observed with the ACC/FOE ignition system borrowed from another program. Due to schedule constraints, the system was removed from test without further development. It is believed that increasing the spark event duration of the ABB ignition system would provide performance similar to the ACC/FOE ignition system.

Turbochargers. The Schwitzer turbocharger performed as expected, well matched to the engine, with flows typically ten percent higher than predicted. The compressor was apparently at its limit during operation at the takeoff rating. The hardware is quite robust having survived many hot shutdowns. Unfortunately time did not permit evaluation of the special Mitsubishi TD09 turbocharger.

Electronic High Speed Unit Injector (HSUI) Fuel System. The HSUI fuel system has been developed to the point where the control system, accumulator and electronic unit injectors are functioning well. A minor problem with fuel leaking from the injectors can be resolved by improved sealing of the leakoff fitting and sealing the electrical wires or replacing them with sealed terminals.

The AMBAC fuel pressure supply pump experienced several failures. To permit continuation of test, a Nippondenso "A" pump was reconfigured for this purpose but it also experienced several failures. The AMBAC M100 head was selected for this system due to its high pressure, high speed capabilities and demonstrated reliability on other applications. It is believed that with further bench testing and development, the M100 can be made to be reliable in this application as well. This step is necessary for the HSUI to be a viable fuel system.

8.4 Overall Summary and Engine Status. During this program, the technology developed during the preceding programs using the single rotor rig engine was applied to the two rotor system. With improvements to the charge air system (intake and exhaust ports and manifolds and turbocharger) the cruise and takeoff power demonstrations were performed with a conventional pump-line-nozzle fuel injection system. With an advanced, electronic high speed unit injector system the cruise rating was again achieved. The fuel consumption was higher than the goal, possibly as a result of an un-tuned exhaust system and low rail pressure. Little optimization was possible due to the limited time available for test once the HSUI system was made operational on the two rotor engine and the repeated pump failures. Further development of the fuel system, turbocharger and exhaust systems should provide the means for the two rotor engine to match the fuel consumption of the single rotor rig engine and thereby achieve the goal.

The two-rotor engine demonstrated several mechanical problems. Corrections were defined and applied to all difficulties encountered. For the majority of these, effectivity has been demonstrated to the extent of the test time accumulated during the contract effort. To be a viable powerplant for any application, further understanding and resolution of the rotor gear attachment failures is required. Much data was obtained during this effort and continued study of the data should provide guidance for this effort.

A high speed electronic unit injector fuel system was synthesized, procured and demonstrated. This advanced fuel injection system progressed to the point of operating well. As is appropriate to this enablement stage, several details remain to be refined in the final development of the system. For an aircraft propulsion system, the advanced fuel system offers substantially increased flexibility of fuel injection timings and flows. This provides an opportunity for reduced fuel consumption over the entire engine operating range. In contrast, a purely mechanical system tends to be optimized for a few (at best) operating points. Properly executed, the electronic control system provides fault recovery and redundancies which are impractical with a conventional system.

9.0 RECOMMENDATIONS

9.0 RECOMMENDATIONS

1. Further testing for optimization of specific fuel consumption in the cruise power regime.

2. Further evaluation of the advanced, high speed unit injector (HSUI) fuel injection system and associated control parameters.

3. Integration of the core power section into a complete experimental flight test engine package including reduction gearing, propeller shaft and basic aircraft required accessories. A near term rating of 250-300 HP (187-225 kW) at Take-off is recommended for initial flight evaluations pending required durability testing for higher ratings.

10.0 APPENDIX

6 October 1994

TO: J. Mack
G. LaBouff

FROM: E. Troc

CC: R. Bazaz
R. Gigon
T. Hofmann
C. Irion
C. Jones
M. Kulina
W. Silvestri
FA File (Q4-340-S)
FA File (Q4-340-N1)
TDS File

SUBJECT: Rotor-Apex Seal Compatibility Tests, LFW-1 Wear Rig, RPI

REF: Following Text

INTRODUCTION:

Castings of 4140 steel and 17-4PH stainless steel materials are being evaluated as rotor components in high power rotary engine applications.

17-4 stainless steel was selected primarily because of high material strength property (tensile, fatigue endurance) requirements for satisfactory operation and durability. This material however, is highly susceptible to fretting, galling and material transfer in high contact stress and relative motion situations such as is experienced in the apex seal-to-rotor slot environment.

To alleviate this 17-4PH material characteristic and improve seal-slot compatibility, a low friction electroless nickel-thallium-boron coating (Ni-Bron) applied to the apex seal slot walls has been moderately successfully, although some fretting has been observed after long term engine test.

4140 steel was selected as an alternate cast alloy based on comparable strength properties, and a material judged to be more compatible with other (apex seal) materials than 17-4PH, but not as tolerant as the predecessor "baseline" nodular cast iron chemical composition.

A wear rig test program was initiated to evaluate the relative compatibilities of current and alternate apex seal and rotor materials, as well as various coatings and/or surface treatments.

The LFW-1 ring-on-block wear tester has shown to be a fairly reliable screening device for determining wear/compatibility of material combinations. If a material couple shows poor compatibility on rig test, that couple would most probably not perform satisfactorily in the engine. If rig testing indicates good wear and compatibility, the combination may prove satisfactory in the particular engine environment.

The rig tests were conducted without lubrication to present the most abusive possible environment (no fuel/metering oil/carbon film) that might be encountered in the close fit apex seal-rotor slot configuration, and also, to generate wear and compatibility characteristics more rapidly. A few of the material couples were tested with a small amount of 90 diesel fuel/10 lube oil mix (engine fuel and meter oil) to observe any difference in couple characteristics.

Each material couple was run continuously at 1000 rpm for a period of 10 minutes at a contact stress of 10,000 psi, followed by an additional 10 minutes at 17,000 psi and 1000 rpm. Maximum friction force was recorded at each stress level, and relative chatter/noise comments at each level were noted.

Ring and block wear features such as scoring, wear scar width, depth, polish, etc. were noted at the end of each test period. Materials included in this evaluation are given below.

ROTOR APEX SEAL SLOT MATERIAL AND SURFACE TREATMENT

1. Cast 17-4 PH Stainless Steel - This investment cast alloy, solution heat treated and age hardened, with no coating or other surface treatment represents the rotor operating bare against an apex seal.

2. Cast 4140 Steel - This investment cast alloy, hardened and tempered to a RC 35 hardness range, with no coating or other surface modification represents a rotor operating bare against an apex seal.

3. NiBRON - A Nickel-Thallium-Boron electroless plated compound (AMS 2433) of Pure Industries featuring low friction coefficient and high hardness.

4. Lube-Lok 7000 - A ceramic based dry film lubricant an E/M Corporation product applied by airborne spray and cured at 1025° F in Argon atmosphere.

5. Enplate NI-428 - An E/M Corporation electroless Nickel/PTFE (Teflon) composite coating featuring high hardness and lubricity.

6. Enplate NI-9095 - An electroless Nickel-Silicon Carbide composite deposit of E/M Corporation that features high hardness and wear resistance.

7. Gas Atmosphere Nitride - Heat treat processing that develops a hard wear resistant surface layer for a specific depth. This treatment was applied to both 4140 steel and 17-4 PH stainless to .007" - .011" case depth.

8. Salt Bath Nitride (Melonite) - A surface treatment in salt baths that develops a thin wear resistant surface layer. This treatment was applied to 4140 steel.

9. Tool Steel Weld Deposit - A tool steel composition identified as DO-14 applied by Tungsten inert gas (TIG) welding.

APEX SEAL MATERIAL AND SURFACE TREATMENT

1. Gopalite (NJS 234) - A wear resistant powder metal composite of tungsten carbide-cobalt particles in a matrix of an iron-cobalt-molybdenum alloy (Clevite 300). The composite is blended, pressed, sintered and HIPed (hot isostatic pressed) in the manufacture of the final product.

2. Ion Implanted Gopalite (NJS 234) - Gopalite composite material apex seal with a chromium nitride surface treatment applied by ion beam mixing.

3. Titanium Nitride Coated Gopalite (NJS 234) - Gopalite composite base material apex seal with a physical vapor deposited (PVD) titanium nitride compound surface treatment.

4. Chromium Nitride Coated Gopalite (NJS-234) - Gopalite apex seal material with a physical vapor deposited (PVD) chromium nitride compound surface treatment.

5. Reinforced Silicon Nitride (CIW-15) - A silicon carbide whisker reinforced silicon nitride ceramic compound with exceptional wear resistance and low friction coefficient. The material is compounded and pressure assisted densified ("PAD") into blanks and diamond ground to finish dimension.

SUMMARY

Based on the results of the LFW-1 wear rig testing, the following material couples not previously engine tested should be considered for evaluation on engine hardware:

ROTOR SLOT TREATMENT/COATING	APEX SEAL
Lube-Lok 7000	Gopalite/Ion Gopalite
Enplate NI-428	Gopalite/Ion Gopalite
Enplate 9095	Gopalite/Ion Gopalite
17-4 PH Bare	CIW-15
4140 Bare	CIW-15
17-4 PH Bare	Gopalite/Ion Gopalite

A total of 42 separate ring-on block tests were run with 29 different combinations. Some of the tests served as "baseline" tests representing current bill of material rotor and apex materials as a basis of comparison and evaluation for "new" material couples. Some tests were run in duplicate or at longer (greater number of cycles) periods of time to confirm results of promising couples. A few tests were declared invalid because of skewed or severely offset contact patterns.

The various test combinations, parameters, measurements, and observations noted are presented in the attached Table (2 pages) entitled Apex Seal Material/Slot Wear Rig Results.

The material couples considered for engine test indicated satisfactory compatibility on the rig.

It is interesting to note that a pilot nozzle performance demonstration test (1058R engine) at 375 and 500 HP using a 4140 steel rotor with no slot treatment (bare) and Gopalite 3 piece design apex seals showed relatively poor compatibility at teardown inspection after only 27 hours of test. The engine run combination exhibited significant slot and apex seal surface degradation (Reference 2). The 4140 and Gopalite wear pair did not rank highly in the wear rig results.

This bare slot steel rotor continued test in the next build equipped with reinforced silicon nitride (CIW-15) 3 piece apex seals, a favorably ranked wear rig test combination. This test was terminated after approximately 21 hours because of poor performance. Disassembly revealed chipping and fracture of the apex seal top bar at the acute angle scarf section of the 3 piece design (Reference 3). In addition the steel rotor had cracked at one of the ribs in the 18-rib rotor configuration (Reference 4).

The C1W-15 top bar did however, exhibit excellent compatibility with the steel rotor, showing no deterioration at the slot-seal side face contact surfaces. CIW-15 also showed no degradation at the trochoid contact radius.

Because of the very encouraging indications of the 17-4 PH rotor CIW-15 seal couple, a new design apex seal system, consisting of a full depth CIW-15 center bar, to eliminate and reduce severe stress concentrations inherent in the FOE 3-piece top bar design (acute angle scarf, sharp corners), was developed. The seal design also included two (2) corner pieces and a lower spring rate apex seal spring to be compatible with the lower weight and density of the CIW-15 seal.

This modified apex seal system with a 17-4 PH rotor was tested in 1058R E/N 75106-1 for 444:35 hours TT and 396:00 Modified Mission Profile Cycle hours, and exhibited excellent wear and compatibility characteristics (Reference 7).

A Lube-Lok 7000 coated 17-4 PH rotor slot - bill of material (B/M) Gopalite apex seal couple, a pair that showed excellent compatibility in wear rig testing, did not exhibit comparable results on engine test after 120:30 hours TT and 100:00 hours cycle time (Reference 5). Slot wall and seal side face fretting at the contact surfaces was observed.

Engine test of a bare 17-4 PH rotor-B/M Gopalite apex seal top bar combination illustrated reasonable compatibility after 392:35 hours TT and 350:30 hours cycle time in 1058R E/N 71104-8 (Reference 6) with minor evidence of chaffing at the seal-slot contact surfaces.

This combination was judged to be marginally satisfactory on wear rig tests.

Based on rig tests and subsequent engine test results and observations, reinforced silicon nitride material exhibits most desirable compatibility with either of the base material alloys (4140 and 17-4) under evaluation for improved rotor durability.

REFERENCES:

1. Memo, Newman to LaBouff, 26 September 1991
2. Test Report, 1058R E/N 71104-3, 24 March 1993
3. Test Report, 1058R E/N 71104-4, 29 March 1993
4. Memo, Troc to LaBouff, 17 June 1994
5. Test Report, 1058R E/N 71104-7, in process
6. Test Report, 1058R E/N 71104-8, in process
7. Test Report, 1058R E/N 75106-1, in process

REPORT DOCUMENTATION PAGE

Form Approved
OMB No. 0704-0188

1. AGENCY USE ONLY (*Leave blank*)	2. REPORT DATE	3. REPORT TYPE AND DATES COVERED
	October 1994	Final Contractor Report

4. TITLE AND SUBTITLE

Two Rotor Stratified Charge Rotary Engine (SCRE)
Engine System Technology Evaluation

5. FUNDING NUMBERS

WU- 505-62-11
C-NAS3- 26920

6. AUTHOR(S)

T. Hoffman, J. Mack and R.Mount

7. PERFORMING ORGANIZATION NAME(S) AND ADDRESS(ES)

Rotary Power International, Inc.
P.O. Box 128
Wood-Ridge, New Jersey 07075

8. PERFORMING ORGANIZATION REPORT NUMBER

E- 9193

9. SPONSORING/MONITORING AGENCY NAME(S) AND ADDRESS(ES)

National Aeronautics and Space Administration
Lewis Research Center
Cleveland, Ohio 44135-3191

10. SPONSORING/MONITORING AGENCY REPORT NUMBER

NASA CR-195395

11. SUPPLEMENTARY NOTES

Project Manager, Thomas N. Strom, Advanced Propulsion Applications Office, NASA Lewis Research Center Organization Code 2701 (216) 433-3408.

12a. DISTRIBUTION/AVAILABILITY STATEMENT

Unclassified-Unlimited
Subject Category 07

12b. DISTRIBUTION CODE

13. ABSTRACT (*Maximum 200 words*)

This report summarizes results of an evaluation of technology enablement component technologies as integrated into a two rotor Stratified Charge Rotary Engine (SCRE). The work constitutes a demonstration of two rotor engine system technology, utilizing upgraded and refined component technologies deriving from prior NASA Contracts NAS3-25945, NAS3-24628 and NAS-23056. Technical objectives included definition of, procurement and assembly of an advanced two rotor core aircraft engine, operation with Jet-A fuel at Take-Off rating of 340 BHP (254kW) and operation at a maximum cruise condition of 255 BHP (190kW), 75% cruise. A fuel consumption objective of 0.435 LBS/BHP-Hr (265 GRS/kW-Hr) was identified for the maximum cruise condition. A critical technology component item, a high speed, unit injector fuel injection system with electronic control was defined, procured and tested in conjunction with this effort. The two rotor engine configuration established herein defines an affordable, advanced, Jet-A fuel capability core engine (not including reduction gear, propeller shaft and some aircraft accessories) for General Aviation of the mid-1990's and beyond.

14. SUBJECT TERMS	15. NUMBER OF PAGES
Stratified Charge; Rotary; Engine; Aircraft; Fuel Injection; Multi-Fuel	16. PRICE CODE

17. SECURITY CLASSIFICATION OF REPORT	18. SECURITY CLASSIFICATION OF THIS PAGE	19. SECURITY CLASSIFICATION OF ABSTRACT	20. LIMITATION OF ABSTRACT
Unclassified	Unclassified	Unclassified	